Performance of IEEE 802.11 MAC Protocol over a Wireless LAN with Distributed Radio Bridges

by

CUPID C. CHOW

B. Sc. (Electrical Eng.) The California State University, Fresno, CA, USA, 1994

A THESIS SUBMITTED IN PARTIAL FULFILLMENT OF

THE REQUIREMENTS FOR THE DEGREE OF

MASTER OF APPLIED SCIENCE

in

THE FACULTY OF GRADUATE STUDIES

DEPARTMENT OF ELECTRICAL ENGINEERING

We accept this thesis as conforming

to the required standard

THE UNIVERSITY OF BRITISH COLUMBIA

April 1999

In presenting this thesis in partial fulfilment of the requirements for an advanced degree at the University of British Columbia, I agree that the Library shall make it freely available for reference and study. I further agree that permission for extensive copying of this thesis for scholarly purposes may be granted by the head of my department or by his or her representatives. It is understood that copying or publication of this thesis for financial gain shall not be allowed without my written permission.

Department of ELECTRICAL ENGINEERING

The University of British Columbia
Vancouver, Canada

Date APR 28, 1999

DE-6 (2/88)

Abstract

In this thesis, the performance, in terms of throughput and access delay, of the proposed distributed Wireless Local Area Network employing the IEEE 802.11 Medium Access Control protocol is analyzed extensively by computer simulations. The proposed network is based on using the same frequency for the entire coverage area with multiple receivers or radio bridges (RBs), with or without capture effect at each receiver. Different channel environments, including the Additive White Gaussian Noise (AWGN) channel, log-normal shadowing channel, Rayleigh fading channel, and log-normal shadowing plus Rayleigh fading channel, are considered in the simulations. The effects of various parameters are also studied.

The results show that the performance can be improved significantly by using more RBs except for AWGN channel. The performance improvement of multiple RBs over one RB depends on the system parameters. In the log-normal shadowing plus Rayleigh fading channel, the throughput with 4 RBs and no capture can be improved by at least 120% over one RB. It is found that multiple RBs are more effective in a system with large number of stations and for channels severely degraded by shadowing or fading. With the use of capture, the performance can be improved by multiple RBs. But the performance improvement of multiple RBs is about the same as no capture cases. The effect of capture ratio is studied. It is found that the performance increases with decreasing the capture ratio.

The performance of one and two dimensional models are found to be slightly different. The throughput does not change with packet size; however, the access delay degrades with packet size. Finally, it is found that the performance is not significantly affected by the length of the acknowledgment time-out.

Table of Contents

List of Tables

List of Figures

Acknowledgment

I would like to express sincere gratitude to my research supervisor, Dr. V. C. M. Leung, who has provided me with many helpful suggestions, constant supervision, and invaluable guidance in both my research and the preparation of this document. I would like to thank Dr. E. Casas for his help in reviewing and verifying the simulation model.

Chapter 1 Introduction

Nowadays, Local Area Networks (LANs) are widely used to interconnect computers to each other, printers, servers, and the Internet. However, installing and maintaining the wiring of a LAN is very expensive, and in some instances technically very challenging. Wireless Local Area Networks (WLANs) provide an attractive alternative which enable flexible location of terminals and can avoid re-wiring when terminals are relocated.

WLANs employ wireless communications for interconnecting wireless terminals among themselves and to wired LANs. A Medium Access Control (MAC) protocol is used by a WLAN to enable multiple terminals to efficiently share the same radio or optical wireless channel. For extending the connectivity of a WLAN, a backbone LAN can be employed. WLAN usually operates in the indoor environment. Fading and shadowing will degrade the performance of the system. Techniques such as diversity reception, equalization, and spread spectrum signalling can overcome the propagation effects to enable reliable communications [1]. When multi-access interference occurs, all the transmitted packets sent by several users collide at the receiver and all the packets are destroyed. Therefore, the throughput efficiency is limited. Fortunately, the capture effect allow the receiver to capture one of several colliding packets correctly due to different signal strengths when the packet reaches the receiver [2][3]. Therefore, the capture effect can increase the throughput efficiency of the system.

To provide coverage in a large building using low power radio transmissions, the centralized architecture can be used. As in a cellular mobile telephone system, the building area is divided into cells which are connected through a backbone LAN. Different radio channels are assigned to adjacent cells to minimize interference. An alternative approach is the distributed

architecture proposed in [1][4][5] which is based on using the same radio channel over the entire coverage area. This architecture avoids the need for frequency coordination and does not need the complicated handoff mechanisms as required in the cellular architecture. Besides, it enables macro-diversity, and it is expected to give improved performance in the presence of propagation effects and hidden terminals. The performance evaluation of the distributed architecture by applying the IEEE 802.11 MAC protocol is the main goal of this thesis.

1.1 Motivations and Objectives of the Thesis

WLAN is an integral and important component in the emerging wireless office. WLAN not only removes the hassle of installing and maintaining cables, but it also provides communication where computers are no longer bounded to a particular location. Currently, WLANs utilize two technologies, infrared and radio access. Both of them require proper access control protocols to allow multiple users to share the channel. In particular, radio access technology requires a proper knowledge of the environment in which the radio WLAN is to be deployed. Therefore, the performance of the radio WLAN systems are very much influenced by the radio propagation effects, especially in indoor environments, and by the MAC protocols as well. Accordingly, in 1990, the IEEE Project 802.11 WLAN Standards Committee was established to recommend an international standard [6][7] for WLANs. The scope of the work is to develop MAC layer and Physical (PHY) layer specifications for wireless connectivity for fixed, portable and moving stations within a local area. The standard describes the MAC procedures to support the asynchronous and time-bounded MAC Service Data Unit (MSDU) delivery services. The basic MAC protocol is a Distributed Coordination Function (DCF) that allows for medium sharing through the use of Carrier Sense Multiple Access with Collision Avoidance (CSMA/CA) and a random backoff time.

The architectures of the WLANs can be addressed in two major areas. They are adhoc and infrastructure networks. Adhoc network is formed by a minimum of two Wireless Terminals (WTs) that are close enough to form direct connections without pre-planning. Both simulations and analysis have been done for this kind of networks. In [8], simulations results are presented for throughput and delays for 10 and 25 stations with different values of inter-frame spacing periods and transmission speeds. It shows that there is no significant difference in normalized throughput for various transmission speed, and the choice of inter- frame space values depends on the type of network. In [9][10][11], simple modifications for the backoff mechanism using weighted probability are presented. A simulation is done with 8 stations with or without hidden terminals, and the results show that the throughput increases by 25% with the modified backoff scheme. However, the optional Ready to Send/Clear to Send (RTS/CTS) mechanism does not completely solve the hidden terminal problem, and only some improvements can be achieved. In [12], voice traffic in the Contention Free Period (CFP) and data traffic in the Contention Period (CP) over an 802.11 WLAN are simulated. The results show that the cooperation of the CP and the CFP limits the number of possible voice conversations and the maximum payload size of the data. In [13][14], a simple analytical model to compute the saturation throughput performance in the presence of a finite number of terminals with the assumption of ideal channel is presented. Besides, an adaptive contention window mechanism is proposed and the optional RTS/CTS is investigated with hidden terminals by simulations. The results show that the basic CSMA/CA suffers from several performance drawbacks. With the adaptive contention window mechanism, the system becomes stable, and it outperforms the standard protocol when the network load and the number of mobile stations are high. In [15][16], the possibility of power capture, and presence of hidden stations is considered. System throughput is computed and fairness properties are

evaluated. The impact of spatial characteristics on the performance of the system and that observed by individual stations is determined. The simulation results obtained for throughput for varying values of capture parameter and probability of hidden stations validate the analytical approach.

In contrast to the adhoc network, infrastructure networks contain Access Points (APs) which are stations that provide access to the backbone LAN. The centralized architecture of the infrastructure networks is used as in a cellular mobile telephone system, with the building area divided into cells which are connected through a backbone LAN. This type of network is studied in [17] with Rayleigh fading, shadowing and power capture effect by using the MAC protocols based on IEEE 802.11. The channel throughput and packet delay are analyzed. In [18][19], the natural hidden terminals problem of this network is analyzed. The analysis includes the effects of the difference in the coverage of the AP and the mobile terminals as well as the capture effect caused by the near far problem. Most of the research and commercial products employ the centralized architecture, such as the Wireless In Building Network (WIN) by Motorola [20], which can handle a combined network traffic demand of approximately 3 Mbps.

In [21][22][23], the performance of the MAC layer is determined by simulating asynchronous data for both adhoc and infrastructure networks. In [21], the sensitivity of network geometry, traffic flow, queueing size, channel models, hardware, backoff parameters and hidden terminal problem on performance are studied. It turns out that the connectivity and the hidden terminal parameter can be used to predict the performance of the system. For [22][23], performance results are provided for packetized data and a combination of packetized data and voice over the WLAN. The results show that the 802.11 WLAN can achieve a reasonably high efficiency when the

medium is almost error-free, but may degrade under fading, and it also shows that time-sensitive traffic such as packet voice can be supported together with packet data.

In [24][25], they both present the modeling and performance analysis of a distributed WIN with multiple receivers and Direct Sequence Spread Spectrum (DSSS). The first one use the Carrier Sense Multiple Access and the second one use the slotted ALOHA medium access control protocol. Besides, in [26], a one-dimensional network model with multiple access ports is studied by using slotted ALOHA medium access control. Therefore, the proposed distributed WLANs has not been studied using the IEEE 802.11 standard MAC protocol.

The objective of this thesis is to investigate by simulations the throughput and delay performance of the IEEE 802.11 MAC protocol employing CSMA/CA in WLANs employing distributed radio bridges (RBs) [1]. We focus on the uplink channel between WTs and the multiple RBs, subject to Rayleigh fading and shadowing, with and without capture effect at the receivers.

1.2 Outline of the thesis

In this thesis, an overview of the IEEE 802.11 WLAN MAC protocol is given in Chapter 2. Chapter 3 presents the architecture and a functional evaluation of the WLAN employing distributed RBs with the IEEE 802.11 MAC protocol. As well, the simulation model using OPtimized Network Engineering Tools (OPNET) [27] is presented. Chapter 4 discusses the model validation and the simulation results for the Additive White Gaussian Noise (AWGN) channel, the Rayleigh fading channel and the Log normal shadowing channel. Chapter 5 presents the simulation results on the performance of the combination of the AWGN, Rayleigh fading and shadowing channel with and without capture effect. Conclusions are given in Chapter 6.

Chapter 2 Background

In this chapter, the architecture components to provide IEEE 802.11 WLAN that support station mobility transparently to upper layers will be described. Then, the functional description of the MAC layer will be presented.

2.1 IEEE 802.11 Architecture Components

The basic building block of an 802.11 LAN is the Basic Service Set (BSS) which is a set of stations controlled by a single coordination function. Figure 2.1 shows two BSSs, each of which has two stations. The ovals is used to define a basic service area (BSA) as the coverage area over which the stations can communicate with each other. The independent BSS is the most basic type of 802.11 LAN. A minimal 802.11 LAN can consist of only two stations.

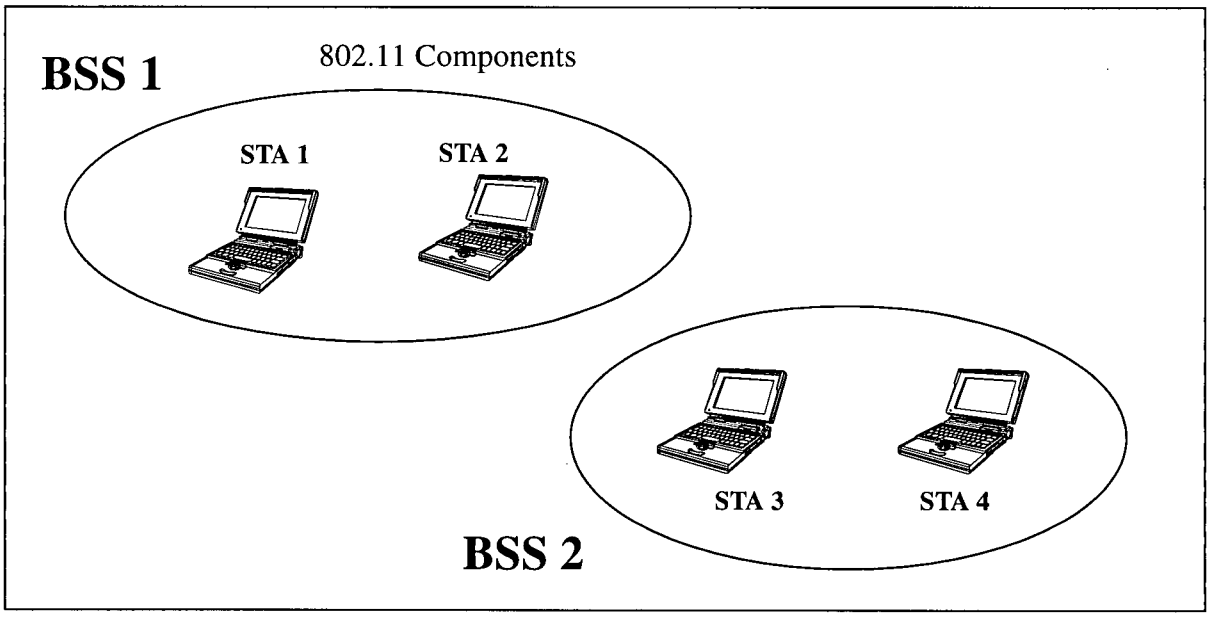

Figure 2.1 Basic Service Set.

The architectures of the WLANs can be addressed in two major areas. They are adhoc and infrastructure networks.

2.1.1 Adhoc Network

Figure 2.1 shows two independent BSSs. In each BSS, the stations are close enough to form a direct connection without pre-planning. This type of operation characterizes as adhoc network. Since, all the stations must be close enough for communications, the range of this type of network is limited.

2.1.2 Infrastructure Network

In contrast to the adhoc network, infrastructure networks can provide wireless users with specific services and range extension. An infrastructure network contains one or more APs which are stations that provide access to the Distribution System (DS). The DS is used to interconnect a set of BSSs to create an Extended Service Set (ESS). Stations within an ESS can communicate and mobile stations may move from one BSS to another (within the same ESS). The BSSs may overlap or be disjoint. The Extended Service Area (ESA) which is not smaller than a BSA, is the area within which members of an ESS can communicate. The DS can be thought of as a backbone network that is responsible for MAC level transport of MSDUs. An ESS can provide access for wireless users into a wired network via a device known as a portal. The Station Services (SS) include authentication, deauthentication, privacy and MSDU delivery by every station. The Distribution System Services (DSS) include association, disassociation, distribution, integration and reassociation and are used to cross media and to address space logical boundaries. Figure 2.2 shows a simple ESS with two BSSs, a DS, and a portal access to a wired LAN.

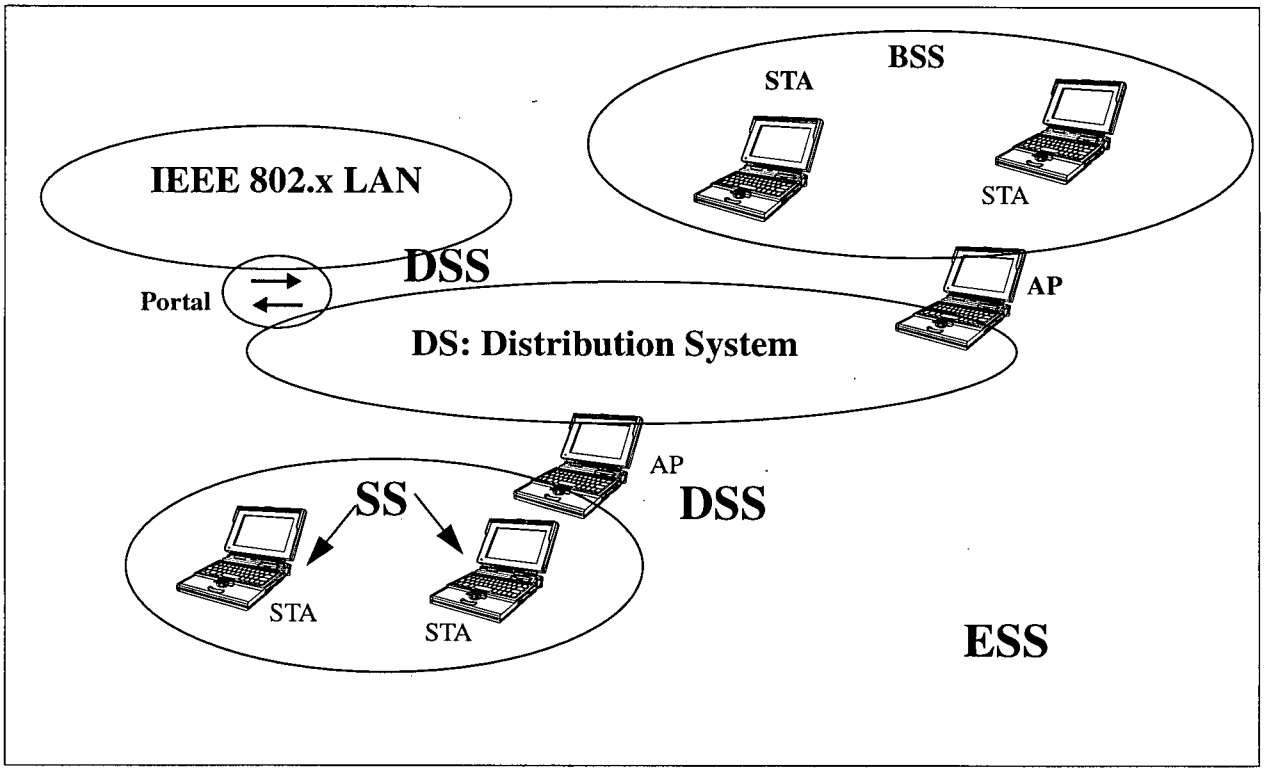

Figure 2.2 An infrastructure network.

2.2 IEEE 802.11 WLAN MAC Protocol

The basic MAC protocol specified in IEEE 802.11 is a DCF that allows for medium sharing through the use of CSMA/CA and a random backoff time. The DCF shall be implemented in all stations and APs. An alternative access method is a Point Coordination Function (PCF) which may be implemented on top of the DCF. This access method uses a point coordinator to determine which station currently has the right to transmit. Since this paper mainly focuses on the DCF part, the system modeling and performance analysis will be based on the DCF. However, both the DCF and the PCF may coexist without interference.

2.2.1 Distributed Coordination Function (DCF)

The fundamental access method of the 802.11 MAC is a DCF knows as CSMA/CA. The

CSMA/CA is designed to reduce the collision probability between multiple stations accessing a medium. Carrier sensing (CS) can be performed both through physical and virtual mechanisms. The physical CS mechanism shall be provided by the PHY and the details of CS are provided in the individual PHY specification section [6][7]. The virtual CS mechanism is achieved by reserving the medium as busy through the exchange of special small RTS and CTS frames before the actual data frame. The RTS and CTS frames activate the Network Allocation Vector (NAV) which contains the duration field for the period of time that the medium is to be reserved to transmit the actual data frame. This information is distributed to all stations within detection range of both the source and the destination stations in order to solve the hidden station problem. However, this can only be used for directed frames. When multiple destinations are addressed by broadcast/ multicast frames, then this mechanism is not used.

2.2.2 Inter-Frame Space (IFS)

The time interval between frames is called the IFS. According to the priority levels for access to the wireless media, there are four different IFSs. The first one is the Short Inter-frame Space (SIFS), and it has both a minimum and maximum specification which depends on the PHY layer. This SIFS is used for an acknowledgment (ACK) frame, a CTS frame, and between frames. The second type is the PCF-IFS (PIFS) and is used only by the PCF to send any of the CFP frames. After a station operating under the PCF detects the medium free for the period PIFS, it is allowed to transmit. The third type is the DCF-IFS (DIFS) and is used to transmit asynchronous MAC Protocol Data Units (MPDUs). After a station operating under the DCF detects the medium free for the period DIFS, it is allowed to transmit, as long as it is not in a backoff period. Extended Inter-frame Space (EIFS) is used by the DCF when the PHY has indicated to the MAC that a frame transmission was begun that did not result in the correct reception of a complete MAC

frame with a correct Frame Check Sequence (FCS) value. The SIFS Time and Slot Time are defined as follows, and are fixed per PHY.

$$\begin{aligned} \text{SIFS Time} &= \text{RxRFDelay} + \text{RxPLCPDelay} + \text{MACProcessingDelay} \\ &\quad + \text{RxTxTurnaroundTime}. \\ \text{Slot Time} &= \text{CCA Time} + \text{RxTxTurnaroundTime} \\ &\quad + \text{AirPropagationTime} + \text{MACProcessingDelay}. \end{aligned} \tag{2.1}$$

The PIFS and DIFS are derived by:

$$\begin{aligned} \text{PIFS} &= \text{SIFS Time} + \text{Slot Time} \\ \text{DIFS} &= \text{SIFS Time} + 2 \times \text{Slot Time} \end{aligned} \tag{2.2}$$

The EIFS is derived from the SIFS and the DIFS and the length of time it takes to transmit an ACK frame at a Mbit/s by the following equation:

$$\begin{aligned} \text{EIFS} &= \text{SIFS Time} + (8 \times \text{ACKSize}) + \text{PreambleLength} \\ &\quad \text{PLCPHeaderLength} + \text{DIFS}. \end{aligned} \tag{2.3}$$

where ACKSize is the length, 14 bytes, the SIFS Time, Slot Time, RxRFDelay, RxPLCPDelay, MACProcessingDelay, RxTxTurnaroundTime, CCA Time, AirPropagationTime, MACProcessingDelay, PreambleLength and PLCPHeaderLength are different for the three PHY layer specifications. The following table lists the default values:

Table 2.1 Lists of the PHY Attributes of FHSS, DSSS and IR.

PHY	Attribute	Default Value
FHSS	Slot Time	50 μs
	CCA Time	27 μs
	RxTxTurnaroundTime	20 μs
	RxPLCPDelay	2 μs
	SIFS Time	28 μs
	RxRFDelay	4 μs
	MACProcessingDelay	2 μs
	PreambleLength	96 μs
	PLCPHeaderLength	32 μs
	AirPropagationTime	1 μs
	CW_{min}	15
	CW_{max}	1023
DSSS	Slot Time	20 μs
	CCA Time	≤ 15 μs
	RxTxTurnaroundTime	≤ 5 μs
	RxPLCPDelay	implementation dependent
	SIFS Time	10 μs
	RxRFDelay	implementation dependent
	MACProcessingDelay	not applicable
	PreambleLength	144 bits
	PLCPHeaderLength	48 bits
	CW_{min}	31
	CW_{max}	1023

PHY	Attribute	Default Value
IR	Slot Time	8 μd
	SIFS Time	7 μs
	RxTxTurnaroundTime	0 μs
	RxPLCPDelay	1 μs
	CCA Time	5 μs
	RxRFDelay	implementation dependent
	MACProcessingDelay	2 μs
	PreambleLength	16 μs (1 Mbps) 20 μs (2 Mbps)
	PLCPHeaderLength	41 μs (1 Mbps) 25 μs (2 Mbps)
	CW_{min}	63
	CW_{max}	1023

2.2.3 DCF Access Procedure

The basic access refers to the mechanism a station uses to determine whether it has permission to transmit. A station with a pending MPDU may transmit when it detects a free medium for greater than or equal to a DIFS time. If the medium is busy, the random backoff time algorithm will be followed. Figure 2.3 shows the basic access mechanism. Figure 2.4 shows the basic transmission procedure for the source, destination and other stations. The source station follows the basic access procedure and transmits the data frame. The destination station returns an ACK frame and other stations defer and follow the backoff procedure.

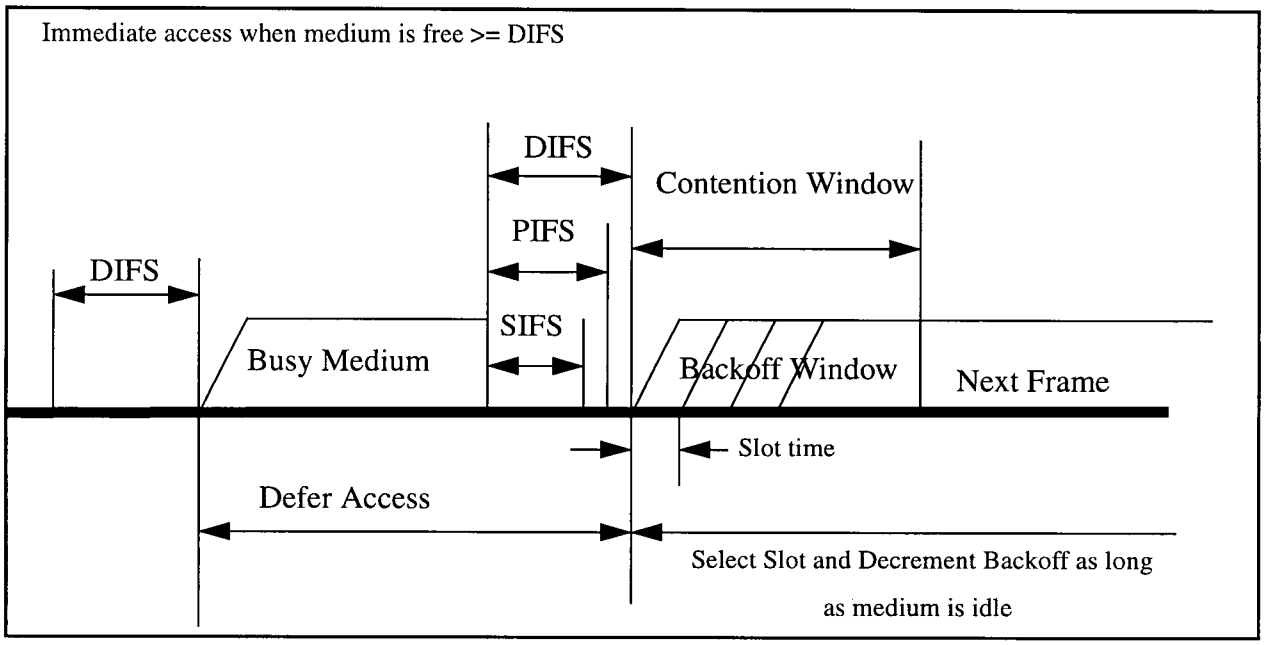

Figure 2.3 Basic Access Method

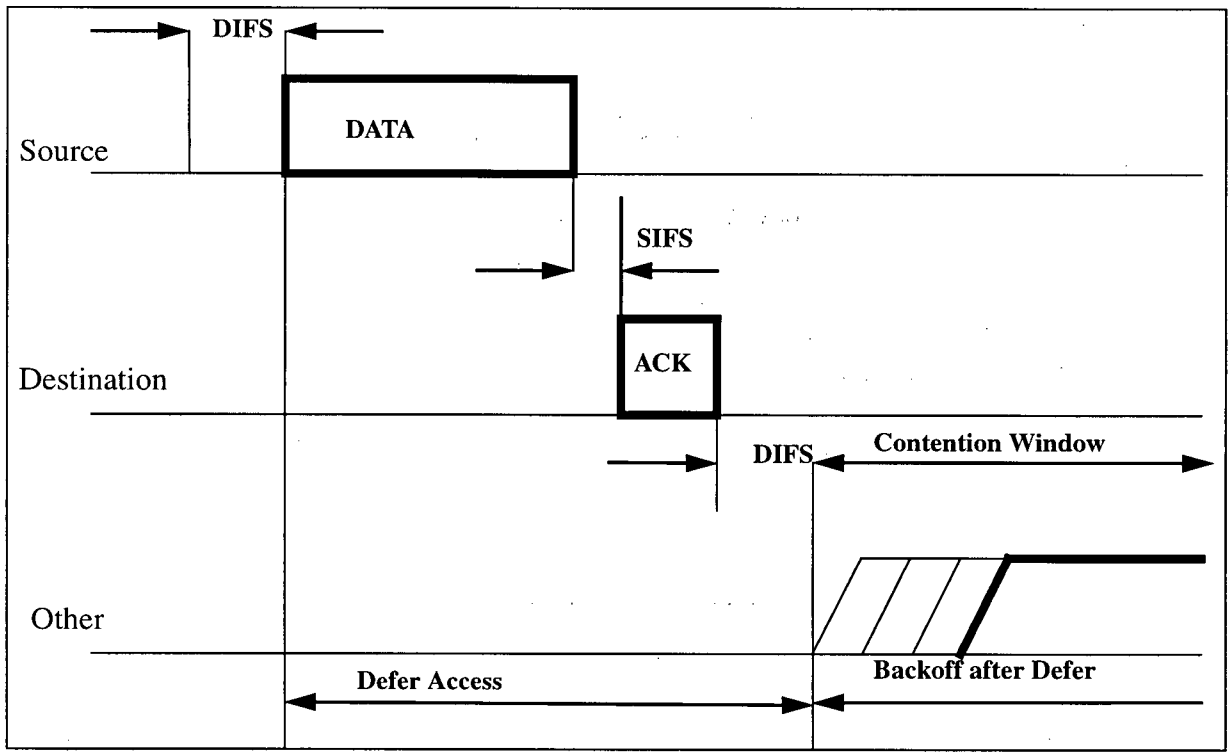

Figure 2.4 Directed MPDU transfer procedure.

2.2.4 Backoff Procedure

When a station intends to transmit an MPDU and finds that the medium is busy, the backoff procedure will be followed. This procedure has a backoff timer which is selected from (2.4). The timer will decrement only when the medium is free for DIFS time and it will be frozen during the busy period. When the timer goes to zero, MPDU transmission begins if the medium is still idle. Figure 2.5 shows the backoff procedure of five stations trying to send their own MPDUs and some of them have to go through the backoff procedure while one of them is sending its own MPDU. In order to provide fairness of access for all the stations, once a station has transmitted a frame and has another frame ready to transmit, it has to perform the backoff procedure.

The backoff time is determined as follows:

$$\text{Backoff Time} = \text{Random}() * \text{Slot Time} \tag{2.4}$$

where:

$$\begin{gathered}\text{Random}() = \text{Pseudo random integer drawn from a uniform} \\ \text{distribution over the interval } [\,0, CW] \\ CW = \text{An integer between } CW_{min} \text{ and } CW_{max}\end{gathered} \tag{2.5}$$

where the Slot Time is defined in equation (2.1) and the default values are listed in Table 2.1. The Contention Window (CW) has an initial value of CW_{min} for every MPDU and is increased exponentially after every retransmission attempt up to CW_{max}. This is done to improve the stability of the access protocol under high load conditions. The default values for the CW_{min} and CW_{max} are in Table 2.1.

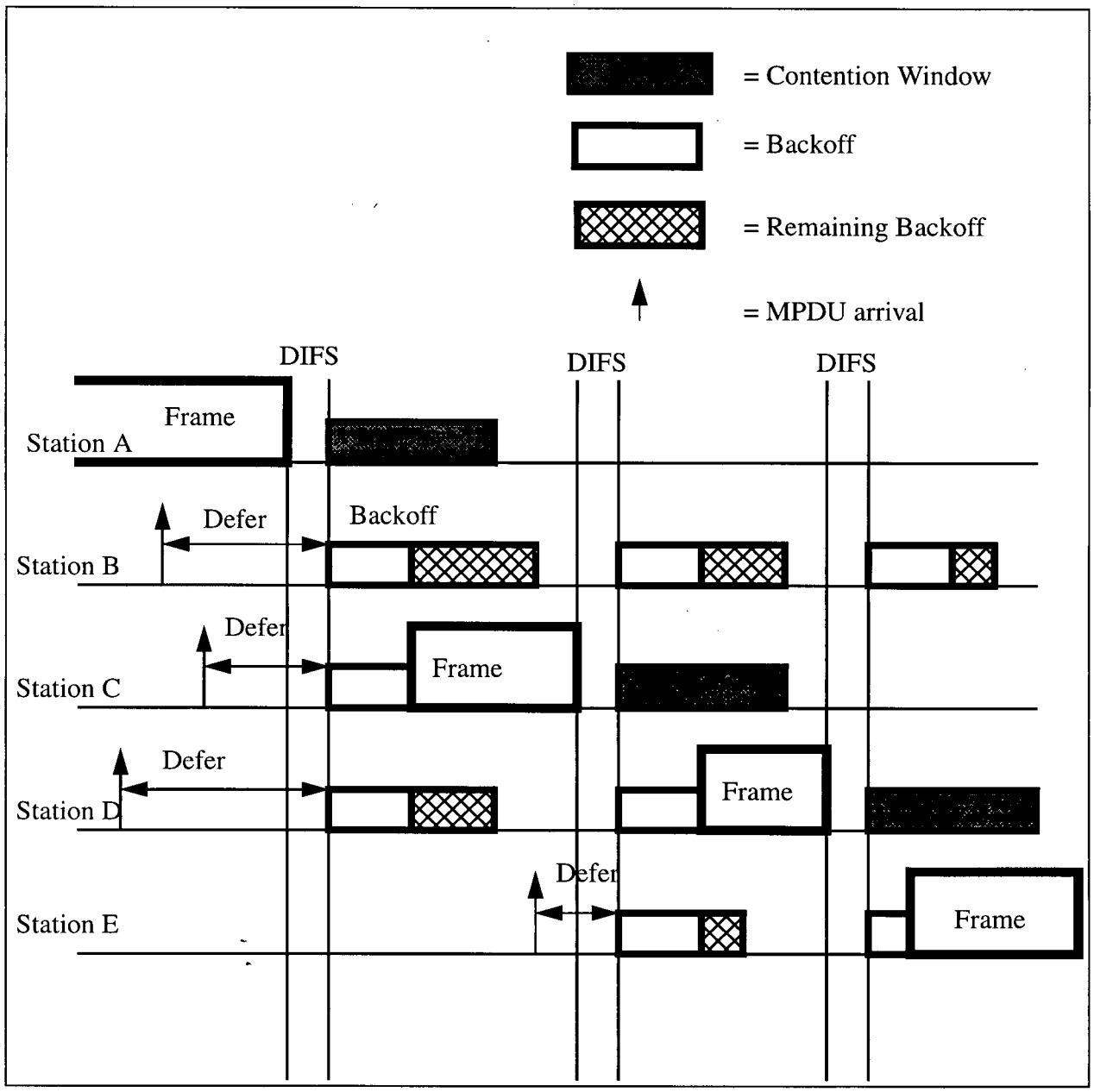

Figure 2.5 Backoff Procedure

2.2.5 Directed MPDU Transfer Procedure using RTS/CTS

Figure 2.6 shows the directed MPDU transfer procedure with the use of RTS/CTS. A station shall use an RTS/CTS exchange for directed frames only and the length of the MPDU will

be used to determine whether RTS/CTS is used. If the length is greater than a threshold, RTS_Threshold = 3000 bits [7], the RTS/CTS exchange is used. From Figure 2.6, the source station sends a RTS frame using the basic access procedure and the backoff procedure. Within the CTS_Timeout, the destination station returns the CTS frame after the SIFS. All other stations will set their NAV to the duration of the whole transmission process. When the source station receives the CTS frame, it will transmit the data frame after SIFS. Finally, the destination station will send back an ACK frame upon successful reception of data after the SIFS.

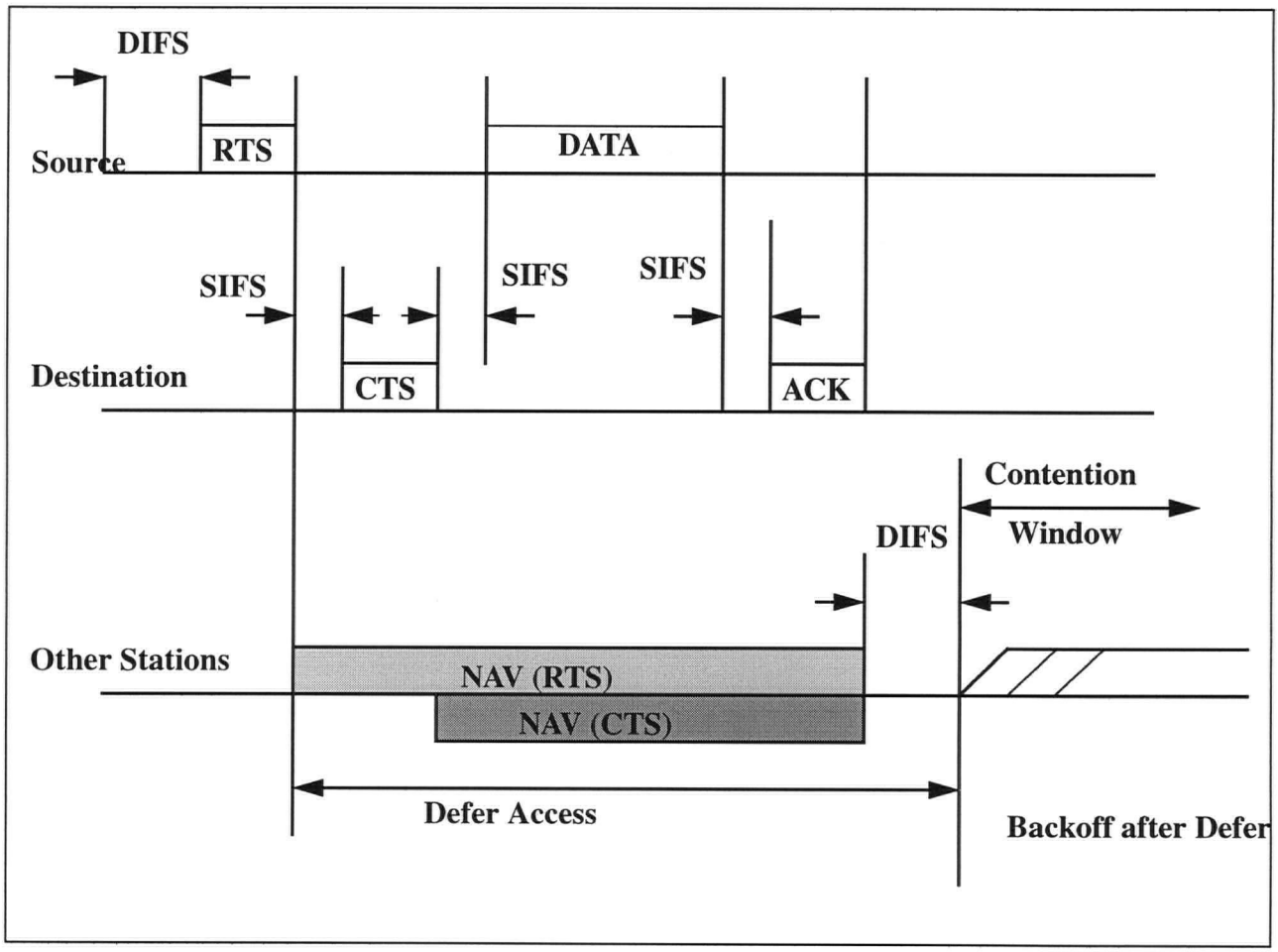

Figure 2.6 Directed MPDU Transfer using RTS/CTS.

2.2.6 RTS/CTS Recovery Procedure and Retransmit Limits

Due to a collision or interference, CTS may not be returned after the RTS transmission. If after a RTS is transmitted, the CTS fails to return within a CTS_Timeout. The Short Retry Count is incremented and then a new RTS will be generated following the backoff procedure. This process will continue until the transmission is successful, or until the Short Retry Count reaches a ShortRetryLimit, and the MSDU or MPDU is discarded. The ShortRetryLimit is 7.

If a directed data frame has been transmitted without RTS/CTS, but an ACK frame has not been received within an ACK_Timeout, it will go through the backoff procedure. The data frame will be retransmitted when the backoff time has reached zero. This process will continue until the Long Retry Count reaches a LongRetryLimit, and then the MSDU or MPDU is discarded. The LongRetryLimit is 4.

2.2.7 Broadcast and Multicast MPDU Transfer Procedure

In the DCF, when broadcast or multicast MPDUs are transferred from a station to stations, only the basic access procedure is used. Regardless of the length of the frame, and no ACK is returned by any destination stations. However, any broadcast of multicast MPDUs transferred from a station to the DS should follow the basic access method and the rules for RTS/CTS exchange. The broadcast/multicast message shall be distributed into the BSS.

2.2.8 ACK Procedure

An AP shall always generate an ACK frame, and a station shall return an ACK frame when it receives a unitcast data frame or management frame. If the source station has not received the ACK frame within the ACK_Timeout, it will conclude that the MPDU was lost.

2.2.9 Duplicate Detection and Recovery

Each frame has an MPDU ID which is a 16 bit hash of the 2 Octet Network ID field, 6 Octet source address and a 1 Octet sequence number maintained by the source station. A destination station checks the MPDU ID with the IDs kept in the MPDU_ID_CACHE and discards the duplicate frame, but it will still follow the ACK procedure.

2.3 IEEE 802.11 Physical Layer

The draft standard includes two types of PHY layer specifications for the 2.4 GHz ISM band, FHSS and DSSS, and Infrared (IR) PHY specification. The FHSS PHY parameters are used in the simulation model in this thesis and the capture model is mainly based on the frequency modulation. 1 Mbit/s and 2 Mbit/s are the only rates currently supported, and the 1 Mbit/s data rate is used in the simulation model. The number of transmit and receive frequency channels is 79 for the North America. Detail information on PHY layer can be found in [7].

Chapter 3 Distributed WLAN Architecture and the Functional Evaluation of the IEEE 802.11 MAC Protocol

This chapter describes the architecture of the distributed WLAN employing multiple RBs and how the frames received by the RBs are forwarded over the LAN. By reviewing the architecture of the distributed WLAN and the IEEE 802.11 MAC methods, this chapter provides an evaluation of the functional aspects of the distributed WLAN using the standard MAC protocol. Moreover, a simulation model of the proposed network using OPNET will be presented. Then, the design of the IEEE 802.11 MAC state machines will be described.

3.1 Distributed WLAN Architecture

Figure 3.1 shows the distributed architecture. This architecture is based on using the same radio channel over the entire coverage area. Each WT is interconnected with multiple RBs to a backbone LAN. This architecture avoids the need for frequency coordination and does not need the complicated handoff mechanisms as required in the cellular architectures. In Figure 3.1, this WLAN consists of multiple WTs transmitting (uplink) to the RBs and receiving (downlink) from the RBs. Each WT consists of a work-station equipped with a wireless transceiver, and each RB incorporates a processing unit which buffers and forwards incoming frames according to a bridging algorithm [1]. The WT employs a MAC protocol to communicate with the RBs within its range over the wireless channel. The locations of the mobile terminals are variable. Sufficient number of RBs are attached to the backbone LAN at fixed locations to provide multiple-site radio coverage of all possible locations of the WTs. The proposed architecture can be expanded easily to increase network capacity and reconfiguration of network topology. WTs can be added in any existing network coverage area but the number of WTs that can be accommodated within a certain

area is limited by the network throughput capacity available over that area. The throughput may be increased by reducing the coverage of each RB in that area, and increasing the number of RBs. The coverage area of the network can be expanded by attaching more RBs to the backbone LAN to cover new areas.

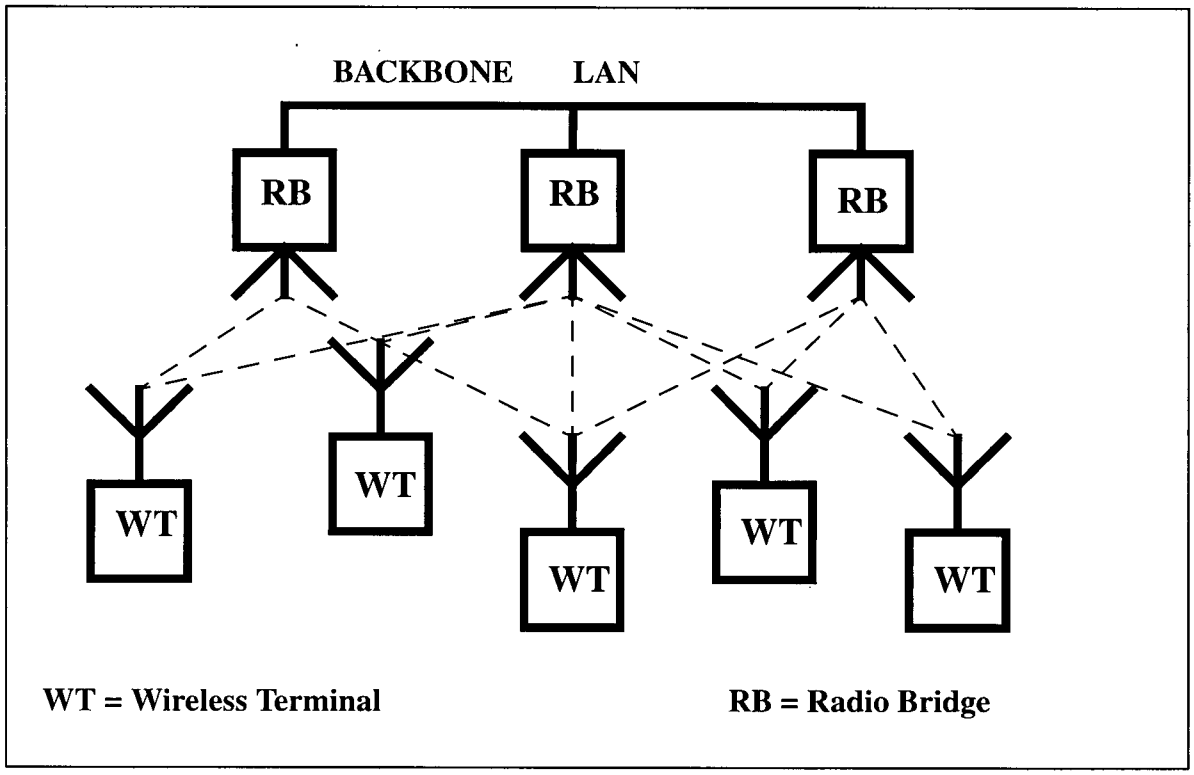

Figure 3.1 The distributed architecture for WLAN, with multiple radio bridges.

3.2 Functional Evaluation of the Distributed WLAN Employing the IEEE 802.11 MAC Protocol

A LAN consists of a collections of devices that share the network's transmission capacity. The function of the MAC protocol is to control access to the transmission medium to provide an orderly and efficient use of that capacity. The IEEE 802.11 MAC protocol is designed to reduce

the collision probability between multiple stations accessing a wireless medium by using the carrier sensing mechanism and the random backoff time mechanism as described in Chapter 2. To illustrate the operation of the distributed network employing the IEEE 802.11 MAC protocol, the following example is given.

3.2.1 An Example of the Distributed WLAN

In Figure 3.2, there are two RBs and three WTs. Each WT can start transmission when it senses the channel free for DIFS time. Besides, each WT can choose either to send the actual data with RTS/CTS or without RTS/CTS. For simplicity reason, all the RBs and WTs in Figure 3.2 are within range. Therefore, there are no hidden terminal in this example.

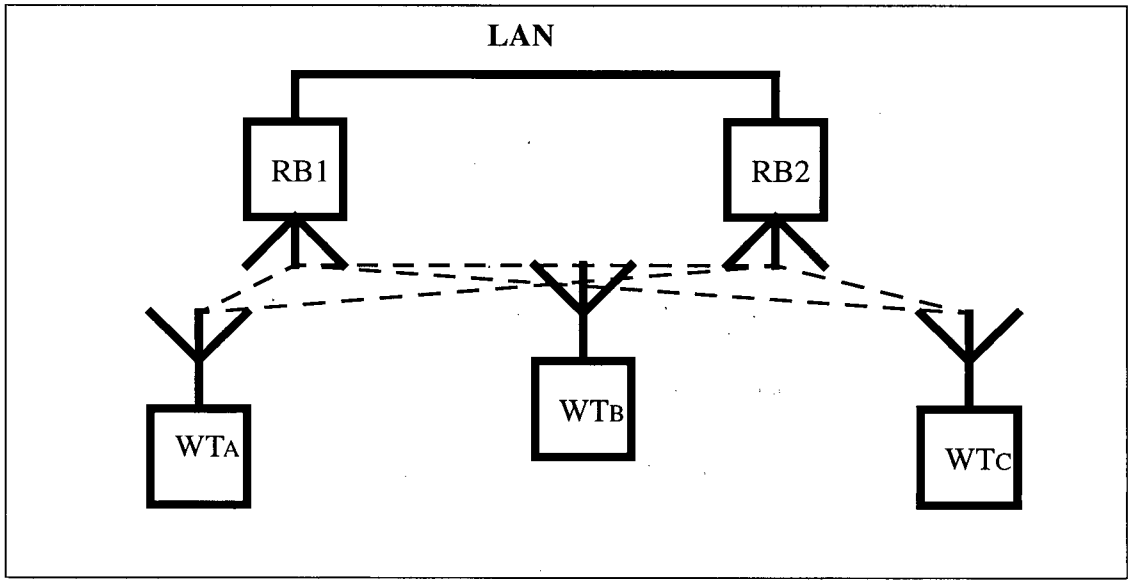

Figure 3.2 An example of the WLAN employing RBs.

Consider that WT_A has a data frame waiting in its transmit queue ready to be sent. WT_A first needs to find out whether the payload length exceeds the RTS_Threshold, and if so RTS will be sent before the actual data frame. The RTS_Threshold can be set from 0 (which means no

MPDU is delivered without the use of RTS/CTS) to maximum MPDU length, and it can be set differently in each station.

In this case, suppose all the MPDU needs to be sent with RTS/CTS. An ACK frame shall be returned by the destination station upon successful reception of a data frame within the ACK_timeout. WT_A first listens to the channel and if it is free for longer than DIFS, then transmits a RTS. Once the transmission has started, all other stations, if they sense the channel busy will defer until the medium is free for DIFS and go into backoff. All the RBs and WTs are within range and receive the RTS at different times because of the propagation delay. RB_1 and RB_2 both receive the RTS at different times and try to return a CTS, and each RB needs to wait for SIFS time and senses the channel before sending the CTS. If RB_1 receives the RTS first, then RB_1 will return a CTS first. In that case, if RB_2 senses the channel while RB_1 has already started transmitting the CTS, RB_2 will delay it transmission and will go back to the wait state. This situation can be vice versa. However, RB_1 and RB_2 sense the channel at the same time and find out that it is free, and then they both return CTS back to WT_A. As a result, two CTSs collide and both are lost. And after the CTS_timeout has expired, WT_A goes into backoff and waits for the next available time for retransmission of the RTS frame. In other words, if the CTS frame is successfully received by WT_A, then the data frame will be sent after SIFS time. The same approach will be followed when RBs receive the data frame and return ACK frame after SIFS. Figure 3.3 shows the timing relationship for the system.

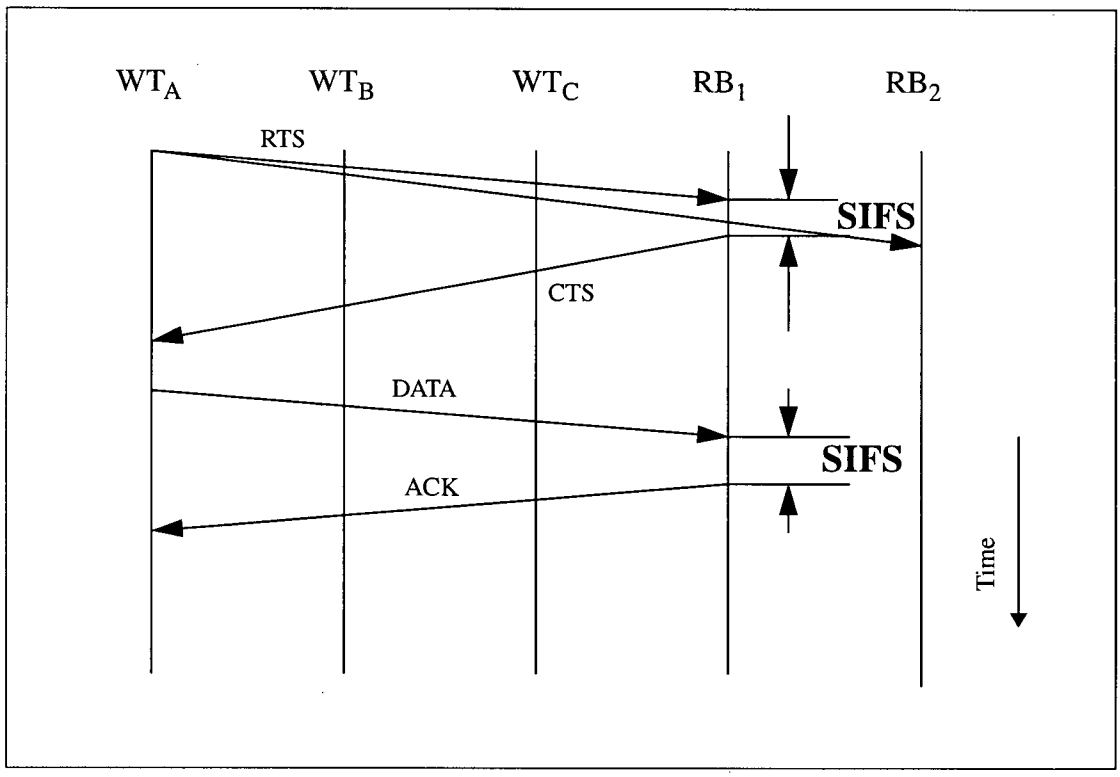

Figure 3.3 The Time-line diagram of the example.

3.2.2 The Advantages and Disadvantages of the proposed WLAN using IEEE 802.11 MAC protocol

The distributed WLAN uses the same radio channel over the entire coverage area. This can eliminate the need for frequency coordination, and can avoid the complicated handoff mechanism. Each WT does not depend only on one particular RB. If a RB fails to work properly, the whole network can still operate without that RB, since each WT needs not access a fixed AP (RB). Besides, when fading occurs, the packets may not reach the destination, if there is only one RB that the WT can communicate with. Multiple RBs can enhance the chances of successful packet reception. However, the disadvantage is that the packet waiting time of a WT is longer because more WTs trying to access the same channel. In other words, a station has a packet to transmit must wait until the channel is free, and therefore, the access delay is high. Moreover,

when the multiple RBs receive a data frame, they will either all return ACKs frames or one of them returns ACK frame, and that will delay the next data packet transmission.

From the example shown in Figure 3.2, a relatively high system throughput can be achieved since multiple receptions can guarantee at least one packet to be successful received by the destination station. When the RTS/CTS exchange is successful, the channel is reserved for both the source station and the destination station, and the data packet has a very high probability to be received correctly.

3.3 Design of the Simulation Model

Simulation plays an important role in the performance evaluation of MAC protocols. In the simulation environment, different models are used to represent real-life situations. However, certain assumptions need to be made to reduce the amount of computations. In this section, a simulation model of the proposed network using OPNET will be presented. Then, the design of the IEEE 802.11 MAC state machines will be described.

3.3.1 The OPNET Simulation Environment

OPNET is a comprehensive engineering tool supporting the modeling of communication networks and distributed systems. The OPNET environment can be used for analyzing the behavior and performance of the modeled systems by a simulation study, including model design, simulation, data collection, and data analysis. There are four model-specification editors, called network, node, process, and parameter. The network editor depends on elements specified in the node editor, and the process editor defines the models in the nodes. The parameter editor is used to define parameter models, such as packet format, antenna pattern and so on.

3.3.2 The Node Model

Figure 3.4 shows the node model for the station (WT) in the simulator. In the node model, there are a packet generator, a sink, a MAC queueing processor, a radio transmitter and a radio receiver. The solid lines interconnect each block representing the packet streams and the dash lines represent the statistic information streams. Individual data frames are generated by the packet generator according to the Poisson random process with exponential interarrival times. Each station has its own packet generator which is statistically independent of others. When the packet is generated, it is passed to the MAC processor and then follows the MAC protocol to be sent out via the transmitter attached to the MAC processor. The receiver uses carrier sensing to determine the state of channel. If the received signal power is above the carrier sensing threshold (CST), the receiver senses the channel busy. Otherwise, the channel is considered free. Moreover, the received signal power of a packet has to be above the receiver sensitivity (RS) in order to be received by the receiver. The sink receives valid data frame from the MAC and then with the statistics from the data frame calculates the throughput and delay.

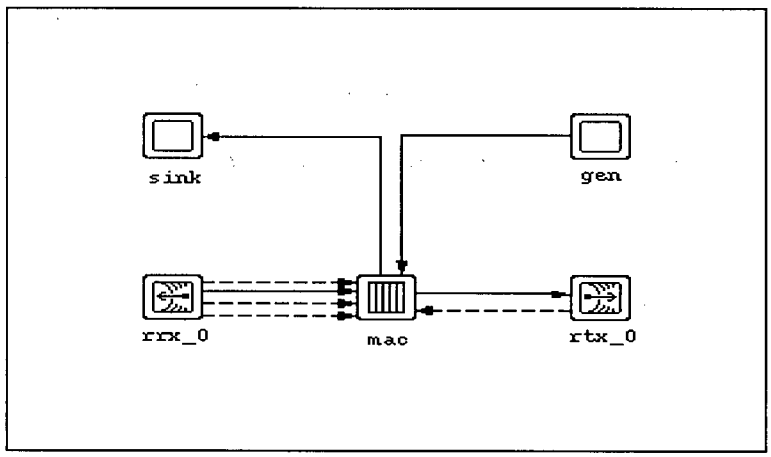

Figure 3.4 The node model for the WT.

3.4 The Channel Models

This section describes the channel models used in the simulation. Indoor radio propagation is dominated by the same mechanisms as outdoor: reflection, diffraction, and scattering [28]. In general, indoor channels may be classified either as line-of-sight (LOS) or Obstructed (OBS), with varying degrees of clutter. Due to multiple reflections from various objects, the electromagnetic waves travel along different paths of varying lengths, and the strengths of the waves decrease as the distance between the transmitter and receiver increases. Propagation models predict the average received signal strength at a given distance from the transmitter.

3.4.1 Path Loss Model

The average received signal power decreases with some power of distance. The average large-scale path loss for an arbitrary transmitter-receiver separation is expressed as a function of distance by using a path loss exponent, γ.

$$PL(dB) = PL(d_0) + 10\gamma\log\left(\frac{d}{d_0}\right) \tag{3.1}$$

$$PL(d_0) = -10\log\left[\frac{\lambda^2}{(4\pi)^2 d_0^2}\right] \tag{3.2}$$

where γ indicates the rate increases with distance, d_0 is the reference distance determined from measurements close to the transmitter, d is the distance between the transmitter and the receiver, and λ is the wavelength in meters. The reference distance is chosen as 1 meter and the path loss exponent, γ is 3 [28]. The received signal power is:

$$P_r(dBm) = P_t(dBm) + G_t(dB) + G_r(dB) - PL(dB) \tag{3.3}$$

where P_r is the received power, which is a function of the transmitter and receiver separation, P_t is the transmitted power, G_t is the transmitter antenna gain, and G_r is the receiver antenna gain.

3.4.2 Rayleigh Fading

In addition to the path loss model, in a mobile radio environment, the short-term fluctuations caused by multipath propagation is called small-scale fading. Small-scale fading is caused by wave interference when two or more multipath components arrive at the receiver over a short period of time. It is generally classified as either flat or frequency selective. If the mobile radio channel has a constant gain and a linear phase response over a bandwidth that is greater than that of the transmitted signal, then the received signal will undergo flat fading. The most common amplitude distribution of the instantaneous gain of flat fading channels is the Rayleigh distribution. The Rayleigh flat fading channel model assumes that the channel induces an amplitude which varies in time according to the Rayleigh distribution. The Rayleigh distribution has a probability density function (pdf) given by:

$$p(r) = \begin{cases} \dfrac{r}{\sigma^2}\exp\left(-\dfrac{r^2}{2\sigma^2}\right) & (0 \le r \le \infty) \\ 0 & (r < 0) \end{cases} \tag{3.4}$$

where $2\sigma^2$ is the average power of the received signal before envelope detection. The probability that the envelope of the received signal does not exceed a specified value R is given by the corresponding cumulative distribution function (CDF):

$$P(R) = Pr(r \le R) = \int_0^R p(r)dr = 1 - \exp\left(-\frac{R^2}{2\sigma^2}\right) \tag{3.5}$$

In simulation, an exponential distributions generator is used to generate a series of numeric values with mean received power for each packet received. In Figure 3.5, the theoretical Rayleigh CDF is used to compare with the simulation results. The mean received power is 3.956 nW. The simulation results closely match the theoretical line.

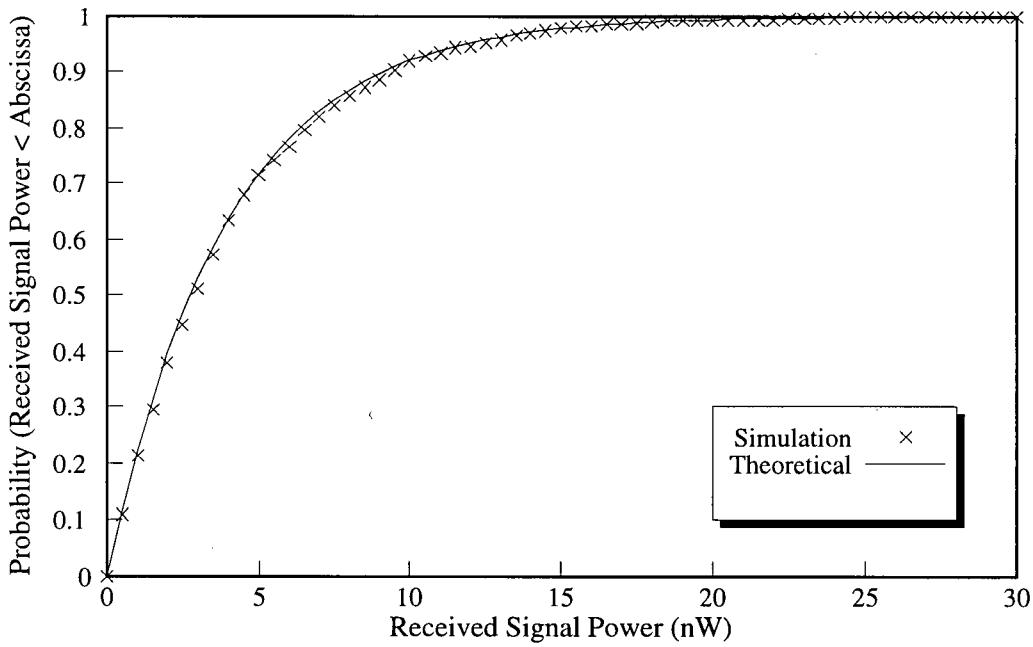

Figure 3.5 Rayleigh CDF vs. Simulation results.

3.4.3 Log-normal Shadowing

Log-normal shadowing is the random shadowing effects which occur over a large number of measurement locations which have the same transmitter-receiver separation, but have different levels of clutter on the propagation path. The shadowing effect will be the same throughout each

simulation, since all the stations (RBs and WTs) are assumed fixed. Besides, the shadowing effect between each transmitter and receiver pair is also fixed. With the effect of log-normal shadowing, the received power $P_{r,L}(dBm)$ will be:

$$P_{r,L}(dBm) = P_r(dBm) + L_\sigma(dB) \tag{3.6}$$

where L_σ is a zero-mean Gaussian distributed random variable (in dB) with standard deviation σ dB. L_σ is calculated for each transmitter and receiver pair before the simulation takes place. For indoor environment [28], a value of 6 dB is used for σ.

3.5 Station Location

All the WTs and RBs are placed along a straight line. This simple one dimensional model can be used to represented a long corridor[26]. The WTs are placed 10.35 meters apart for 15 WTs and 5 meters for 30 WTs in the network. The RBs are evenly distributed throughout the network. Figure 3.6 shows the different arrangements for different numbers of RBs.

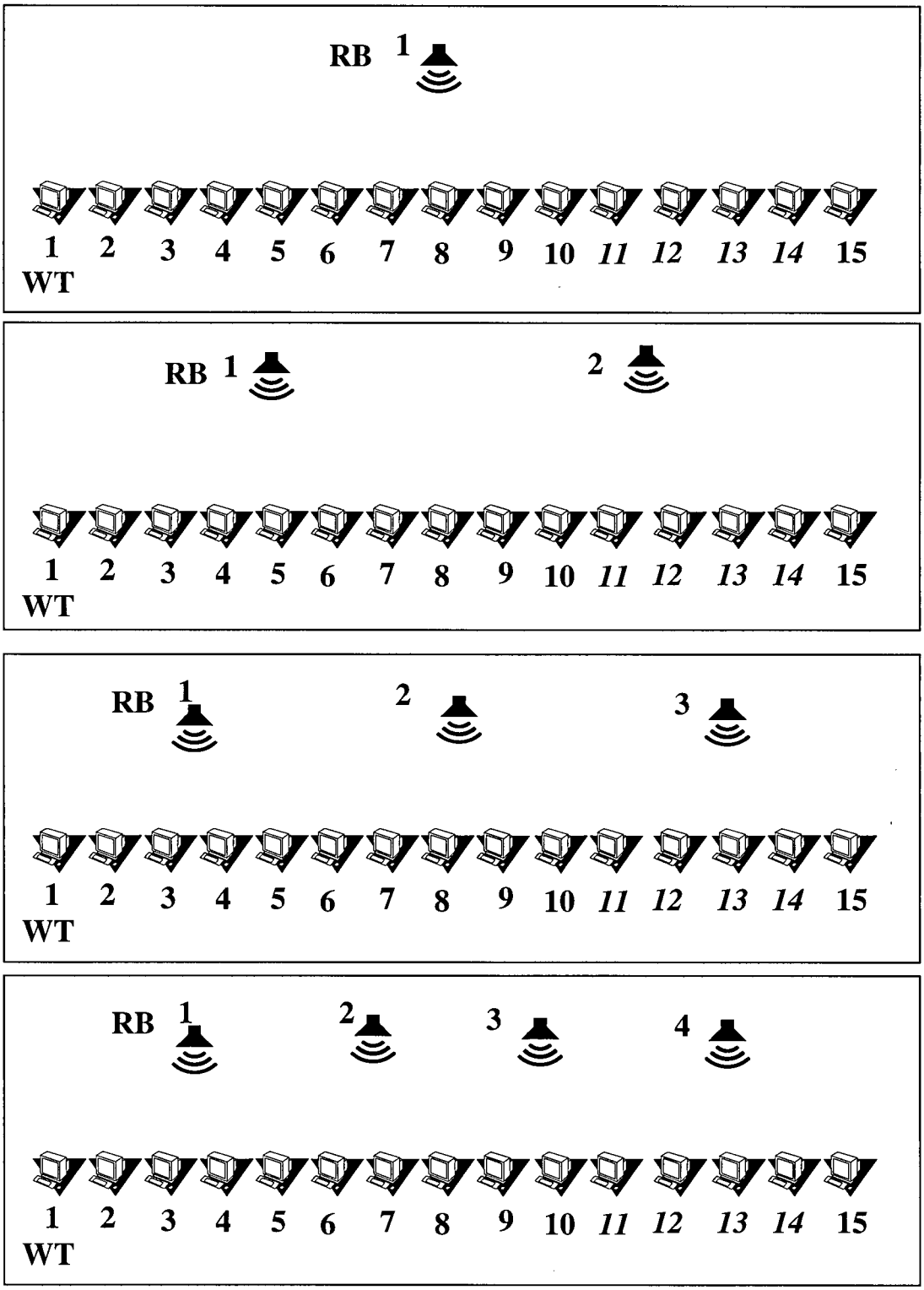

Figure 3.6 Four sets of network arrangement

3.6 Design of the IEEE 802.11 MAC Process

The process model of the MAC is the core of the simulator. The way to implement the 802.11 MAC protocol is to use a finite state machine which defines the transition conditions for changing states.

In order to avoid complicated implementation, some assumptions are made. The RBs and WTs are treated as individual stations, so that each WT can generate packets. Besides, only one channel is used for both uplink and downlink traffic. Therefore, a station cannot be transmitting and receiving at the same time. This type of transmission is referred as half-duplex. There are two different methods that the RBs will use to return ACKs. The first method is that only one of the RBs will return ACK upon successful packet reception. With this method, the ACK might be lost due to collision, fading or shadowing. Therefore, the second method is introduced. This method requires all the RBs which successfully receive the packets to return ACKs. The first RB will return ACK after the SIFS, and the second RB will return ACK after the SIFS plus the transmission time of the ACK, which is $28\mu s + 112\mu s$. This is because the RB does not sense the channel before sending the ACK. If two RBs return ACKs after SIFS, both ACKS will collide. The third RB will wait two times the transmission time of the ACK plus the SIFS and the fourth RB will wait three times the transmission time of the ACK plus the SIFS before sending the ACK. This can make sure that all the ACKs will not collide with each other. This method provides multiple ACKs. Thus, even though one of the ACKs is lost because of fading or shadowing, the additional ACK can still be received in order to prevent retransmission of the packet. When more than one frame is received at a station, all frames collide and are assumed to be lost without the capture effect. Since all the WTs might receive packets from more than one RBs at the same time, the

capture method described in 5.2 can improve the throughput of the system.

3.6.1 The Finite State Machine of the 802.11 MAC Protocol

There are nine states in the state machine and there is a function block written in C programming language providing additional functions for the entire process. The states and their transitions are described in Table 3.1 and Figure 3.7.

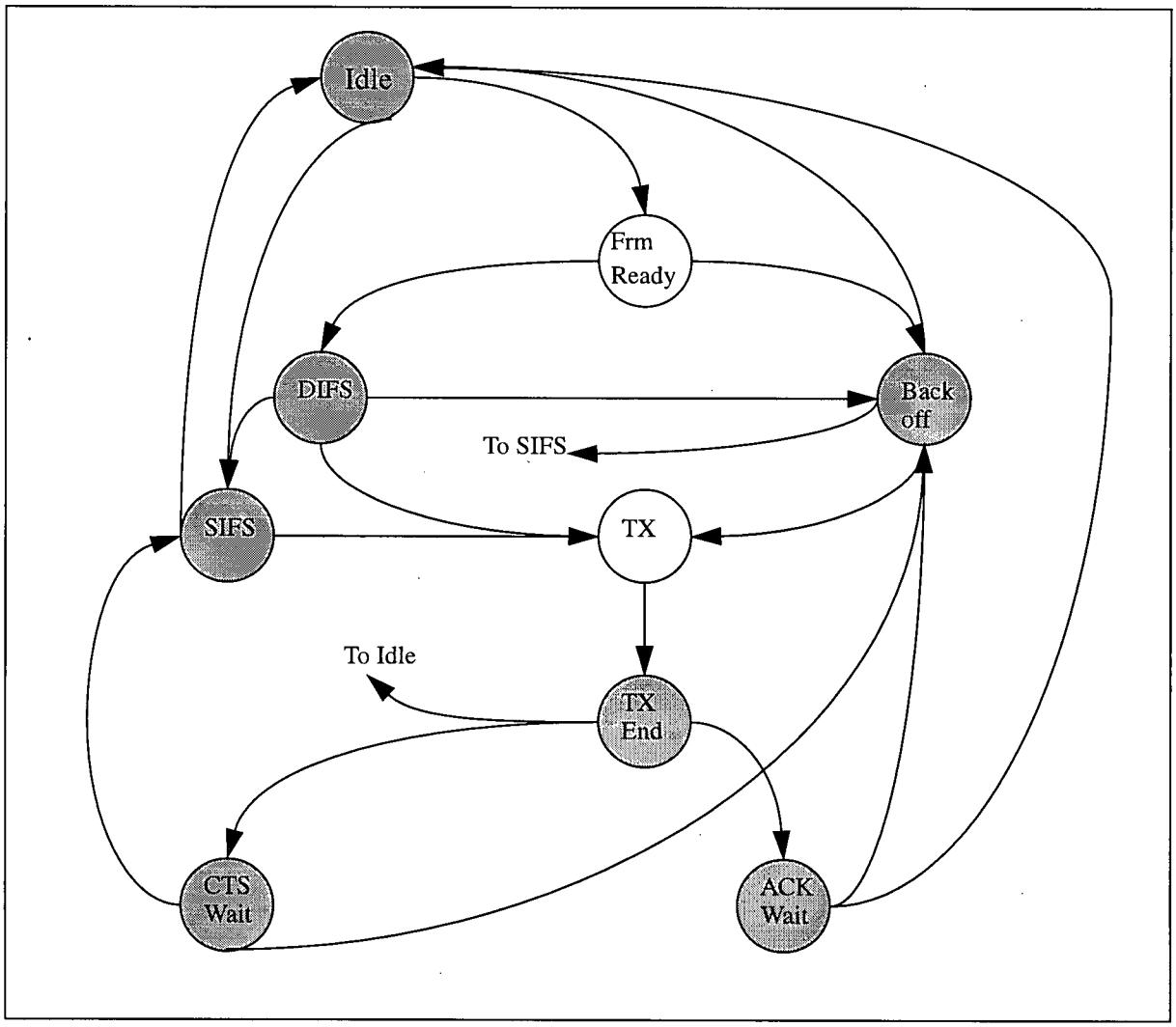

Figure 3.7 The state machine of the 802.11 MAC protocol.

In Figure 3.7, the grey circles indicate unforced states and all these states can receive packet from the upper layer (the generator) or from the lower layer (the radio receiver). The receiving functions are written in the function block. When a packet is received from the upper layer, it will be inserted into the transmit queue. When a packet is received from the lower layer, it will be tested and corresponding action will be initiated. In Table 3.1, all the conditions for transitions are described for all the states.

Table 3.1 Summary of all states and transitions of the 802.11 MAC protocol.

State	Next State	Transitions
Idle	Frm_ready	When a station is idle, no frame has been received from the generator or the radio receiver. If it receives a frame from the generator, it will go to the Frm_ready state.
	SIFS	When a station is idle, a valid frame has been received and a replying frame has been prepared, it will go to the SIFS, and then wait for the SIFS times.
Frm_ready	DIFS	This transition occurs, when the station senses the channel and it is free.
	Backoff	This transition occurs when the station senses the channel and it is busy.
DIFS	Backoff	This transition occurs when the channel is free for less than DIFS time.
	Transmit	This transition occurs when the channel is free for DIFS time. A RTS or data frame is being sent to the radio transmitter.
	SIFS	When a valid frame has been received and a replying frame has been prepared. It will go to the SIFS, and then wait for the SIFS times.

State	Next State	Transitions
Backoff	Transmit	This transition occurs when the backoff timer has expired. A RTS or data frame is being sent to the radio transmitter.
	Idle	This transition occurs when the maximum number of retransmission is reached. The frame will be discarded.
	SIFS	This occurs, when a valid frame has been received and a replying frame has been prepared.
Transmit	Tx_end	This transition occurs when the packet has been sent to the radio transmitter.
Tx_end	ACK_wait	This transition occurs after a station has transmitted a data frame and is waiting for an ACK frame.
	CTS_wait	This transition occurs after a station has transmitted a RTS frame and is waiting for a CTS frame.
	Idle	This transition occurs after a station has transmitted a CTS or an ACK frame.
ACK_wait	Backoff	This transition occurs when an ACK frame is not received in time, or an ACK frame has been received within the time required but a frame is waiting in the queue.
	Idle	This transition occurs after a station has received an ACK frame within the time required, and no other frame is waiting or in the queue.
CTS_wait	SIFS	This transition occurs after a station has received a CTS frame. Then, the data frame will be sent after the SIFS time interval.
	Backoff	This transition occurs when a CTS frame is not received in time.
SIFS	Transmit	This transition occurs when a station has waited for SIFS time interval. According to the specification, carrier sensing is done only when a CTS frame will be sent.
	Idle	This transition occurs when a station senses the channel before sending a CTS frame and the channel is busy, and then the CTS frame will be discarded.

3.6.2 The Simulation Parameters

The simulation parameters can be set during the model specification. This is done via the OPNET Editors. The other method is to promote the attributes to the top level of the system model and then they will be specified at the start of the system's simulation. The first method is appropriate for those parameters that are constant during the simulation run, and the second method is used when the values need to be changed for each simulation run. Table 3.2 lists the simulation parameters.

Table 3.2 The simulation parameters.

Parameter	Description	Default
ShortRetryLimit	Maximum number of transmission attempts of a frame, the length of which is less than or equal to a RTSThreshold.	7
LongRetryLimit	Maximum number of transmission attempts of a frame, the length of which is greater than a RTSThreshold.	4
RTSThreshold	The number of Octets in an MPDU. An RTS/CTS handshake shall be performed for all frames where the length of the MPSU is greater than this threshold.	3000 bits (RTS/CTS not used in simulations unless specified.)
DIFS	Distributed Coordination Function Inter-frame Space.	128 μs
SIFS	Short In-frame Space.	28 μs
Slot_Time	Slot Time as defined in Equation (2.2).	50 μs
ACK_Timeout	The maximum waiting time for the ACK frame.	300 μs
CW_min	Minimum Contention Window.	15
CW_max	Maximum Contention Window.	1023
RTS_frm	RTS frame length.	160 bits
CTS_frm	CTS frame length.	112 bits
ACK_frm	ACK frame length.	112 bits
DATA_frm (N)	DATA frame length.	8000 bits
QueueSize	Size of the FIFO Queue.	10 frames
Bit_rate	Data rate.	1 Mbit/s
Frequency	Carrier Frequency.	2.4 GHz
$P_t(T_x)$	Transmitter Power.	100 mW
RS	Receiver Sensitivity.	-85 dBm
CST	Carrier Sensing Threshold.	-85 dBm
c	Capture Ratio.	10 dB
γ	Path Loss Exponent.	3
σ	The Standard deviation of the log-normal shadowing.	6 dB
G_t	Transmitter antenna gain.	0 dB
G_r	Receiver antenna gain.	0 dB

3.6.3 Data Collection

The objective of most modeling efforts is to obtain measures of a system's performance or to make observations concerning a system's behavior. Both scalar and vector statistics can be computed and recorded automatically for a set of predefined statistics. Predefined statistics in OPNET are related to values that can be measured at specific objects within the model. Custom statistics can be declared by process models and OPNET provides support for both local statistics, which are maintained separately for each processor or queue, and global statistics, which are shared and contributed to by many entities in the model, such as the performance of the system. The following Table 3.3 summarizes the statistics generated by the MAC process model. Moreover, OPNET provides a large number of built-in local statistics, such as transmission delay, propagation delay, received power, signal to noise ratio and bit error rate.

Table 3.3 The Statistics collected by the process.

Type	Name
Local	Actual Load (bits)
	Actual Load (bits/sec)
	Actual Load (data packets)
	Actual Load (data packets/sec)
	Number of Collisions
	Access Delay (sec)
	Throughput (bits)
	Throughput (bits/sec)
	Throughput (data packets)
	Throughput (data packets/sec)
	Queueing Delay (sec)
Global	Actual Load (bits)
	Actual Load (bits/sec)
	Actual Load (data packets)
	Actual Load (data packets/sec)
	Number of Collisions
	Access Delay (sec)
	Throughput (bits)
	Throughput (bits/sec)
	Throughput (data packets)
	Throughput (data packets/sec)
	Queueing Delay (sec)

Chapter 4 Simulation Results and Discussion - Part 1

In this chapter, the performance of the proposed distributed WLANs using IEEE 802.11 MAC protocol in different channel environments will be studied by computer simulation. No capture is assumed in this chapter. First, the parameters and the assumptions used in the simulation are described and then a model verification is provided. The simulation results obtained in additive white Gaussian noise (AWGN), Rayleigh fading and log-normal shadowing channels will be presented and discussed. The effects of various parameters, such as number of WTs, number of RBs, n, transmitted power levels, T_x, and standard deviation, σ, of the log-normal shadowing will be examined. For all the simulation results, a 95% confidence interval within $\pm 5\,\%$ of the average values is shown and the worst case is within $\pm 10\,\%$.

4.1 Simulation Descriptions

4.1.1 Performance Measurement

The performance is measured in terms of normalized throughput, η, and the access delay, τ, versus the normalized offered load, ρ. The ρ is defined as the average number of bits per second generated at the source stations (WTs) and normalized by data rate. The η is defined as the average number of bits per second successfully received by the destination (RBs), and normalized by the data rate. The τ is calculated when the (potential) packet is dequeued at the WT until the first bit of the packet is successfully received at the RBs.

4.1.2 Network Arrangement

A linear (one-dimensional) network arrangement with a length of 145 meters is assumed

in the simulation. There are two different network sizes, with 15 WTs and 30 WTs. The WTs are evenly placed in the system. The number of RB, n, used in the network is from one to 4. Two different methods (A and B) will be used for the RBs to return the ACK. Method A is that only one of the RBs which successfully receives the data packets will return the ACK (in the figure legend, it is noted as n RBs). Method B is that all the RBs that successfully receive data packets return ACK frames (in the figure legend, it is noted as n RBs (all)). For the simulation in this and Chapter 5, the default T_x for the WTs/RBs is set to be 100 mW and the default value of the σ for log-normal shadowing is 6 dB.

4.1.3 Error-Free Channels

The bit-error rate (BER) is obtained as a function of signal-to-noise power ratio. The signal power is computed based on path loss equations (3.1), (3.2) and (3.3) in Chapter 3. The receiver noise floor is obtained based on the ambient noise temperature at the receiver antenna and noise figure, F. The effective noise temperature, T_e is calculated as

$$T_e = (F-1)T_0 \tag{4.1}$$

where T_0 is ambient room temperature (290 K to 300 K). In the simulation, the values of F and T_e used are 1.07 (0.3 dB) and 20° C. The receiver noise floor P_n, is given by

$$P_n = k(T_e + T_b)BW \tag{4.2}$$

where k is Boltzmann's constant given by 1.38×10^{-23} Joules/Kelvin, T_b is the effective background temperature, 290 K, and BW is the equivalent bandwidth of the receiver, 1000 kHz.

Thus, the receiver noise floor is -113.7 dBm. Since the RS is -85 dBm, i.e., the minimum signal-to-noise ratio (SNR) is 28.7 dB, there is no packets error at the RBs or WTs.

4.2 Simulation Model Validation

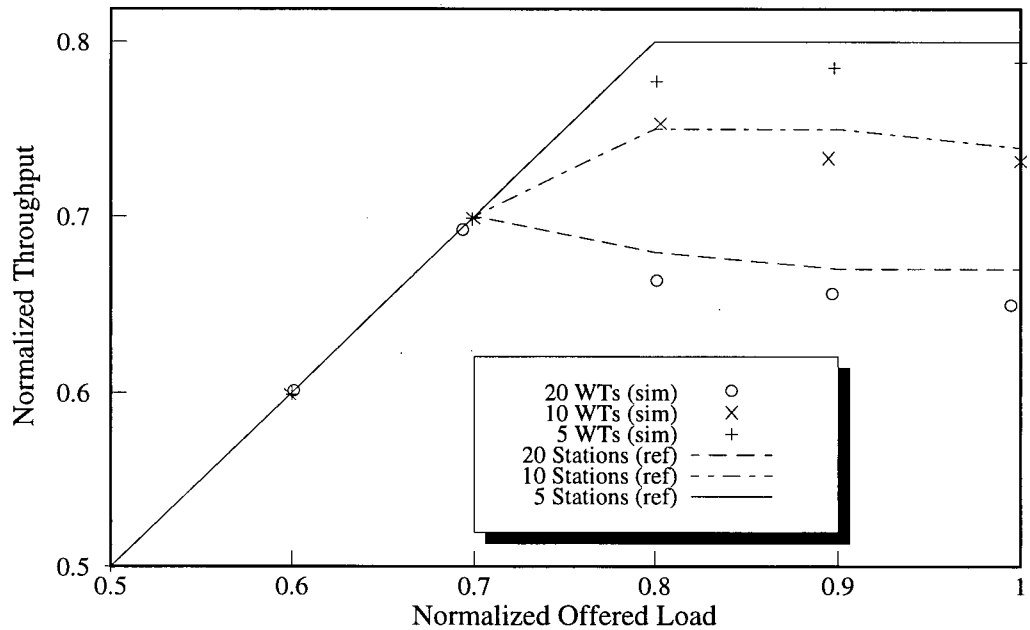

Figure 4.1 Normalized throughput versus normalized offered load for 5, 10 and 20 stations with CWmin = 32 and CWmax = 256 for adhoc and infrastructure networks.

The throughput performance and access delay obtain from the ideal channel (no fading or no transmission error) model are used to compared with those in [13]. The results from [13] are obtained from an adhoc network, in which all the stations can communicate with each other such that any station can be a destination. In the (infrastructure) model, all the stations send packets to an AP as destination. Figure 4.1 shows the throughput for 5, 10 and 20 stations with CWmin = 32 and CWmax = 256. It can be seen that the throughput of the infrastructure model is slightly lower than that in [13] for $\rho > 0.7$. In the infrastructure model, there is an extra AP which is not in

adhoc model. Since the AP sends the ACK to the stations, the amount of contention is increased and the performance is degraded slightly. Figure 4.2 shows the access delay for different values of CWmin and CWmax with 5 stations. It can be seen that the results are close to those in [13].

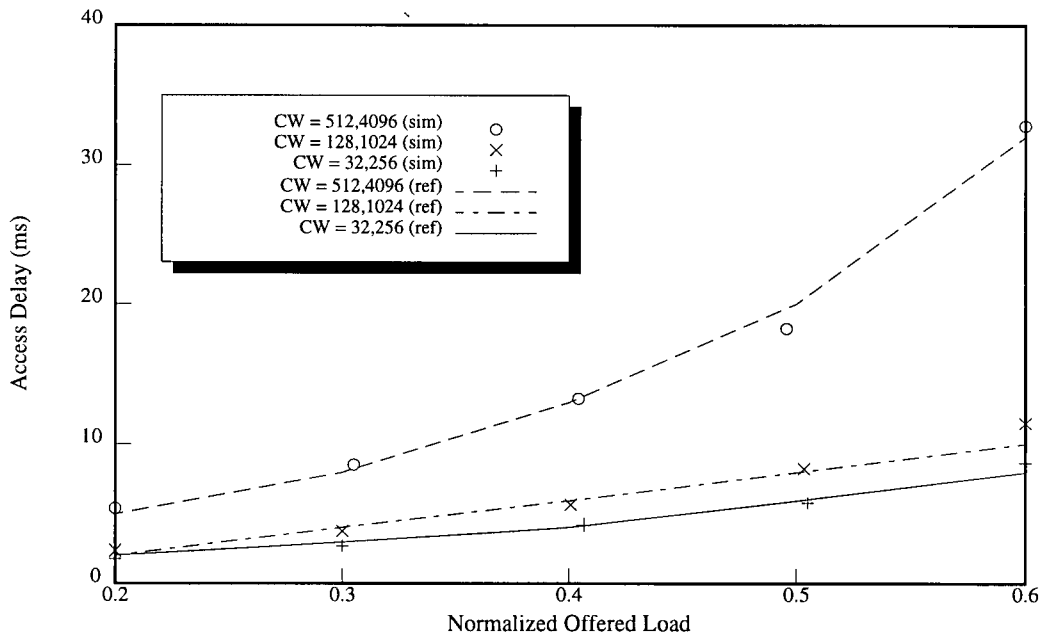

Figure 4.2 Access delay versus normalized offered load with different values of CW(min/max) for 5 stations for adhoc and infrastructure networks.

4.3 AWGN Channel

The T_x of the WTs/RBs is set to be 100 mW so that the received power of the packets at the WTs/RBs is above the CST/RS. Thus, all the packets can be received[1] at the RBs or sensed at the WTs. Since the channel is assumed to be error-free, all the received packets at the RBs contain no error. Therefore, the packets are discarded only when multiple packets collide at the RB(s). Since the received power of the packets at the WTs is always above the CST, the WTs are able to

[1] A packet is assumed to be received at the RB if the received power of that packet is above the RS.

sense the channel status correctly in order to avoid the occurrence of hidden terminals in the network. Thus, the probability of more than one WTs sending packets within a short period of time is very low due to the use of carrier sensing.

4.3.1 Simulation Results

In this section, the simulation results in AWGN channel are presented. The normalized throughput for 15 WTs using Method A and B are shown in Figure 4.3(a) and (b) respectively. In Figure 4.3(a), the saturated throughput, *S,* is quite high, about 0.9, because the probability of collision is very low. For $\rho < 0.9$ the throughput increases linearly with ρ since there is no packets lost due to collision. For $\rho > 0.9$, the probability of more than one WTs sending the packets increases and thus η is kept at about 0.9. The reason why η is below one is because some channel time is used for returning ACKs, for DIFS and for SIFS. It can be seen that η is independent of n. Because all the packets sent from the WTs can be received by one RB. Hence, adding more RBs does not increase the chance of receiving more packets. In Figure 4.3(b), η decreases with n. In Method B, the potential packets at the WTs cannot be sent until all the ACKs returned from the RBs have been transmitted, because the channel is sensed as busy by other WTs when the RBs are transmitting the ACKs, thus, the multiple ACK frames increase the waiting time for the WTs to send their potential packets and the number of packets transmitted from the WTs is decreased. Similar observation can be obtained in Figure 4.4 for 30 WTs. The η for 15 and 30 WTs are about the same.

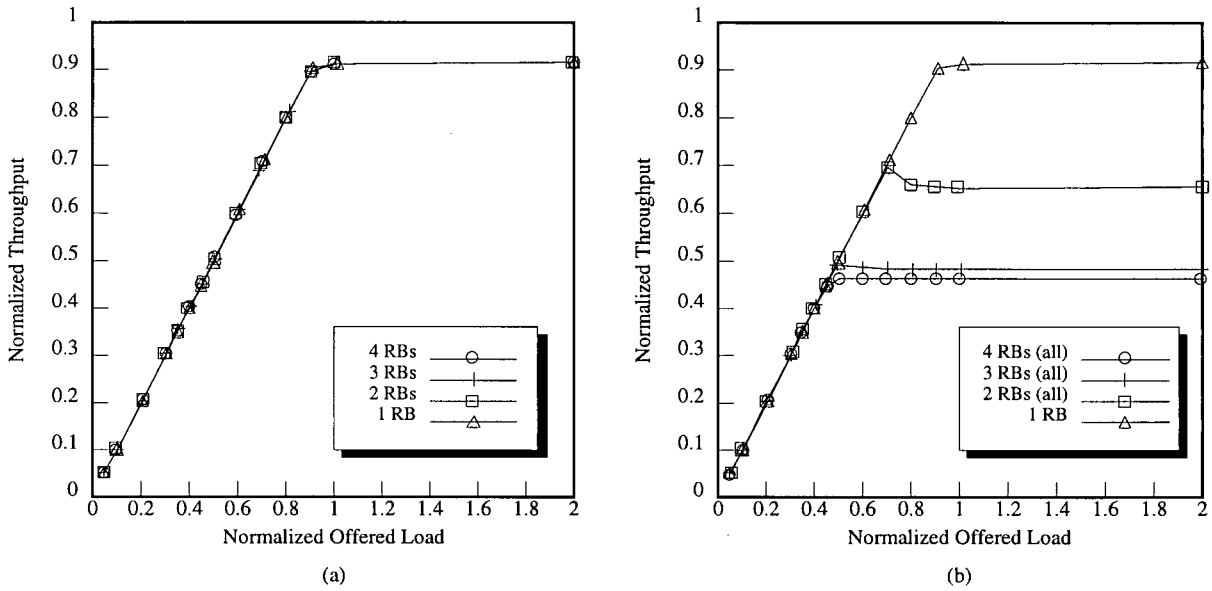

Figure 4.3 Normalized throughput versus normalized offered load for 15 WTs in AWGN channel using (a) Method A and (b) Method B.

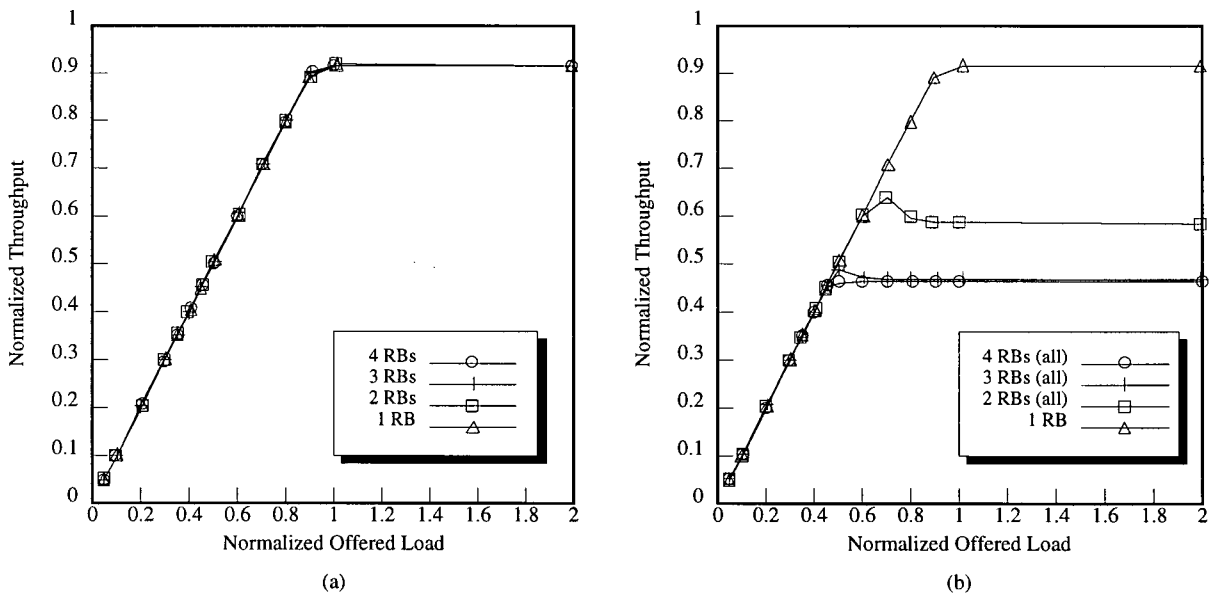

Figure 4.4 Normalized throughput versus normalized offered load for 30 WTs in AWGN channel using (a) Method A and (b) Method B.

The access delay for 15 WTs using Method A and B are shown in Figure 4.5(a) and (b) respectively. In Figure 4.5(a), the access delay is the same for any n. Because only one of the RBs returns ACK, it does not increase the waiting time of sending the potential packets at the WT. Since the ACK is always received correctly at the desired WT, the packets are not required to retransmit. In Figure 4.5(b), the access delay increases with n due to the additional ACK returned to increase the waiting time. The access delay for 30 WTs using Method A and B are also shown in Figure 4.6(a) and (b) respectively. Although η for 15 and 30 WTs are about the same, the access delay for 30 WTs is much longer than that for 15 WTs. This is because more WTs are sending packets in the network and thus the waiting time for sending a packet becomes longer.

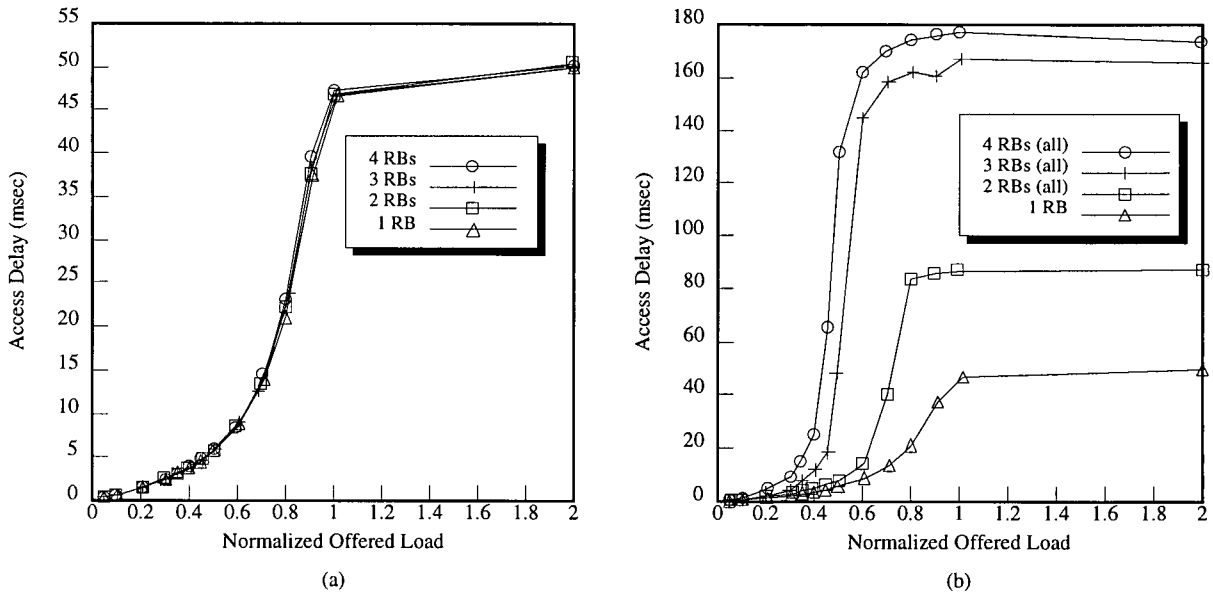

Figure 4.5 Access delay versus normalized offered load for 15 WTs in AWGN channel using (a) Method A and (b) Method B.

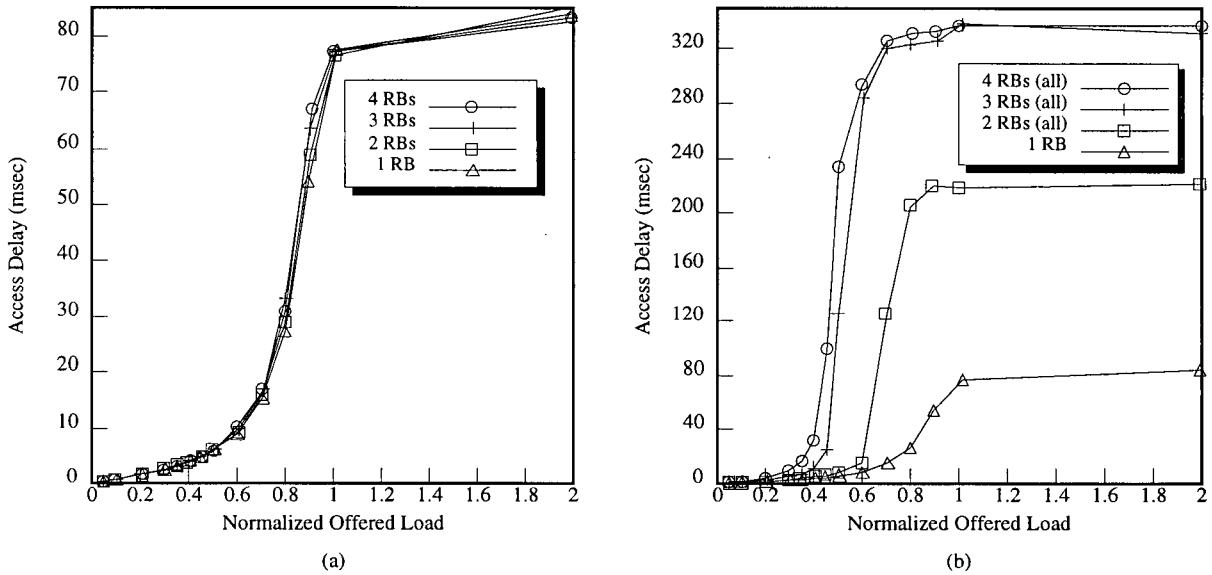

Figure 4.6 Access delay versus normalized offered load for 30 WTs in AWGN channel using (a) Method A and (b) Method B.

4.4 Rayleigh Fading Channel

In addition to the receiver noise floor and the path loss in AWGN channel, we assume a very slow Rayleigh fading channel in this section. Thus, the signal strength is assumed to be constant over a packet. If the packet sent from WT_A arrives at WT_B and its received power is below the CST due to fading effect, WT_B cannot correctly sense the channel status as a busy channel. Then, WT_A is hidden from WT_B. So, a collision might occur if WT_B sends a packet. In Rayleigh fading channel, a packet will not be received when its received power at the RB is below RS, and it will be discarded if it collides with other packets at the RB.

4.4.1 Simulation Results

The throughput curves for 15 WTs using Method A and B in a Rayleigh fading channel are shown in Figure 4.7(a) and (b), respectively. Compared to results for the AWGN channel in

Figure 4.3 where no hidden terminal is assumed, the saturated throughput, S, in a Rayleigh fading channel is much lower. With no hidden terminal, the WTs can sense the channel status (idle or busy) accurately in order to avoid collision. However, in a Rayleigh fading channel, there is a possibility of some terminals hidden from the WTs so that the WTs cannot sense the channel busy when transmitting their packets. Thus, it increases the chance of collisions and degrades the performance. In a Rayleigh fading channel, a packet may not be received by the RB if the packet is faded[2] and its received power is below RS. By using more RBs, the probability of the packet being faded, at all the RBs is decreased. Thus, it can increase the chance of a packet to be received by, at least, one of the RBs in order to increase the throughput. It can be seen that S increases with n. In Figure 4.7(a), S for 2 RBs is increased by 18% compared to that for one RB. For 4 RBs, S can be increased by 38%. In Figure 4.7(b), the performance is not increased by much as n increases. The S for 2 and 4 RBs is increased by 14% and 21% respectively compared to that for one RB. With 3 or 4 RBs, S with Method B is lower than that with Method A. In Method A, a single ACK is returned from one of the RBs even though 2 or more RBs may receive the packet. If the ACK is faded at the desired WT, the packet needs to be retransmitted. The fundamental idea of multiple ACKs in Method B is to increase the chance of ACK reception at the WTs in order to avoid the retransmission of the packets. However, the probability of an ACK being faded at the desired WT is not high. In other words, the desired WT can always receive one of the first two ACKs. Because if a packet sent from the WT can be received (not faded) at the RB, then the ACK sent from that RB can also be received (not faded) at the desired WT with a fairly high probability. Therefore, more ACKs sent from the RBs may not be necessary. Even though more RBs can increase the chance of packets reception, in Method B, the waiting time of the WTs to send their

---

[2] A packet is assumed to be faded at a WT (RB) if the received power of that packet at the WT (RB) is below the CST (RS).

potential packets is increased due to multiple ACKs. Therefore, more RBs or multiple ACKs increases the waiting time of the potential packet to be sent and the throughput decreases with n in Method B. In Figure 4.8(a), the access delay for 15 WTs using Method A decreases with n. The τ for 2, 3 and 4 RBs can be reduced by about 10%, 20% and 30% respectively compared to one RB. This is because the throughput increases with n as shown in Figure 4.7(a). However, τ in Method B does not decrease very much as n increases as shown in Figure 4.8(b). The τ for 4 RBs is only reduced by 10% compared to one RB. Because the WTs cannot send their potential packets until all the RBs have returned their ACKs which increase the waiting time (access delay) for the WTs to send packets.

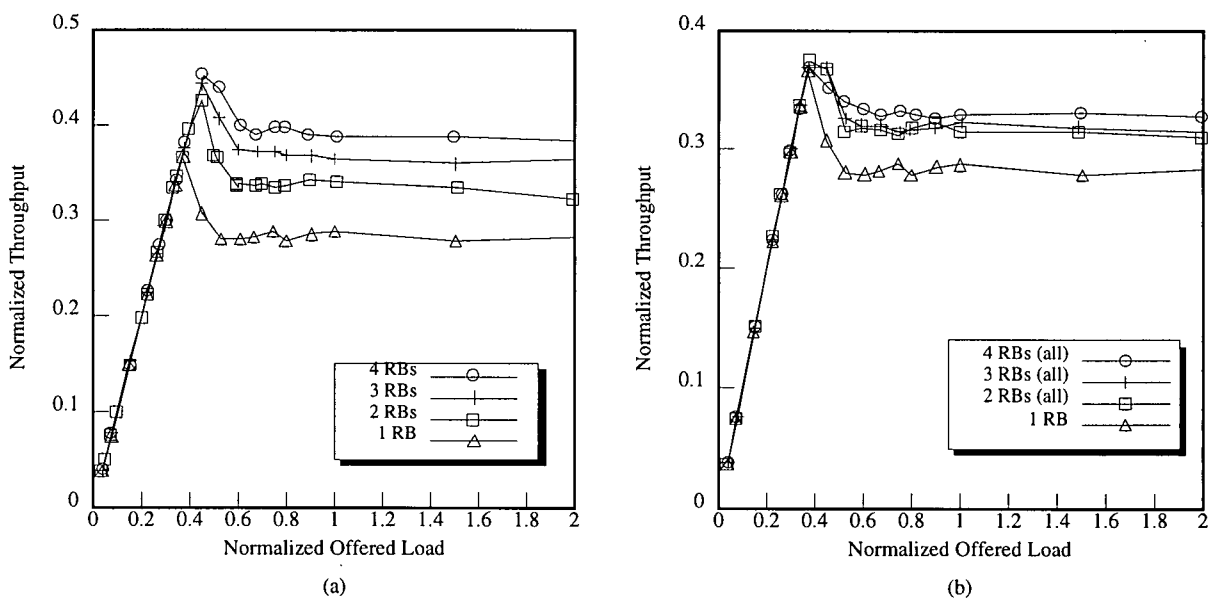

Figure 4.7 Normalized throughput versus normalized offered load for 15 WTs in Rayleigh fading channel using (a) Method A and (b) Method B.

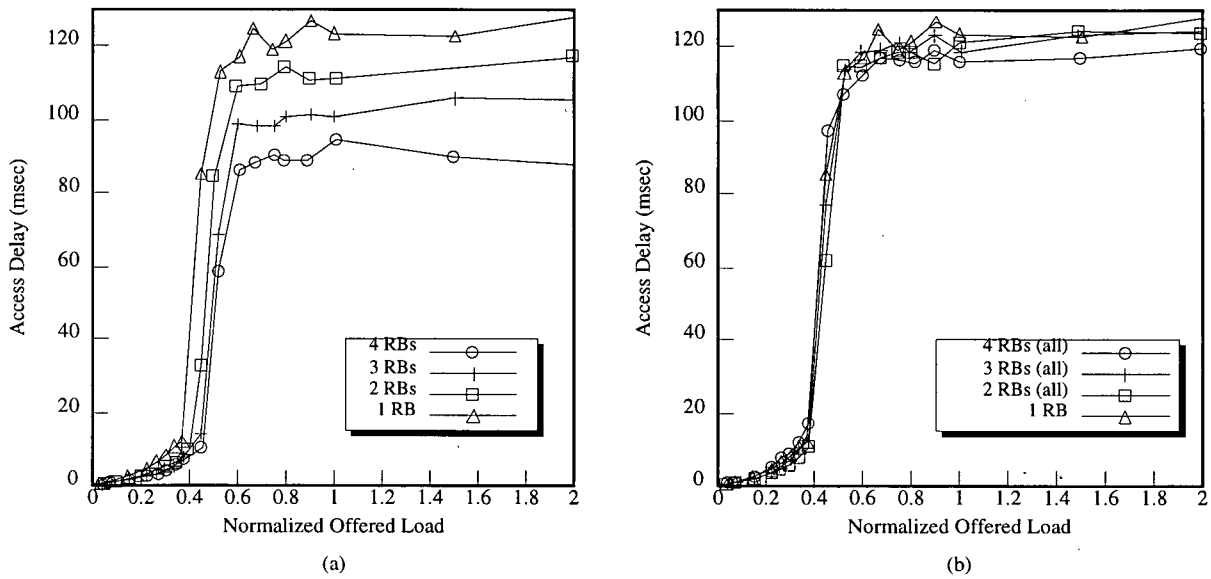

Figure 4.8 Access delay versus normalized offered load for 15 WTs in Rayleigh fading channel using (a) Method A and (b) Method B.

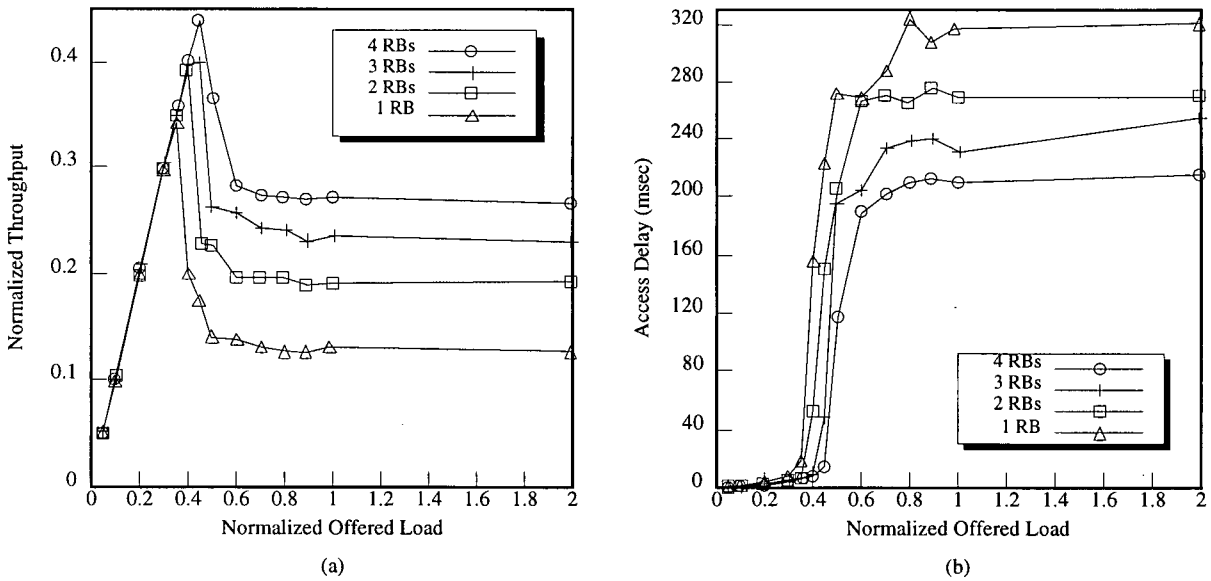

Figure 4.9 (a) Normalized throughput and (b) access delay versus normalized offered load for 30 WTs in Rayleigh fading channel using Method A.

The normalized throughput and access delay for 30 WTs using Method A are depicted in Figure 4.9(a) and (b) respectively. It shows that for the same number of RB, η and τ for 30 WTs are worse than those for 15 WTs. This is because there are more hidden terminals and hence collisions occur more frequently. With one RB, S for 30 WTs is about 50% less than that for 15 WTs. With 4 RBs, S for 30 WTs is about 35% less than that for 15 WTs. It can be seen that S for 2, 3 or 4 RBs can be increased by about 50, 85 and 110% respectively compared to one RB. The performance improvement for 30 WTs is greater than that for 15WTs. Therefore, adding more RBs is more efficient for a system with a large number of WTs. In Figure 4.9(b), τ for 2, 3 and 4 RBs can be decreased by 14%, 28% and 38%, respectively. In the Rayleigh fading channel, for one RB, τ with 30 WTs is about 2.5 times longer than that with 15 WTs. In contrast, over the AWGN channel, τ with 30 WTs is about 60% longer than that with 15 WTs.

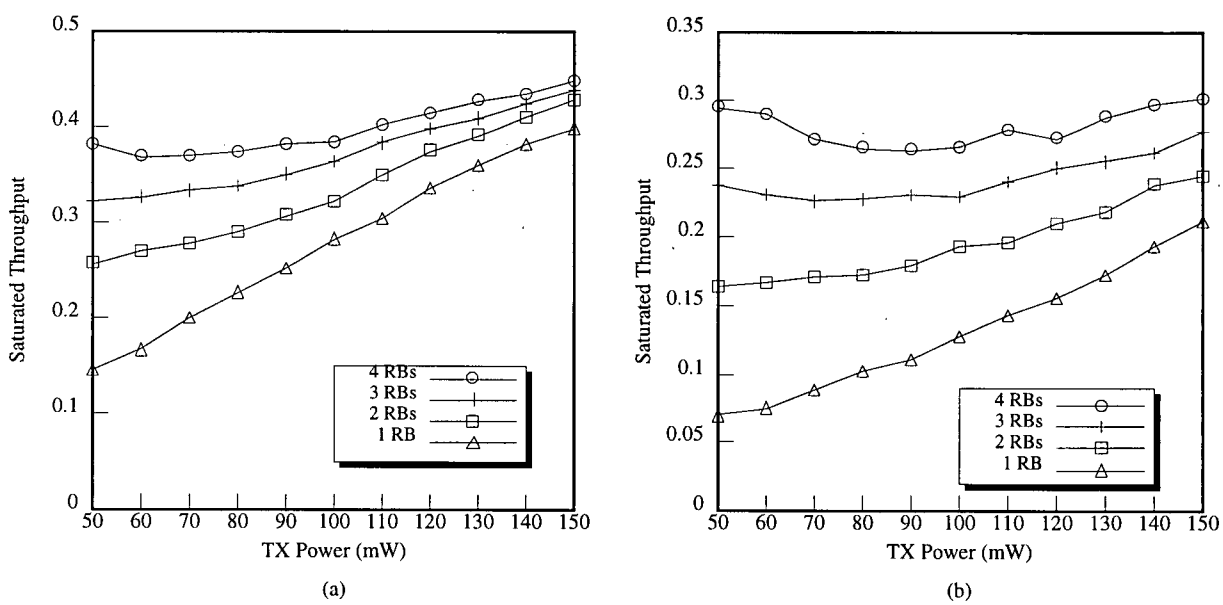

Figure 4.10 Saturated throughput versus transmitted power in Rayleigh fading channel using Method A for (a) 15 WTs and (b) 30 WTs.

The saturated throughput with 15 WTs and 30 WTs using Method A for transmitted power from 50 mW to 150mW are shown in Figure 4.10(a) and (b). It can be seen that S increases with T_x. For one RB at low T_x, the probability of packets being faded (not received) at the RB is high, especially for the packets sent from the WTs further away from the RB. Thus, the RB might not be able to cover all the WTs as shown in Figure 4.11.

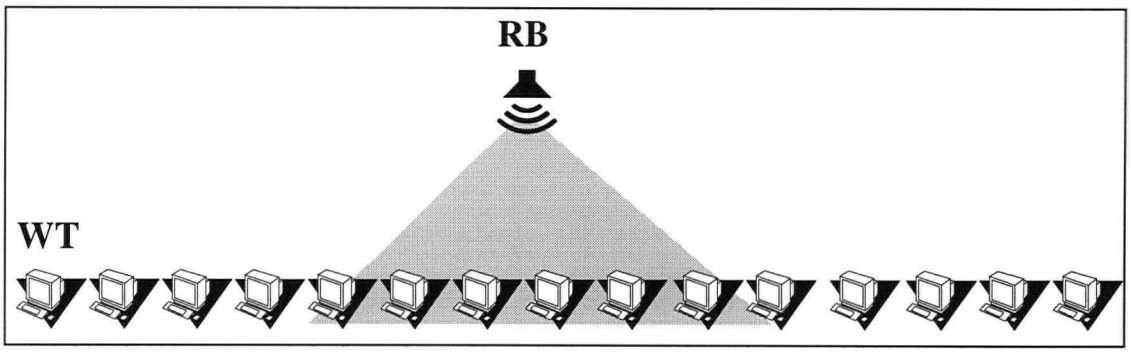

Figure 4.11 The coverage area of one RB for 15 WTs at low T_x.

The WTs beyond the coverage area[3] means that the probability of packets sent from those WTs being received at the RB is quite low due to fading. In addition, the number of hidden terminals for the WTs is also very high because the probability of packets being faded (below CST) at the WTs is high for low T_x. It increases collisions and reduces the chance of packet reception at RB. Therefore, S is quite low at low T_x. As T_x increases, the coverage area increases and the number of hidden terminals is reduced. Thus, more packets can be received at the RB. In Figure 4.10, it can be seen that S increases with n because the chance of a packet being received by RBs increases with n. However, the rate of performance increases as a function of T_x decreases

[3] The coverage area means that there is a high probability of packet reception at the RB if the WTs are located within the coverage area of the RB.

with n because increasing T_x does not increase the packet reception probability by much for high n, i.e., $n = 4$. This is because all the WTs can be covered by at least one RB as shown in Figure 4.12.

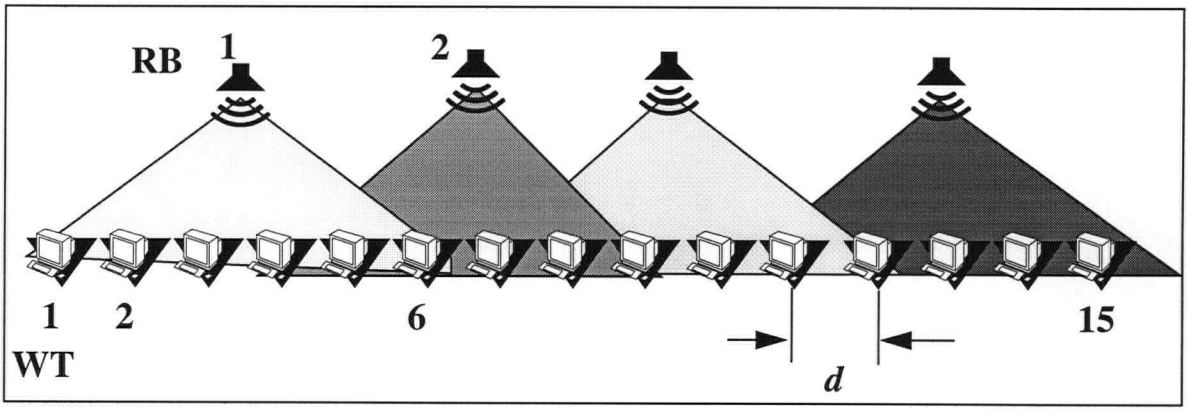

Figure 4.12 The coverage area for the 4 RBs with 15 WTS at low T_x.

The relative performance improvement for using more RBs with 30 WTs is greater than that with 15 WTs for all the evaluation range. However, the actual performance of 30 WTs is still worse than that of 15 WTs due to frequent collisions and longer waiting time for the potential packet transmission. In both figures, the performance improvement for using more RBs compared to one RB decreases as T_x increases. In Figure 4.10(a), S of one, 2, 3 and 4 RBs are very close together. This is because as T_x increases, more WTs can be covered by the RBs and the number of hidden terminals decreases. Eventually, for a very high T_x, the performance will be similar to that in AWGN channel in previous section in which the performance becomes the same for any n.

Figure 4.13 shows the access delay with different T_x for 15 and 30 WTs. The τ decreases with T_x and the decreasing rate decreases with n. The reasons are the same as the observation for S in Figure 4.10. The τ for 30 WTs is longer than that for 15 WTs because of more collisions due to

more hidden terminals and the waiting time of transmitting the potential packets at the WTs.

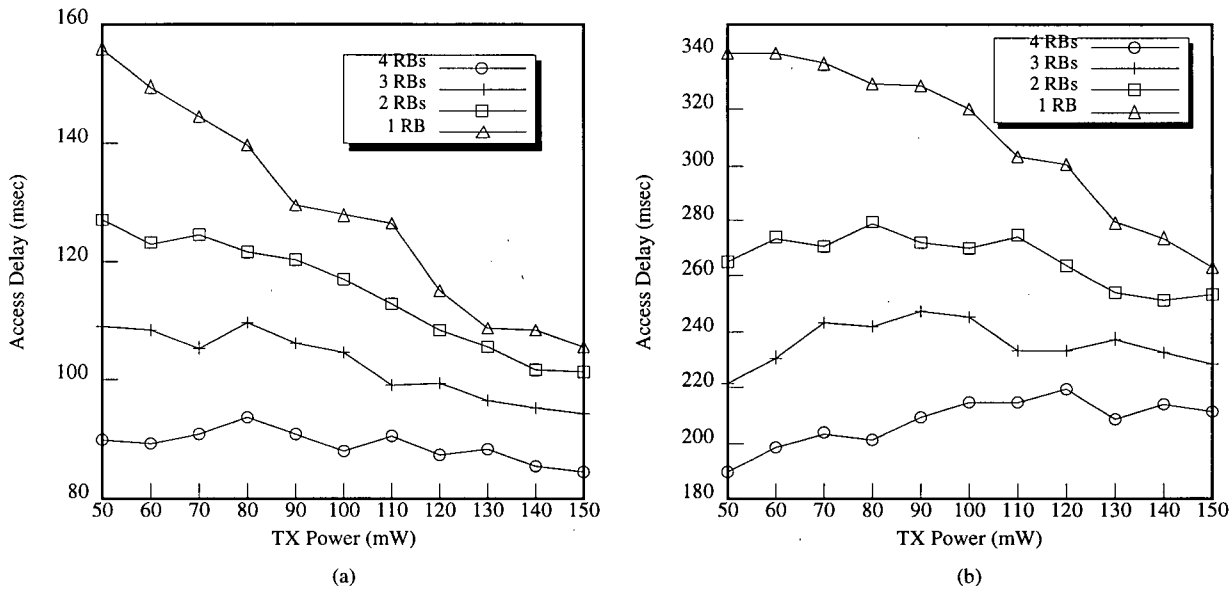

Figure 4.13 Access delay versus transmitted power in Rayleigh fading channel using Method A for (a) 15 WTs and (b) 30 WTs.

The distribution of the saturated throughput on each WT for one RB with 15 WTs at T_x = 50 mW and 150 mW are shown in Figure 4.14(a) and (b) respectively. It can be seen that for T_x = 50 mW, S is mostly concentrated on the WTs near the RB which are WT 6, 7, 8, 9 and 10. Thus, one RB at T_x = 50 mW can cover few WTs as illustrated in Figure 4.11. For T_x = 150 mW, the distribution looks similar to T_x = 50 mW. The S is similarly concentrated on WT 5, 6 7, 8, 9, 10. Thus, the coverage area does not increase with increasing T_x = 150 mW. This is just because the T_x = 150 mW is not high enough to increase the coverage area significantly. But it can be seen that S on each WT for T_x = 150 mW is higher than that for T_x = 50 mW due to the increasing of the packet reception and reducing the number of hidden terminals. The distribution of the saturated throughput on each WT for 4 RBs with 15 WTs at T_x = 50 mW and 150 mW are shown in Figure

4.14(c) and (d) respectively. For T_x = 50 mW, S is more or less evenly distributed in each WT because each RB can evenly cover few WTs in the network as shown in Figure 4.12. However, for T_x = 150 mW, S is more concentrated on the middle WTs. Because the middle WTs can be covered by more RBs as the coverage area of each RB increases. It can be expected that the distribution will become more even when increasing T_x.

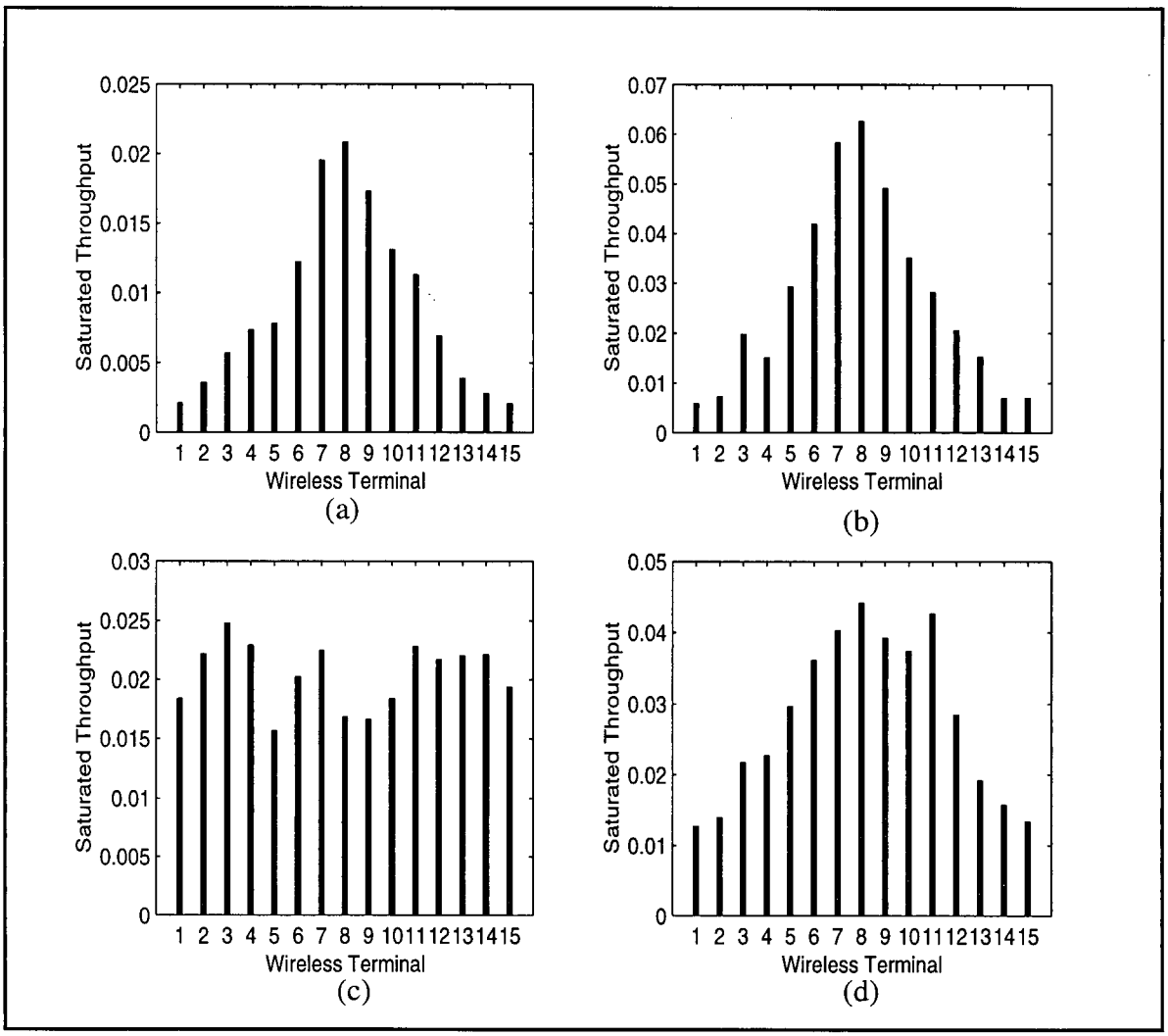

Figure 4.14 The saturated throughput distribution on each of the 15 WT for (a) one RB with T_x = 50 mW, (b) one RB with T_x = 150 mW, (c) 4 RBs with T_x = 50 mW and (d) 4 RBs with T_x = 150 mW.

4.5 Log-Normal Shadowing Channel

In this section, the simulation results are presented for a log-normal shadowing channel which has a log-distance path loss in addition to receiver noise floor. The parameter considered is the standard deviation, σ (in dB), of the log-normal shadowing. The values of σ used in the simulation are from 4 dB to 14 dB. The received power of a packet will be calculated based on equation (3.6) in Chapter 3.

4.5.1 Simulation Results

The saturated throughput versus σ in a log-normal shadowing channel for 15 WTs using Method A and B are shown in Figure 4.15.

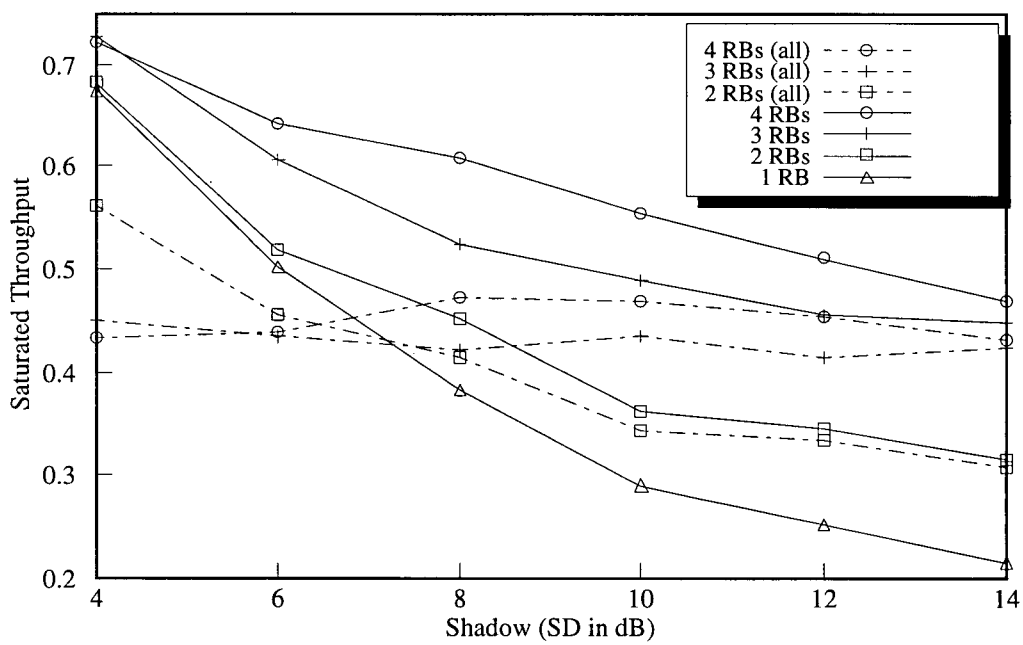

Figure 4.15 Saturated throughput versus σ in log-normal shadowing channel for 15 WTs using Method A and Method B.

Again, S of Method B is lower than that for Method A because of longer waiting time for the multiple ACKs. In Figure 4.15, it can be seen that for Method A, S decreases with σ. Because for a large value of σ, the coverage area of each RB is smaller and more terminals will be hidden from each other. Therefore, there will be more unsuccessful received packets or collided packets at the RBs. At low σ, S of any n approaches about 0.7 whereas S in AWGN channel is about 0.9. This is because as σ decreases, the effect of log-normal shadowing diminishes and hence, the performance will approach that in AWGN channel. The reasons are similar to the high T_x for Rayleigh fading channel in previous section where the probability of packet reception increases and the number of hidden terminal decreases. The performance improvement of using more RBs compared to one RB is increased with σ. For $\sigma = 6$ dB, the performance of using 2, 3 and 4 RBs is improved by 4%, 22% and 28% respectively compared to one RB. For $\sigma = 12$ dB, the performance of using 2, 3 and 4 RBs can be improved by 55%, 110% and 130%. Since there are more hidden terminals for a high value of σ, multiple RBs can improve the performance significantly.

Figure 4.16 shows the access delay for 15 WTs using Method A. For $\sigma < 8$ dB, τ for one RB is better (less) than that for multiple RBs, but S of one RB is worse (lower) than that for multiple RBs for any values of σ as in Figure 4.15. This is because one RB might not be able to receive the packets from a few (one or two) WTs due to shadowing. Using more RBs, it always increases the chance of receiving a packet sent from the WTs received by at least one of the RBs. Therefore, S of one RB is always lower than that of multiple RBs. But this is different from τ because τ of a packet is calculated if and only if the packet is successfully received at the RB. Since the total number of WTs being covered by one RB is lower than that by 4 RBs, there are

fewer WTs which packets can be successful received by the RB. Therefore, there are fewer ACKs for each WT to wait to send its potential packet. As σ increases, τ for one RB becomes higher than that for multiple RBs. In this case, the probability of a packet not being received by one RB is increased due to more hidden terminals and faded packets. Thus, more retransmissions are required. For more RBs, the probability of a packet being received by any one of the RBs is higher and the number of retransmissions can be reduced. The saturated throughput and access delay for 30 WTs using Method A are shown in Figure 4.17(a) and (b). Both figures look similar to the results for 15 WTs, but the overall performance is lower.

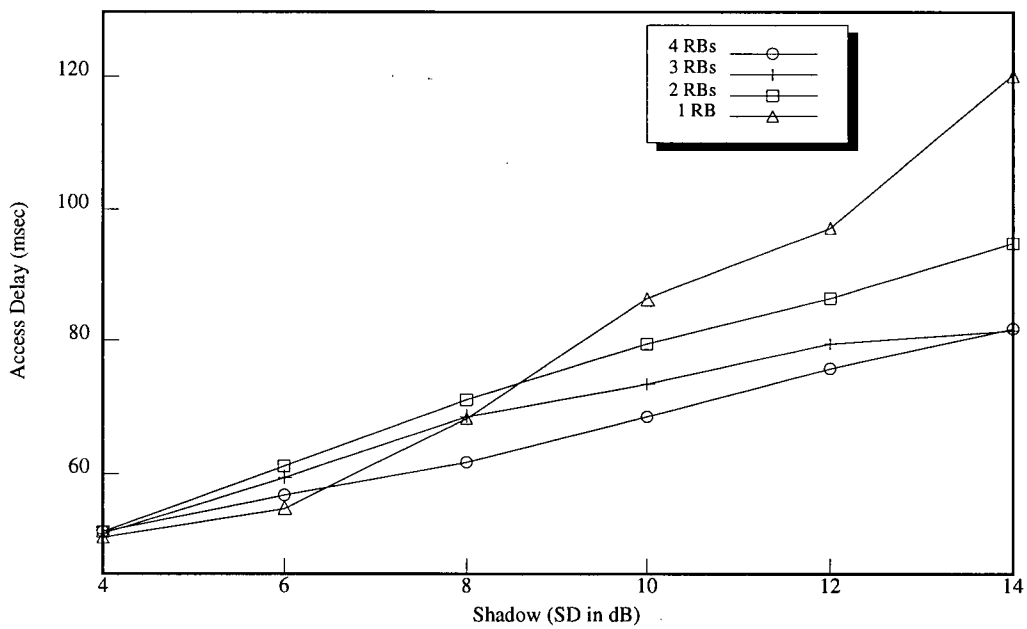

Figure 4.16 Access delay versus σ in log-normal shadowing channel for 15 WTs using Method A.

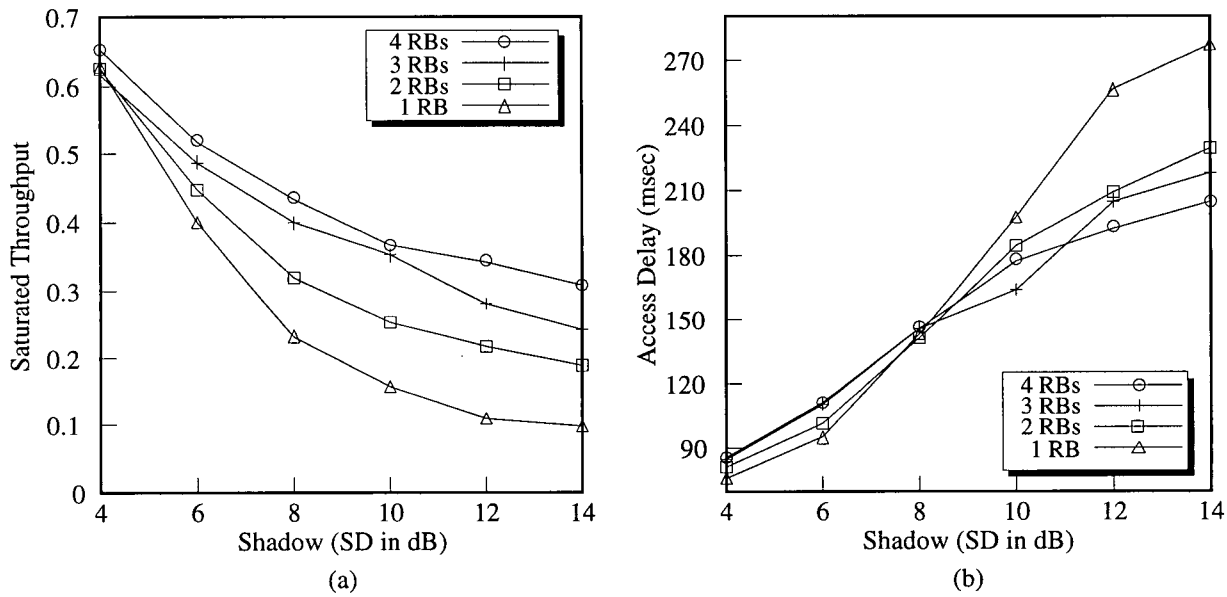

Figure 4.17 (a) Saturated Throughput and (b) access delay versus σ using Method A for 30 WTs.

Chapter 5 Simulation Results and Discussion - Part 2

In this chapter, the performance of the proposed distributed WLANs using IEEE 802.11 MAC protocol will be studied with and without capture effect. A channel model with receiver noise floor, log-distance path loss, Rayleigh fading and log-normal shadowing will be used. Since the performance with Method A is always better than that with Method B as shown in previous chapter, only Method A will be considered in the simulation. The effects of changing the number, n, of RBs, transmitted power levels, the standard deviation of the log-normal shadowing on the performance will be investigated. In order to get insight into the study of distributed networks, a two-dimensional network model will be used as comparison for one-dimensional model. In addition, the length of packet size and the ACK_Timeout will also be studied. The T_x = 100 mW and $\sigma = 6$ will be used as default values.

5.1 Log-normal Shadowing Plus Rayleigh Fading Channel With No Capture

In this section, the simulation results with no capture in a log-normal shadowing plus Rayleigh fading channel will be presented. Figure 5.1(a) and (b) show the normalized throughput for 15 and 30 WTs respectively. It can be seen that η for 30 WTs is lower than that for 15 WTs because of more collisions and longer waiting time. Compared to the Rayleigh fading channel in Figure 4.7(a), η with one or 2 RBs is lower in this channel. This is because the probability of a packet being received successfully in log-normal shadowing plus Rayleigh fading channel is generally lower than that in a Rayleigh fading channel due to the additional degradation from log-normal shadowing. The η with 3 or 4 RBs is about the same in both channels, because the probability of a packet being successfully received increases with n, alleviating the effect of the

log-normal shadowing. For 30 WTs, η for $n \geq 2$ is about the same as that in a Rayleigh fading channel as shown in Figure 4.9(a). The S with 4 RBs for 15 WTs and 30 WTs can be increased by about 100% and 200% respectively compared to that for one RB.

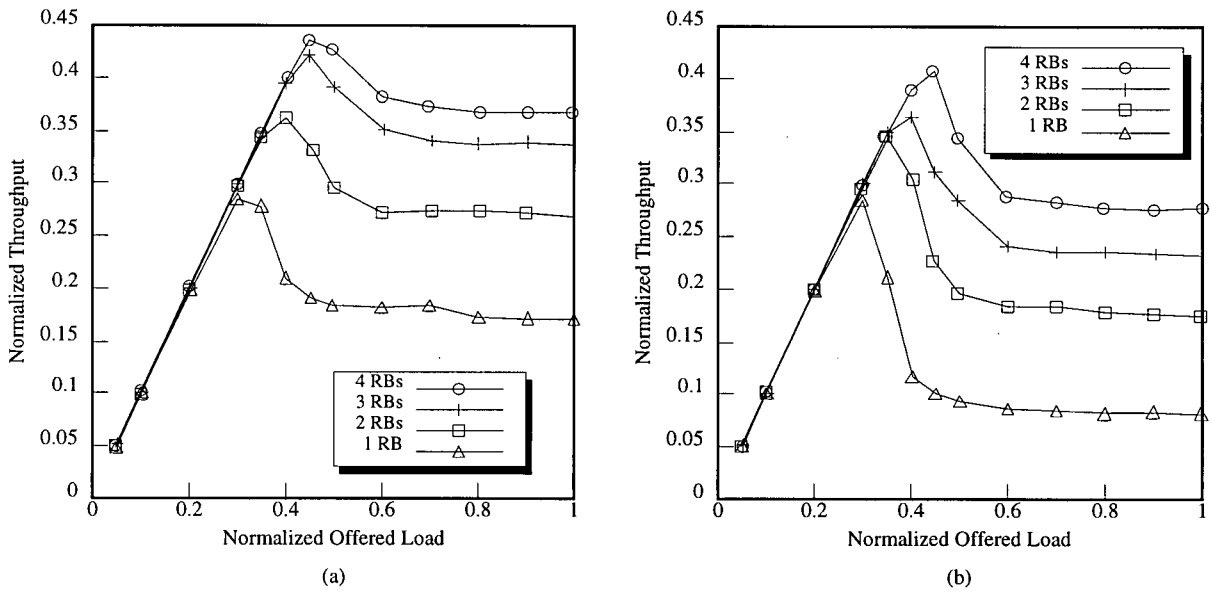

Figure 5.1 Normalized throughput versus normalized offered load in log-normal shadowing plus Rayleigh fading channel for (a) 15 WTs and (b) 30 WTs.

The access delay for 15 and 30 WTs are shown in Figure 5.2(a) and (b) respectively. For 15 WTs, the access delay of one and 2 RBs is higher than that in a Rayleigh fading channel. For 30 WTs, the access delay for any n is about the same in both channels. Thus, the performance, η and τ, for $n \geq 2$ is about the same as in both the Rayleigh fading channel and log-normal shadowing plus Rayleigh fading channel, with $\sigma = 6$ dB and $T_x = 100$ mW. However, compared to the results for the log-normal shadowing channel in Section 4.5, presented in Figure 4.16 and Figure 4.17, τ (S) in log-normal shadowing plus Rayleigh fading channel is doubled (40% lower). Hence, the performance in a log-normal shadowing plus Rayleigh fading channel is much worse

than that in a channel with log-normal shadowing only for any n with $\sigma = 6$ dB and $T_x = 100$ mW. This is because the effect of Rayleigh fading degrades the performance significantly.

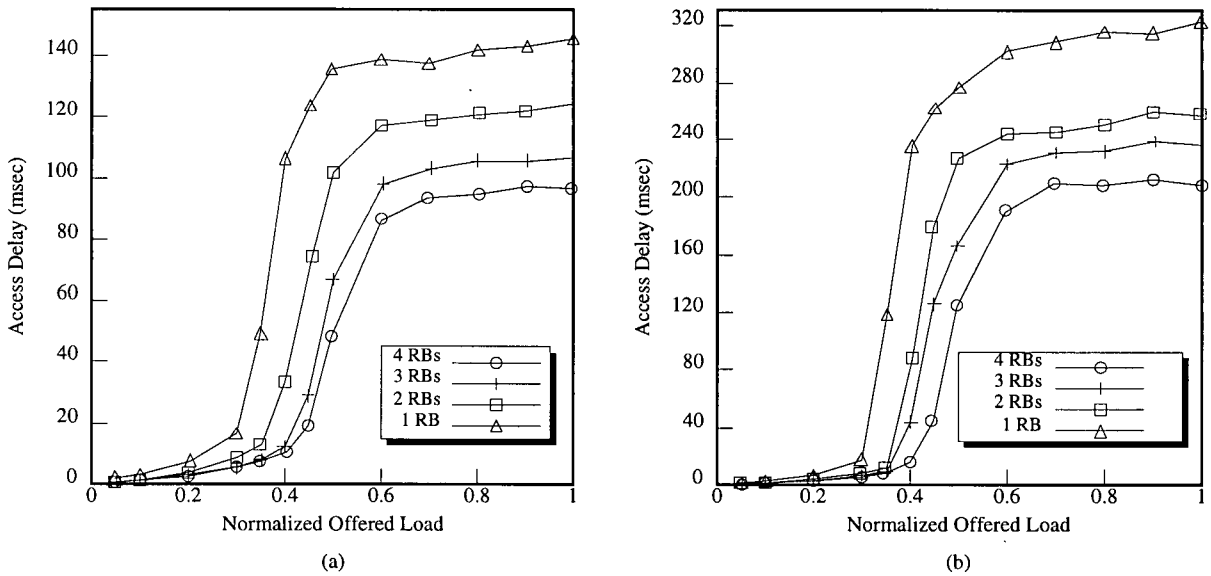

Figure 5.2 Access delay versus normalized offered load in log-normal shadowing plus Rayleigh fading channel for (a) 15 WTs and (b) 30 WTs.

The saturated throughput for 15 and 30 WTs with different transmitted power are shown in Figure 5.3(a) and (b), respectively. It can be seen that S increases with T_x but the rate of increase decreases as n increases. The explanation is the same as that for the Rayleigh fading channel for different T_x in Figure 4.10 in Section 4.4. The performance improvement, on average, of 4 RBs over one RB for 15 WTs and 30 WTs are 120% and 220%, respectively, as shown in Figure 5.3. Thus, it is more efficient to use more RBs in a network with a larger number of WTs. Compared to the Rayleigh fading channel in Figure 4.10, it can be seen that S with any n in both channels is about the same at low $T_x = 50$ mW. For $T_x > 60$ mW, S in a log-normal shadowing plus Rayleigh fading channel becomes lower and the difference increases as T_x increases.

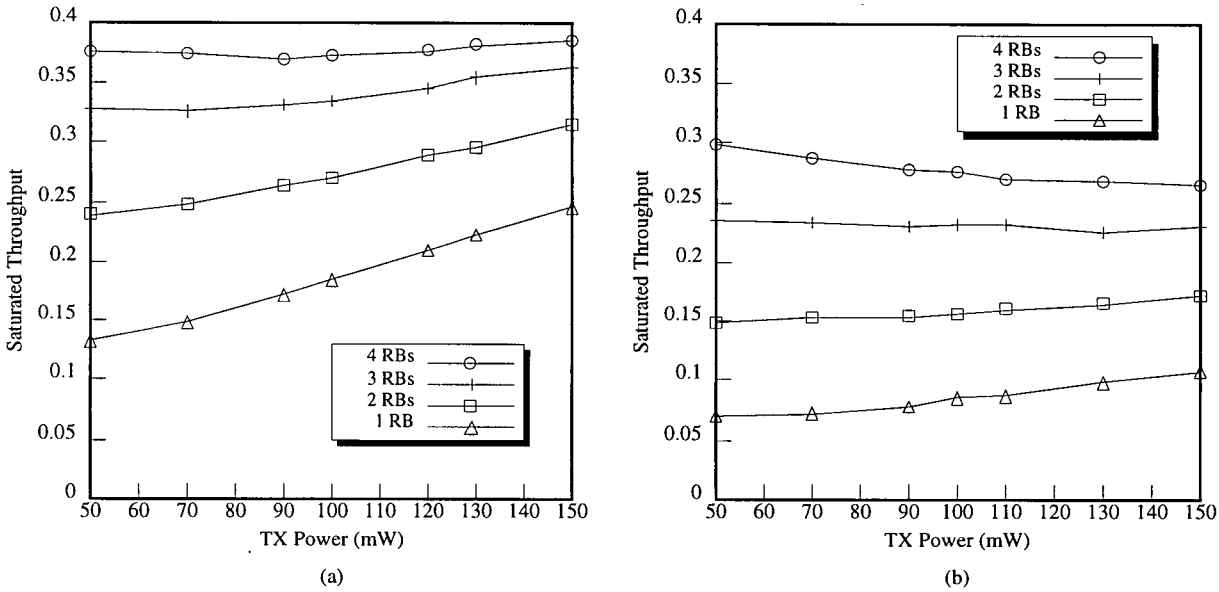

Figure 5.3 Saturated throughput as a function of transmitted power with $\sigma = 6$ dB in log-normal plus Rayleigh fading channel for (a) 15 WTs and (b) 30 WTs.

For low T_x, the probability of a packet being non-faded at RB/WTs with Rayleigh fading is already low. Thus, the additional effect of log-normal shadowing of $\sigma = 6$ dB does not increase the non-faded probability by much. Hence, S in both channels is about the same. As T_x increases, the non-faded probability with Rayleigh fading increases. Then, the additional effect of log-normal shadowing can significantly decrease the non-faded probability. Therefore, S is lower in a log-normal plus Rayleigh fading channel and thus the difference in two channels increases with T_x. For 3 or 4 RBs, the performance difference in the two channels is small. This is because the degradation of performance due to log-normal shadowing can be alleviated by adding more RBs. The performance improvement of 4 RBs to one RB for 15 WTs at low and high T_x in a log-normal shadowing plus Rayleigh fading channel is 200% and 60%, respectively, whereas the performance improvement at low T_x and high T_x in a Rayleigh fading channel is 150% and 20%, respectively. Therefore, the performance improvement degrades rapidly in a Rayleigh fading channel. The

access delay for 15 and 30 WTs are shown in Figure 5.4(a) and (b), respectively. For one or 2 RBs, τ for T_x = 50 mW in a log-normal shadowing plus Rayleigh fading channel is about the same as in a Rayleigh fading channel as shown in Figure 4.13. Similarly, τ for $T_x > 60$ mW in a log-normal shadowing plus Rayleigh fading channel is higher than that in a Rayleigh fading channel and the difference increases with T_x. It can be seen that the performance improvement by using more RBs is greater in a log-normal shadowing plus Rayleigh fading channel than in a Rayleigh fading channel.

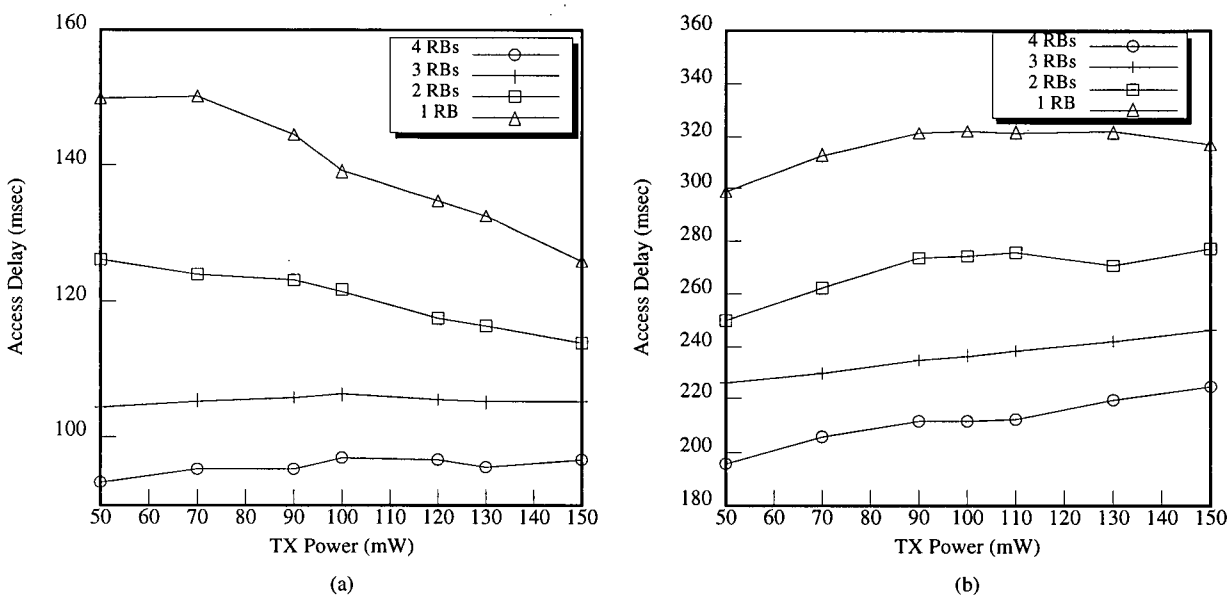

Figure 5.4 Access delay as a function of transmitted power with σ = 6 dB for (a) 15 WTs and (b) 30 WTs.

The effect of σ on the performance of throughput and access delay for 30 WTs is presented in Figure 5.5(a) and (b) respectively. In Figure 5.5(a), it can be seen that S does not

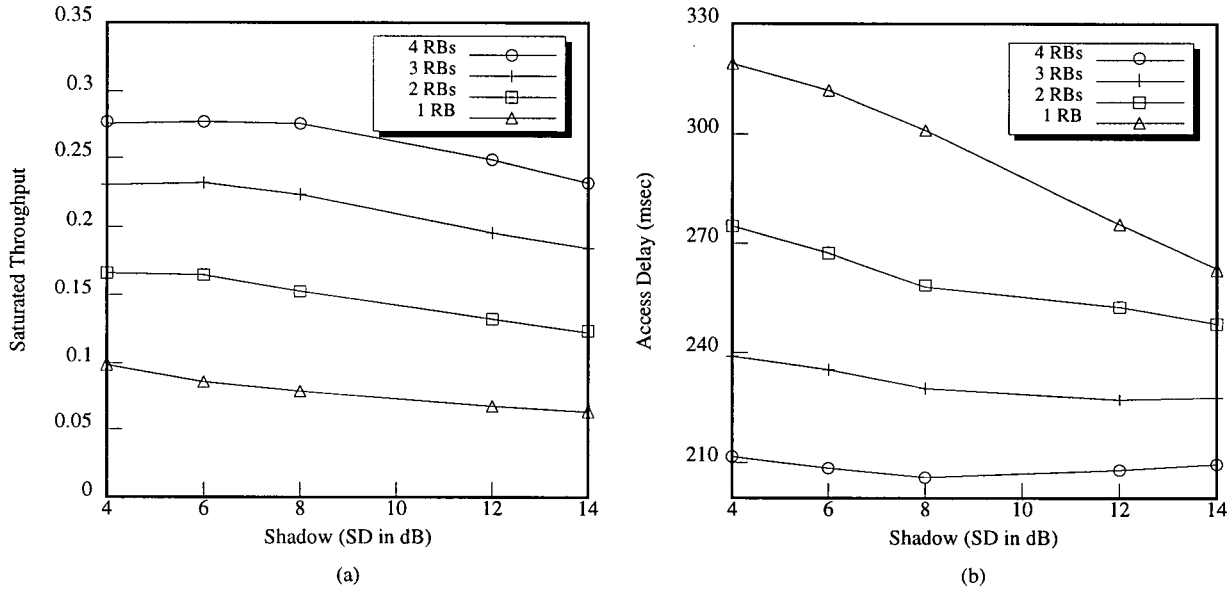

Figure 5.5 (a) Saturated throughput and (b) access delay as a function σ for 30 WTs.

change with σ by much whereas in Figure 4.17(a) in a log-normal shadowing channel, S decreases with σ significantly. The performance improvement of 2, 3 and 4 RBs over one RB is about 67%, 160% and 225% respectively for any values of σ. Compared to a log-normal shadowing channel, S for small values of σ in this channel is much lower. The difference becomes smaller as σ increases. For small values of σ, the performance is degraded mainly due to Rayleigh fading, because the effect of log-normal shadowing is relatively small and does not degrade the performance very much at small σ. This can be observed in Figure 4.17(a) where S is quite high, about 0.65, at small $\sigma = 4$ dB. As σ increases, the effect of Rayleigh fading diminishes relatively compared to log-normal shadowing. Thus, at $\sigma = 14$ dB, the effect of Rayleigh fading becomes negligible and S in a log-normal shadowing plus Rayleigh fading channel is about the same as in a log-normal shadowing channel. The τ in this channel is also

worse (higher) than that in a log-normal shadowing channel as seen in Figure 4.17(b). As σ increases, the difference gets smaller. For example, at $\sigma = 4$, τ for one RB in this channel can be 3 times more than that in a log-normal shadowing channel. For one RB, τ decreases with σ. However, the throughput does not increase with σ. This is because when there is only one RB and 30 WTs, there will be more collisions and more WTs shadowed from the RB as σ increases. Therefore, the number of WTs that can reach the RB is reduced, and that can reduce the waiting time of the packet. Since the access delay is only calculated for the packets which can be received correctly at the RB, the number of correctly received packets is reduced as σ increases. For $n \geq 2$, τ does not vary much with σ. In conclusions, the performance in a log-normal shadowing plus Rayleigh fading channel of $n \geq 2$ is not affected by T_x or σ significantly.

5.2 Log-normal Shadowing Plus Rayleigh Fading Channel With Capture

5.2.1 Capture Model

For the simulation results of throughput and access delay obtained in the previous sections, no capture is assumed to be used. Hence, if two or more packets arrive at the receiver with any amount of overlap in time, all the packets are unusable and discarded due to collision. Since frequency modulation exhibits a so-called *capture effect* characteristic [28], the performance can be improved by considering that the receiver can successfully *capture* a packet with the largest received power amount several packets that arrive at the receiver at about the same time. It is assumed that the received signal powers are more or less constant over a packet duration. In general, two common conditions for a receiver to capture packet A, $A \in \{1, 2, \ldots, m\}$ where m is the number of packets arriving at the receiver simultaneously, can

be used [2][3], i.e.,

$$\frac{\Gamma_A}{\max\{\Gamma_i\}} > c, \qquad i = 1, 2, \ldots, m, \quad i \neq A \tag{5.1}$$

and

$$\text{SIR} = \frac{\Gamma_A}{\sum_{i=1,\, i \neq A}^{m} \Gamma_i} > c \tag{5.2}$$

where Γ_j, j=1,2,..., m, is the received power of packet j and c is the capture ratio. The value of c will depend on the particular modulation and coding technique used in the system. In (5.2), SIR is defined as the signal-to-total interference power ratio.

In the simulation, the second capture model is employed because the first capture model is somewhat unrealistic and optimistic. A packet with the largest received power can be captured by the receiver if and only if the SIR is greater than c for the duration of the packet duration. For example, if two packets, A and B, arrive at the receiver at about the same time (within a packet duration) with overlap as shown in Figure 5.6, there will be three possible outcomes, i.e.,

(i) packet A will be captured if $\frac{\Gamma_A}{\Gamma_B} > c$,

(ii) packet B will be captured if $\frac{\Gamma_B}{\Gamma_A} > c$,

(iii) otherwise, both packets will be discarded.

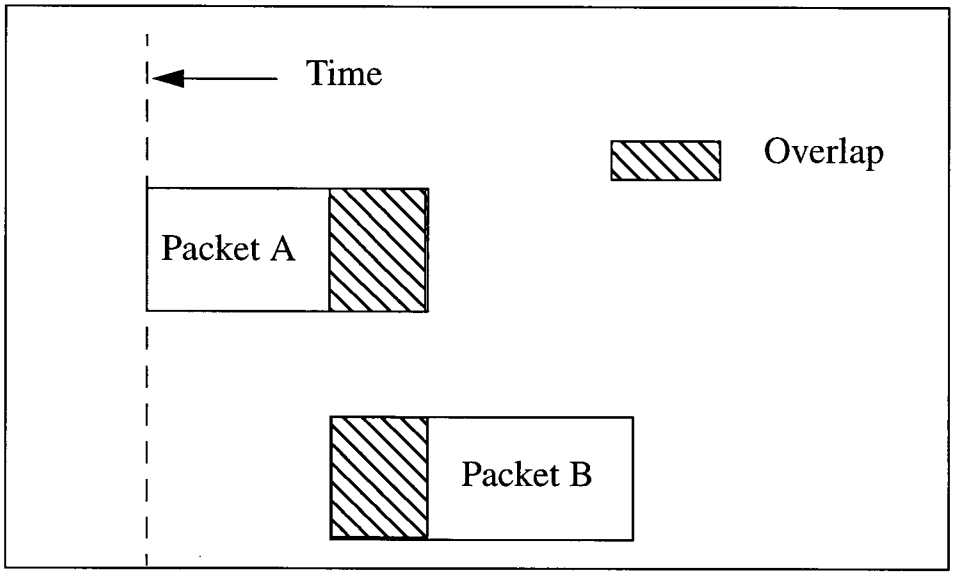

Figure 5.6 The capture model.

5.2.2 Simulation Results

In this section, the simulation results are obtained for a log-normal shadowing plus Rayleigh fading channel with capture. The default value of c is chosen to be 10 dB. The throughput performance for 15 WTs in a log-normal shadowing plus Rayleigh fading channel with capture using Method A is presented in Figure 5.7(a). It can been seen that η with capture is much higher, about 2-3 times more, than that with no capture as in Figure 5.1(a). Because capture can increase the chance of packet reception, especially for those WTs near a RB. The η can be greater than 1 for $n \geq 3$ because there is a higher possibility that two or more packets can be received in the RBs at about the same time. For example, three packets, A, B and C, are sent from three WTs within a packet duration. If the received power of Packet A at RB_1 is higher than the sum of the received power Packet B and Packet C, then Packet A will be captured. Similarly, Packet B may be captured at RB_2 if the received power of Packet B is greater than the sum of

other two packets. In this case, both packets A and B can be received by the RBs within a packet duration. The performance improvement of 2, 3 and 4 RBs over one RB is 66%, 120% and 160% which the performance improvement is greater than that in no capture cases as in Figure 5.1(a). Because capture with more RBs can receive multiple packets. The access delay is shown in Figure 5.7(b).

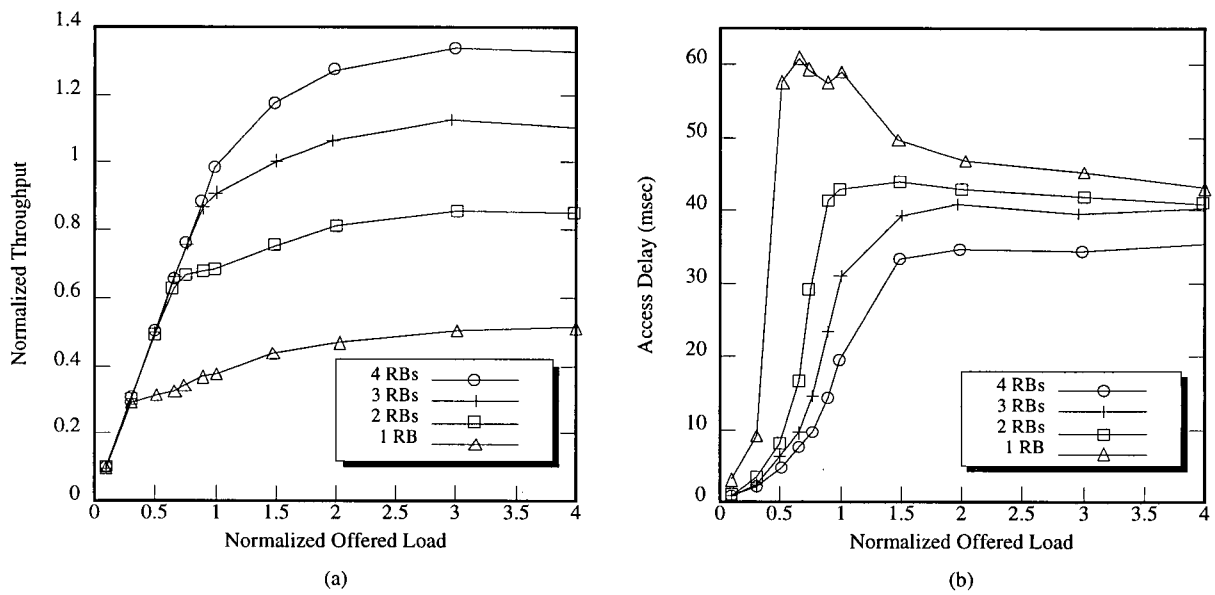

Figure 5.7 (a) Normalized throughput and (b) access delay versus normalized offered load in log-normal shadowing and Rayleigh fading channel with capture for 15 WTs using Method A.

Compared to no capture in Figure 5.2(a), τ with capture is much lower because the number of retransmissions due to collisions is reduced. For one RB, τ goes up when the traffic load is low and drops when the traffic load increases ($\rho > 1.0$). This is because when the traffic load is low, the probability of collision is low and the packets sent from most of the WTs can be received at the RB with several retransmissions. However, as load increases, the probability of collision increases, only the packets sent from those WTs close to the RB can be received due to

power capture. In other words, those packets sent from the WTs which are far away from the RB can never be received by the RB. Therefore, the access delay is calculated based on those packets sent from few WTs that are close to the RB.

The distribution of S at each WT for n = 1, 2, 3 and 4 with no capture and capture is shown in Figure 5.8 and Figure 5.9, respectively. In Figure 5.8(a) for one RB, it can be seen that S is more concentrated on WTs 5 to 11 which are more or less under the coverage area of the RB. On other WTs, S is comparatively smaller. As n increases, S at each WT is distributed more evenly. In Figure 5.9(a) for one RB, S is highly concentrated at WTs 7, 8 and 9, especially for WT 8 at which S is about 40% of the total S in the system. Because a packet is captured based on the largest received power which is inversely proportional to the third power of the distance between the transmitter and receiver, packets from a WT which is close to the RB can be captured more frequently. Since WTs 7, 8 and 9 are the closet WTs to the RB as shown in Figure 3.6, their packets can always be captured by the RB. The S at other WTs is significantly lower, which is about the same as no capture cases shown in Figure 5.8(a). Since their packets cannot be captured due to the larger distance, the performance of these WTs is similar to no capture cases. As n increases as shown in Figure 5.9, it can be seen that S is mostly concentrated on the WTs near the RBs. The performance is improved only for the WTs near the RBs. In conclusion, capture takes advantage of the near-far effect which causes an unfair traffic performance for each WTs even though the total system performance is increased.

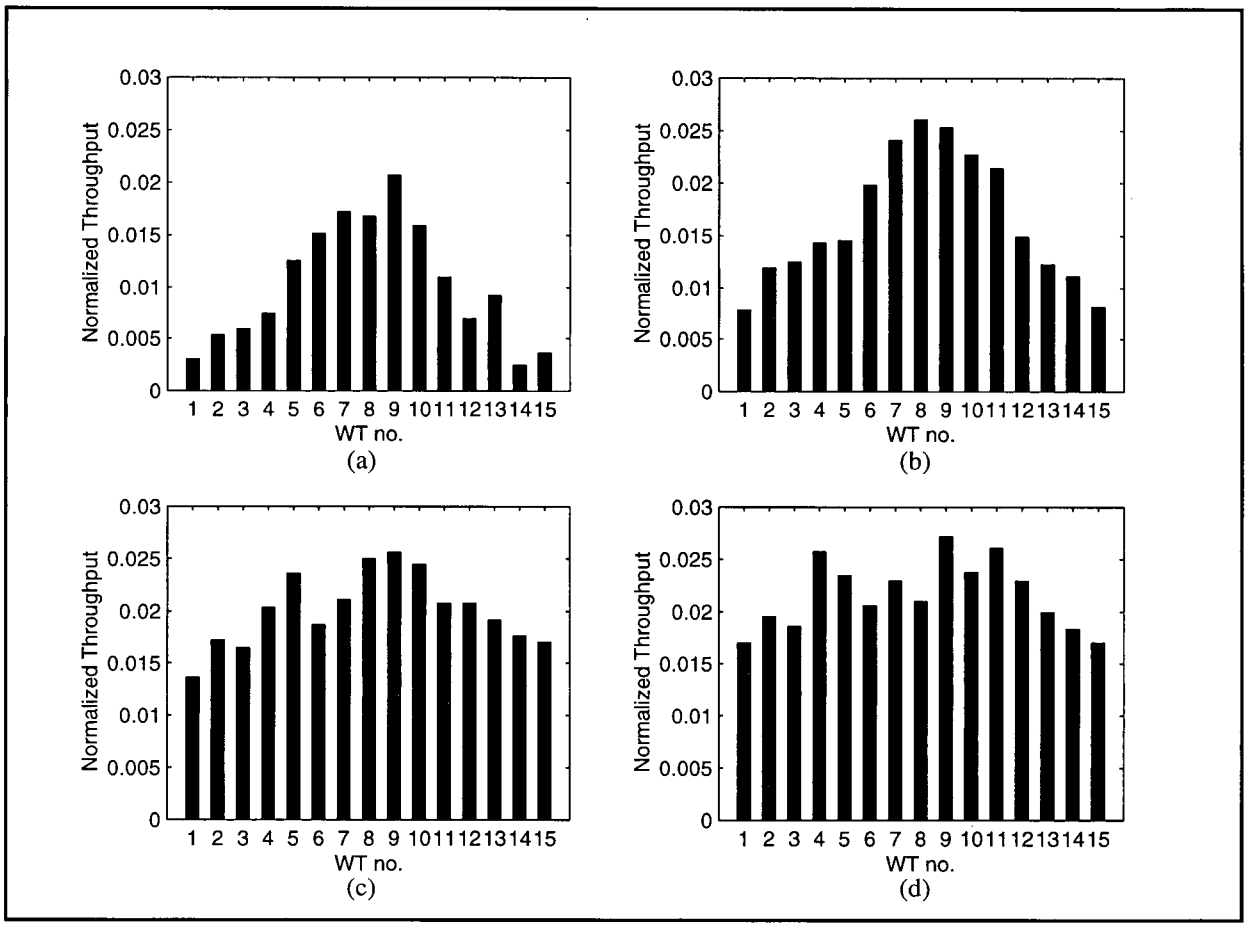

Figure 5.8 The throughput distribution of 15 WTs with no capture for (a) one RB, (b) 2 RBs, (c) 3 RBs and (d) 4 RBs.

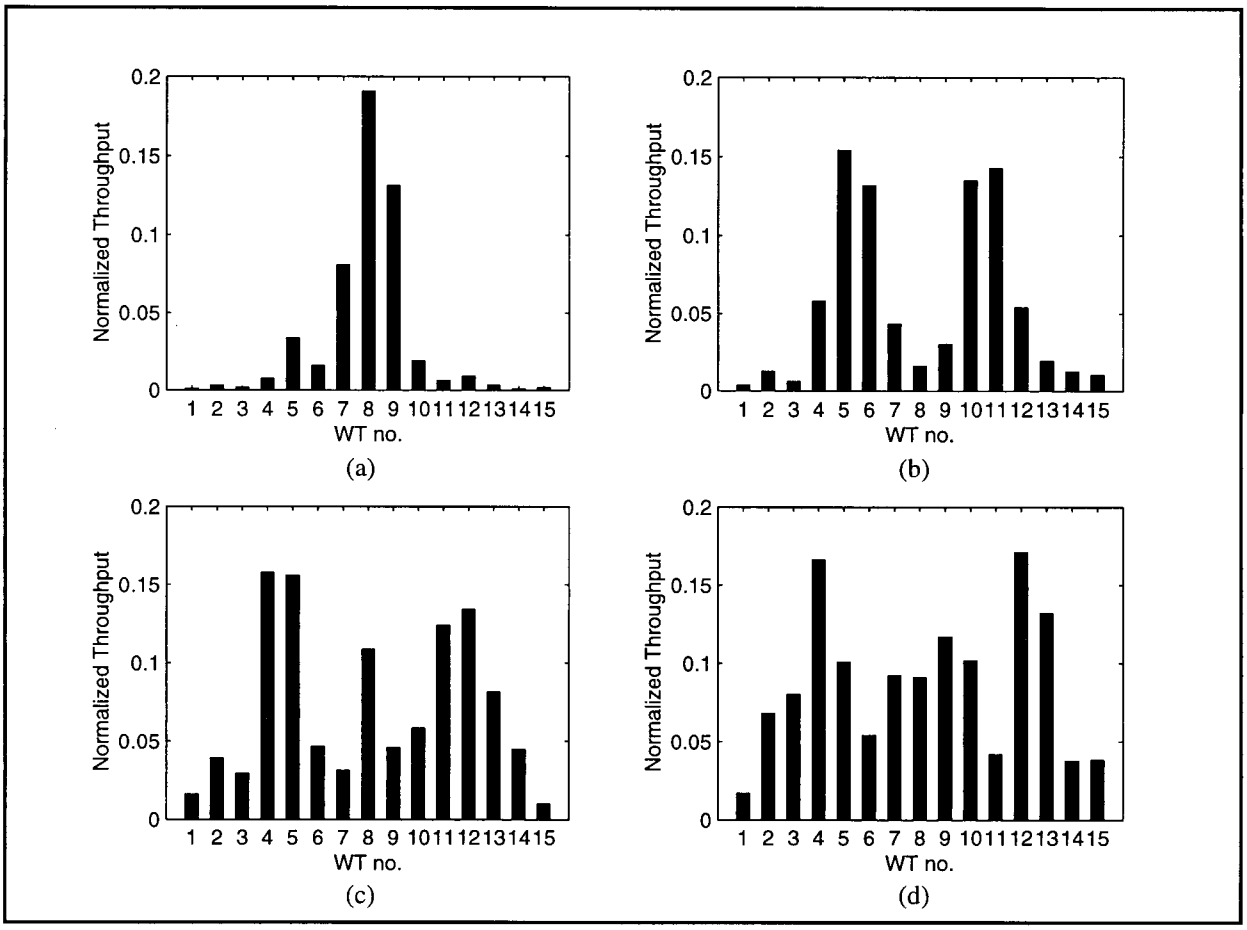

Figure 5.9 The throughput distribution of 15 WTs with capture for (a) one RB, (b) 2 RBs, (c) 3 RBs and (d) 4 RBs.

The saturated throughput and access delay for 15 WTs in a log-normal shadowing plus Rayleigh fading channel using Method A with capture for $\sigma = 6$ dB with different transmitted power are shown in Figure 5.10(a) and (b) respectively. It can be seen that S is not affected by T_x very much. This observation is different from the results for no capture in which S increases with T_x as shown in Figure 5.3(a). The reason is as follows. The received packet powers at the RB are higher for the WTs near it. The total number of WTs close to the RB is not changed whether T_x is high or low.

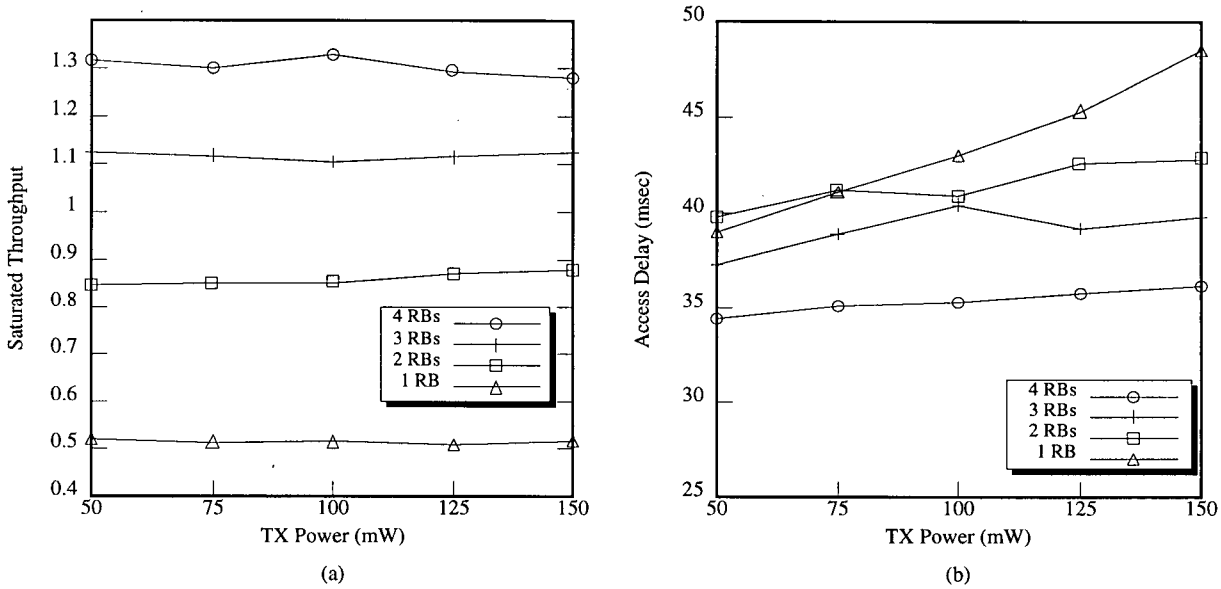

Figure 5.10 (a) The saturated throughput and (b) access delay as a function of transmitted power in log-normal plus Rayleigh fading channel at $\sigma = 6$ dB for 15 WTs using Method A with capture.

As an example of one RB case, the received packet powers from WTs 7, 8 and 9 are always largest at the RB no matter if the T_x of WTs is high or low. Besides, for high or low T_x, the probability of a packet sent from a close WT being received (non-faded) at the RB is quite high because if is close to the RB. Thus, S is about the same at any T_x for the evaluation range because the packets from the closest WTs can always be captured and the reception (non-faded) probability of the packets from these WTs are quite high at any T_x. In Figure 5.10(b), τ with one RB increases with T_x because the non-faded (above CST) probability of packets at WTs decreases with T_x and the time of busy channel sensed by WTs becomes longer. Thus a longer waiting time is required for WTs to send packets. For $n \geq 2$, τ is not changed with T_x by much. Although the waiting time for WTs to send packets increases with T_x, the chance of a packet being successfully received at RBs is increased as well due to multiple RBs. Thus, τ can be kept at about the same.

The throughput and access delay for 15 WTs in a log-normal shadowing plus Rayleigh fading channel using Method A with capture at T_x = 100 mW with different values of σ are shown in Figure 5.11(a) and (b) respectively. The S for $n \geq 2$ decreases slightly with σ because the probability of WTs being shadowed at the RBs increases. Therefore, the chance of the WTs being covered by multiple RBs is reduced. Since there is no multiple RBs' effect for one RB case, S is not affected by σ. Similarly τ with one RB decreases with σ because the probability of packets being non-shadowed or detected at the WTs is decreased with σ. Since the shadowing effect increases, the number of WTs shadowed from the RB increases. Therefore, the time for fewer stations completing for accessing the channel become less. For $n \geq 2$, τ is not changed much with σ because packets can be received by multiple RBs.

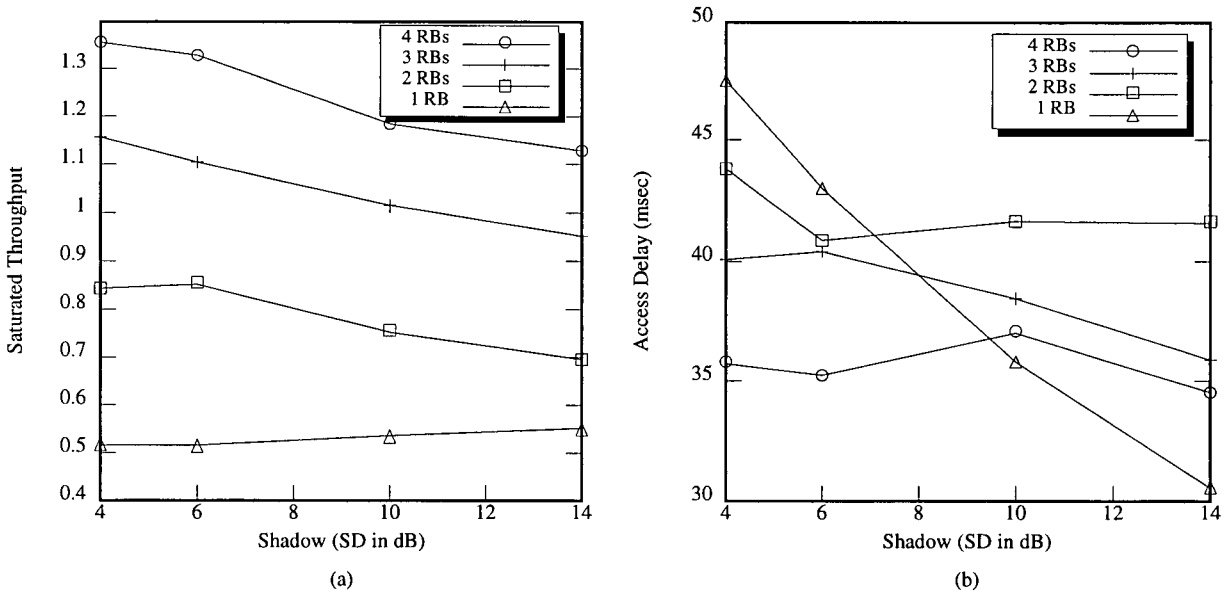

Figure 5.11 (a) The saturated throughput and (b) access delay as a function of σ in log-normal plus Rayleigh fading channel at T_x = 100 mW for 15 WTs using Method A with capture.

5.3 Other System Parameters

In this section, the simulation results will be obtained for different system configurations or parameters. A two-dimensional model will be used to compare the performance obtained from one-dimensional. The effect of *c*, packet length and ACK_Timeout will be considered.

5.3.1 Two-dimensional Model

The previous results are obtained from one-dimensional model. This section will present the simulation results for a two-dimensional model for comparison. The two-dimensional model contains 15 WTs located in three different rows as shown in Figure 5.12.

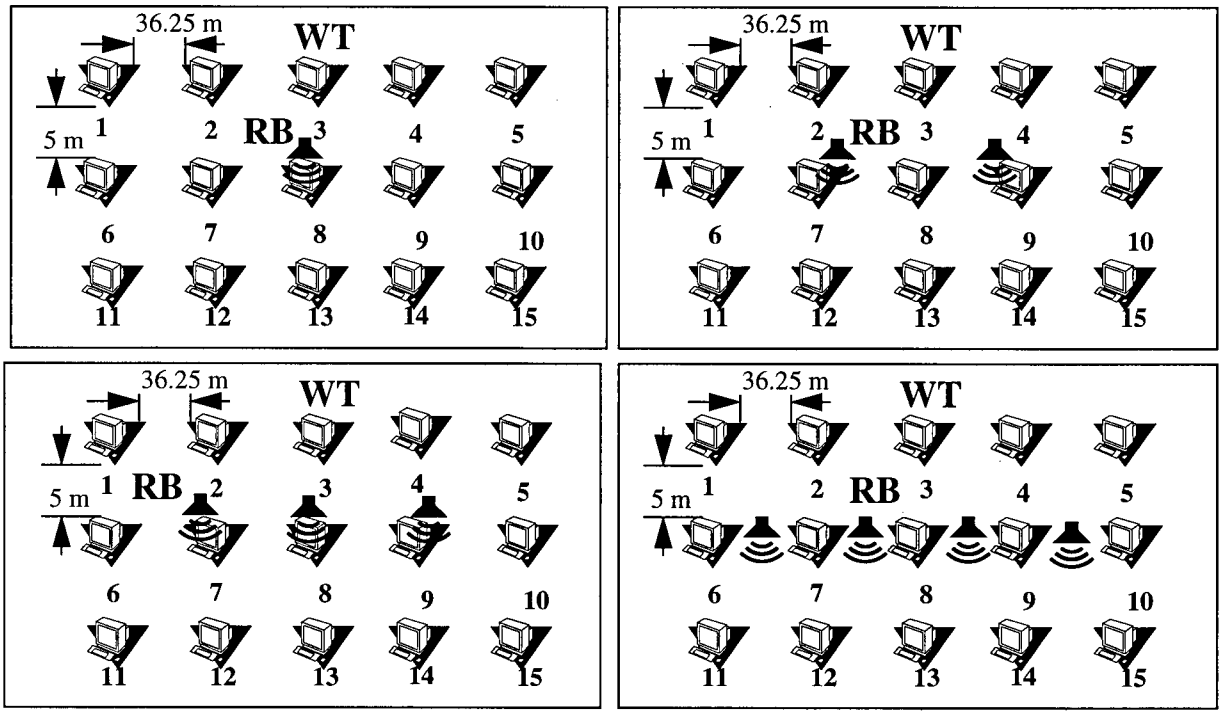

Figure 5.12 The station location for 15WTs and different number of RBs in a two-dimensional model.

Each row has 5 WTs and the distance between the WTs is 36.25 meter. Therefore, the network range is still about 145 meter. The distance between each row is 5 meter. The RB(s) are placed in the middle row and spaced evenly. The network arrangement for the system with n = 1, 2, 3 and 4 is shown in Figure 5.12(a) to (d).

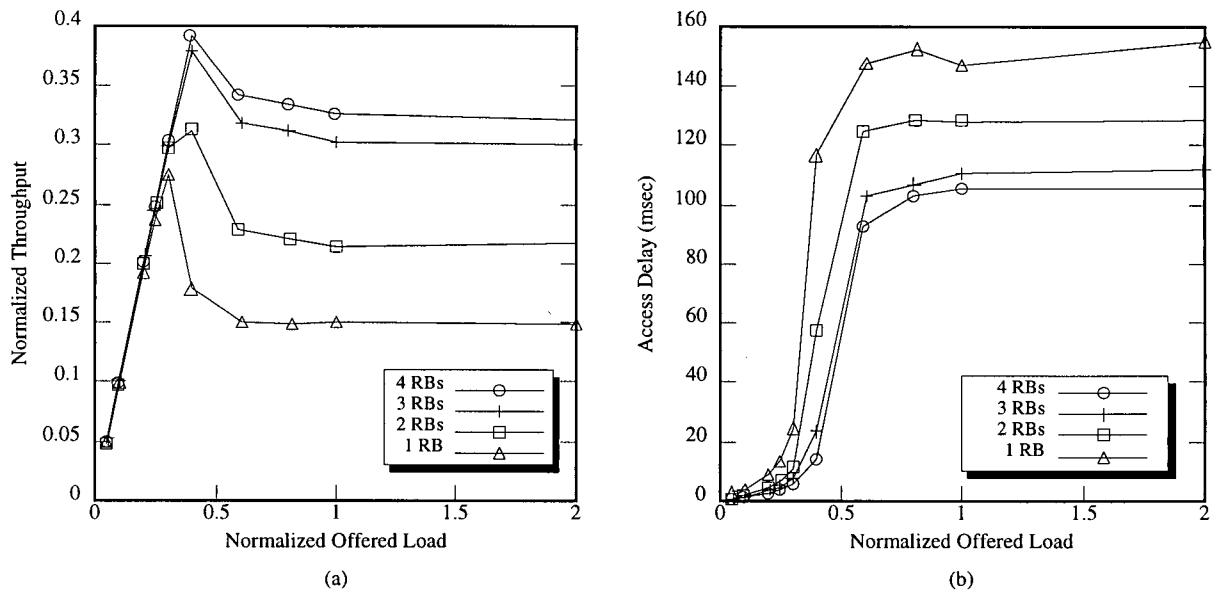

Figure 5.13 (a) Normalized throughput and (b) access delay versus normalized offered load in log-normal shadowing plus Rayleigh fading channel for no capture in two-dimensional model.

The η and τ for 15 WTs in a log-normal shadowing plus Rayleigh fading channel with no capture using Method A in a two-dimensional model are presented in (a) and (b), respectively. The η and τ are slightly worse than those in one-dimensional model in Figure 5.1(a) and Figure 5.2(a). The distribution of S on each WT in a two-dimensional model is shown in Figure 5.14. Compared to one-dimensional model in Figure 5.8, it can be seen that S on each WT is slightly lower in two-dimensional model. The first reason is that there are more packets being faded at the RB in a two-dimensional model because there are more WTs located far away from RB. An example of a single RB in one-dimensional model, there are two WTs 1 and 15 located farthest

away from RB. But, in a two-dimensional model, there are more WTs 1, 5, 6, 10, 11 and 15 located farthest away from RB. The second reason is that there are more possible hidden terminals for each WT. For example, two terminals are hidden from each other if the distance between them is larger than about 70 m. Then, for one-dimensional model, WT 1 has only one hidden terminal, WT 15. However, for a two-dimensional model, WT 1 has three hidden terminals, WTs 5, 10 and 15. Thus, more possible hidden terminals increase the occurrence of collisions.

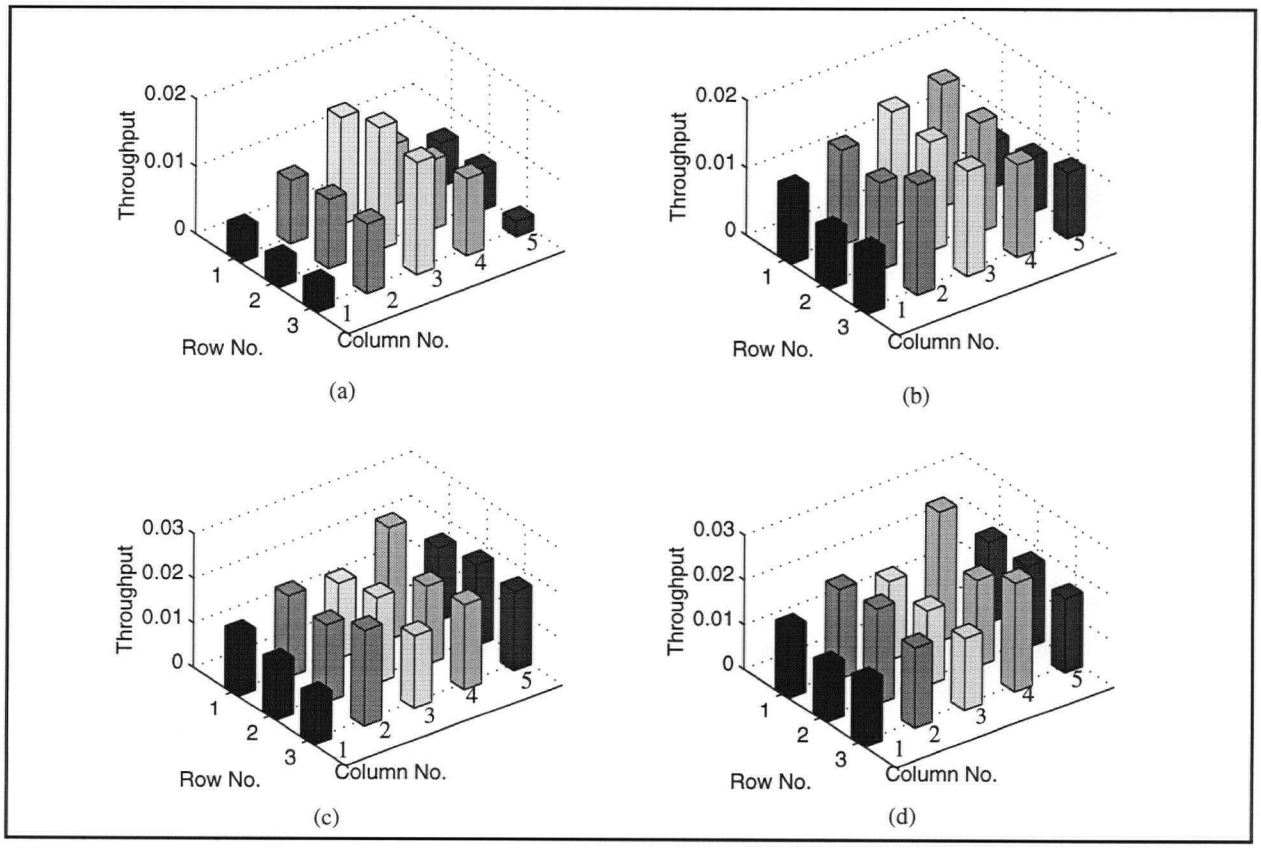

Figure 5.14 The saturated throughput distribution for 15 WTs on each WT with no capture in a two-dimensional model for (a) one RB, (b) 2 RBs, (c) 3 RBs and (d) 4 RBs.

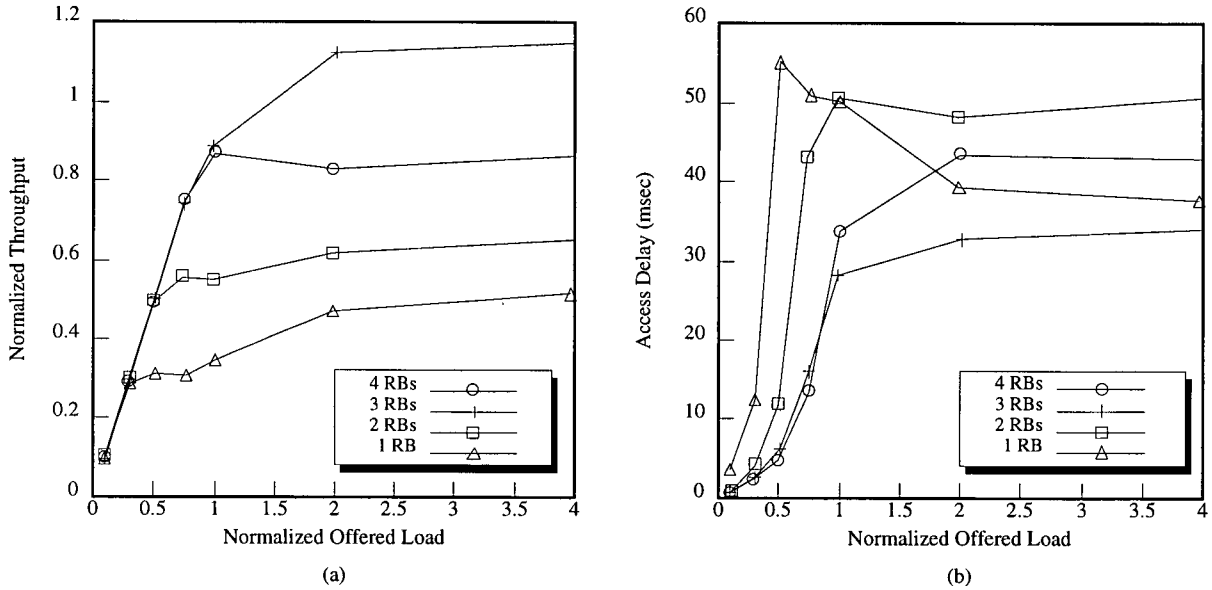

Figure 5.15 (a) Normalized throughput and (b) access delay versus normalized offered load in log-normal shadowing, $\sigma = 6$, and Rayleigh fading channel at $T_x = 100$ mW with capture for 15 WTs using Method A in a two-dimensional model.

The η and τ for 15 WTs in a log-normal shadowing plus Rayleigh fading channel with capture using Method A in a two-dimensional model are presented in Figure 5.15(a) and (b), respectively. The performance with capture is much better than that with no capture. Compared to one-dimensional model in Figure 5.7, the performance in a two-dimensional model for $n = 1$ is about the same, but the performance is worse for $n \geq 2$. In a two-dimensional model, the performance of 3 RBs is better than that for 4 RBs whereas in previous results, the performance of 3 RBs is worse than that with 4 RBs. This can be explained by looking at the distribution of S on each WT as shown in Figure 5.16. With capture, most of the packets being received or captured are sent from the WTs near the RB. For example with one RB as shown in Figure 5.16(a), most of the packets captured by the RB are sent from WTs 3, 8 and 13 which are close to the RB. The S for other WTs is similar to that of the no capture cases as seen in Figure 5.14(a). For three RBs'

case, each RB is located in columns 2, 3 and 4. Similarly, most of the packets being captured are from the WTs located in columns 2, 3 and 4 as seen in Figure 5.16(c). For four RBs' case, each RB is located between columns. For example, if a RB is located between columns 1 and 2, the received power from the WTs in these two columns at the RB will be more or less the same. Hence, if two packets are sent from these two columns, the RB may not effectively capture one of the packets. The throughput is low in column 3 than that in columns 2 and 4 is because the interference level for column 3 is higher. For example, a RB is located between columns 2 and 3. If a packet is sent from a WT in column 2, the interference power comes from the WTs in columns 1, 3, 4, and 5. If a packet is sent from a WT in column 3, the interference power comes from the WTs in columns 1,2, 4, and 5. In addition, the received power of both packets is the same at the RB. Obviously, the total interference power of columns 1, 3, 4, and 5 is lower than that of columns 1, 2, 4, and 5. The Throughput is low in columns 1 and 5, because there is only one RB close by but there are at least two RBs located between columns 2, 3, and 4.

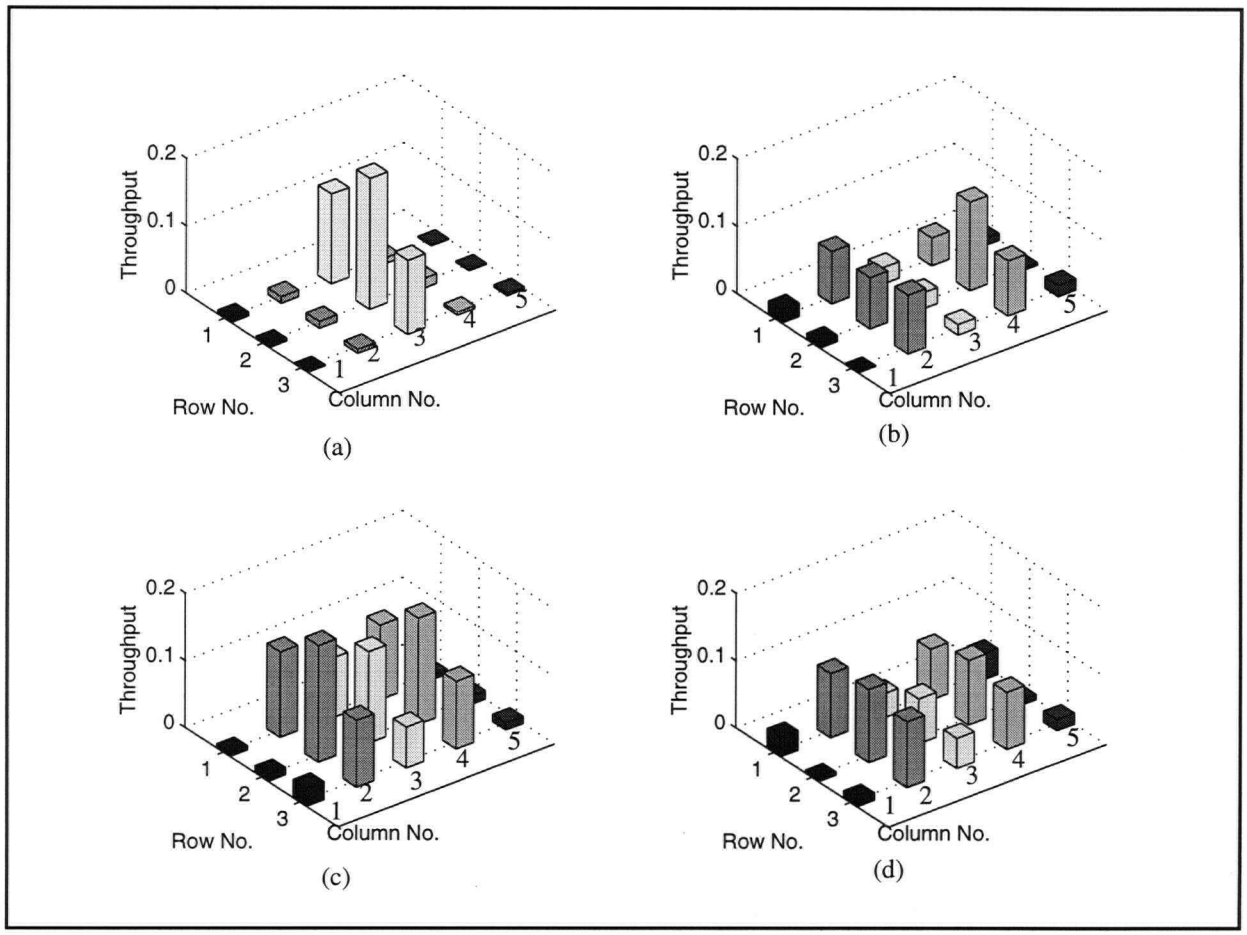

Figure 5.16 The saturated throughput distribution for 15 WTs on each WT with capture in a two-dimensional model for (a) one RB, (b) 2 RBs, (c) 3 RBs and (d) 4 RBs.

The saturated throughput and access delay for 15 WTs a in log-normal shadowing plus Rayleigh fading channel using Method A with capture for $\sigma = 6$ dB with different transmitted power are shown in Figure 5.17(a) and (b) respectively. Similar to a one-dimensional model in Figure 5.10, S or τ for any n is not affected by T_x very much except that τ for one RB increases with T_x.

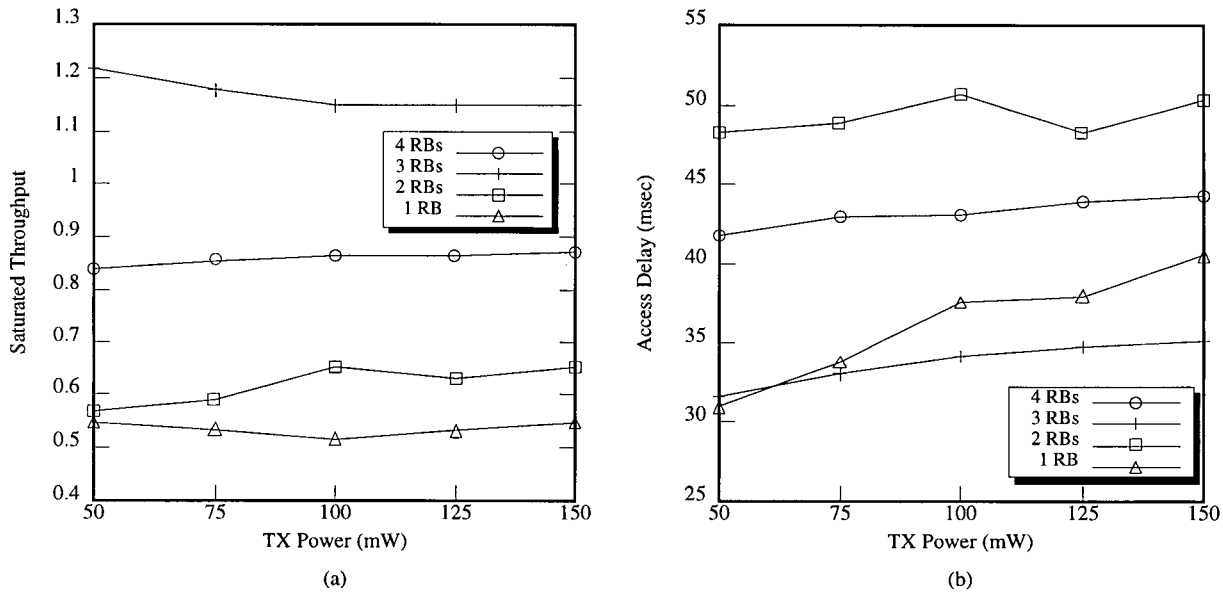

Figure 5.17 (a) Saturated throughput and (b) access delay as a function of transmitted power in log-normal plus Rayleigh fading channel at $\sigma = 6$ dB for 15 WTs using Method A with capture in a two-dimensional model.

5.3.2 Packet Length

The packet length used in the previous simulations is 8000 bits. In this section, the effect of the packet size, N, on the performance will be examined. The saturated throughput in a log-normal shadowing plus Rayleigh fading channel for 15 WTs with capture for different N is shown in Figure 5.18. It can be seen that S is more or less constant with N for any n. For a given period of time, the number of packet received is smaller for a longer packet. But a longer packet contains more information bits. Hence, the throughput in terms of average number of bits per second successfully received will be the same for any N. Even though S is independent of N, τ increases with N as shown in Figure 5.18(b). Since the transmission time is longer for larger N, the channel will be sensed as busy for a longer time. Thus, the WTs need to wait for a longer time to send their packets. In conclusion, longer packet size does not improve the throughput, but it degrades the

access delay. However, the length of packet size mainly depends on the types of message being delivered. Longer packets reduce the fraction of packet overhead.

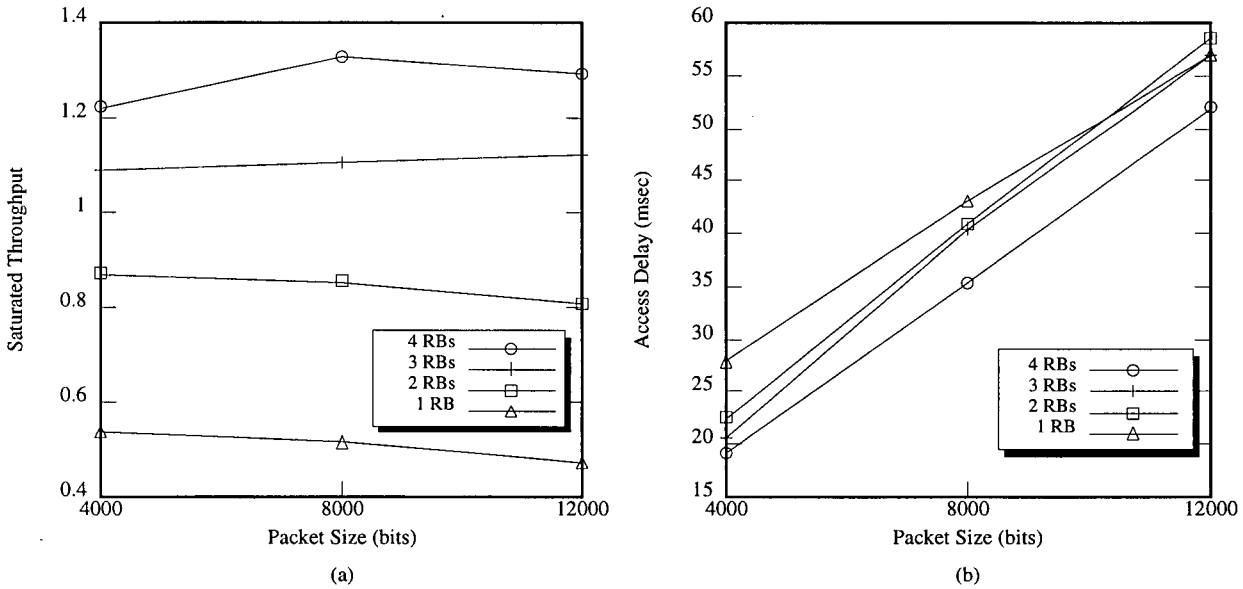

Figure 5.18 (a) Saturated throughput and (b) access delay as a function of packet size in log-normal shadowing, $\sigma = 6$, and Rayleigh fading channel at $T_x = 100$ mW with capture for 15 WTs using Method A.

5.3.3 Effect of ACK_Timeout

The default value of ACK_Timeout is 300 μs in the previous results. The saturated throughput and access delay for 15 WTs in a log-normal shadowing plus Rayleigh fading channel with no capture and capture as a function of ACK_Timeout are shown in Figure 5.19 and Figure 5.20. The access delay with no capture and capture are shown in Figure 5.21 and Figure 5.22 respectively. It can be seen that the performance, S and τ, is not changed with ACK_Timeout for both Method A and B. For Method A, since only a single ACK is returned from a RB, the desired WT after sending a packet is required to wait for the transmission time of the ACK, 112 μs, SIFS, 28 μs, and the propagation time, < 1 μs, which is about 141 μs. If the ACK is lost, the desired

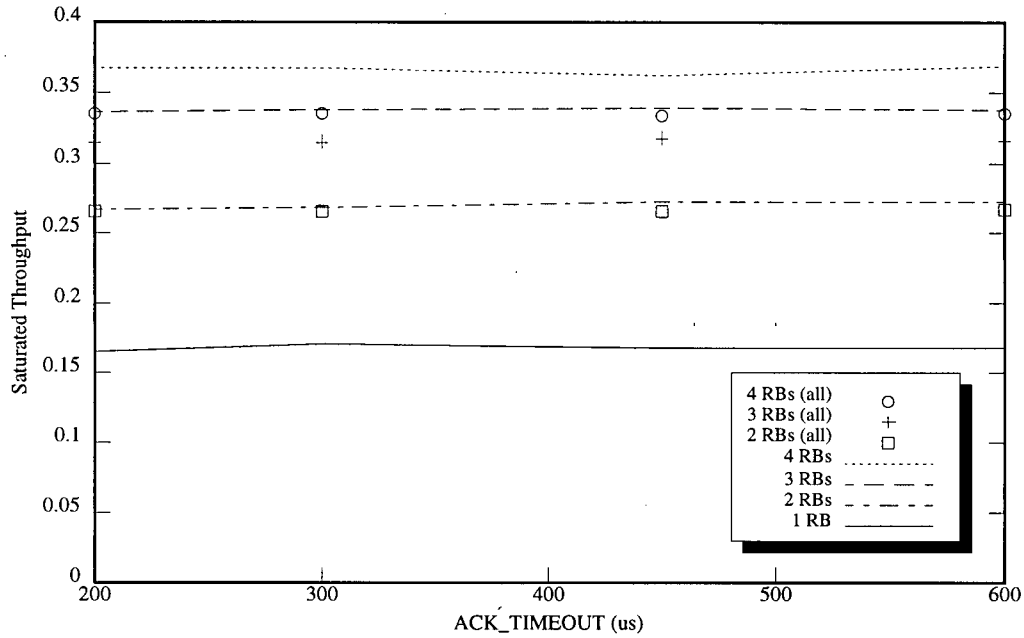

Figure 5.19 Saturated throughput as a function of ACK_Timeout for 15 WTs with no capture in log-normal shadowing plus Rayleigh fading channel using Method A and Method B.

WT will follow the backoff procedures to retransmit the packet only when the ACK_Timeout is expired. If the ACK_Timeout is longer, the desired WT needs to wait for a longer time to retransmit the packet and thus the performance is degraded. In all four figures, however, it can be seen that the performance does not degrade with increasing ACK_Timeout. This is because most of the ACK can be received correctly by the desired WT. The reason is that if the packet sent from the desired WT can be successfully received at the RB, the ACK returned from that RB can also be received at the desired WT with a equally high probability. With capture, the chance of receiving a ACK is higher. It can be seen that the performance of Method B is lower than that of Method A. This is because multiple ACKs increase the channel busy time.

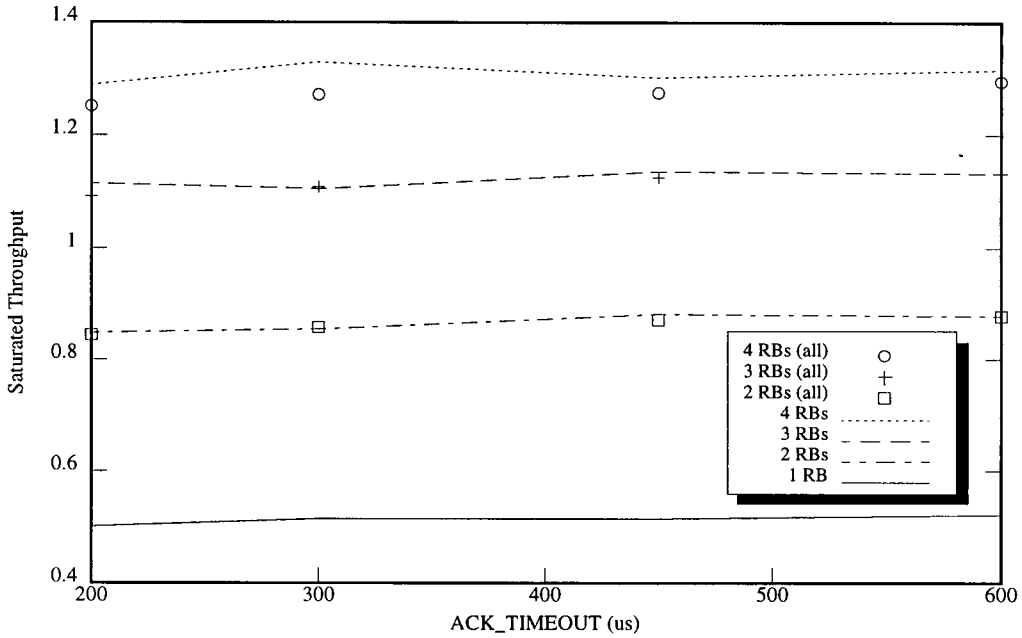

Figure 5.20 Saturated throughput as a function of ACK_Timeout for 15 WTs with capture in log-normal shadowing plus Rayleigh fading channel using Method A and Method B.

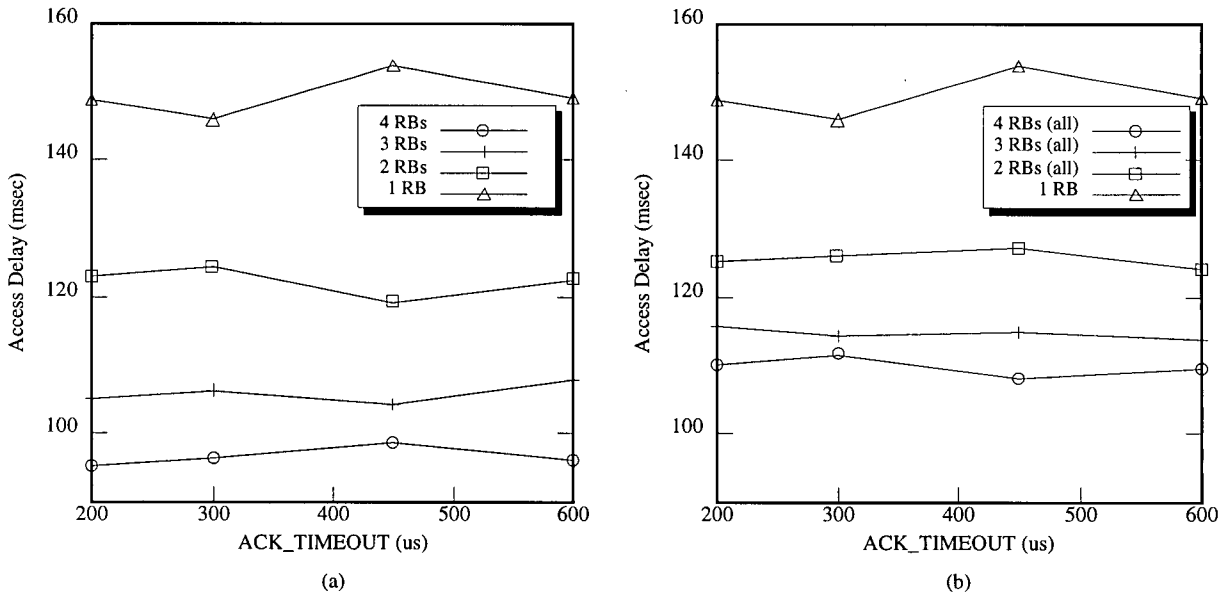

Figure 5.21 Access delay as a function of ACK_Timeout for 15 WTs with no capture in log-normal shadowing plus Rayleigh fading channel using Method A (a) and Method B (b).

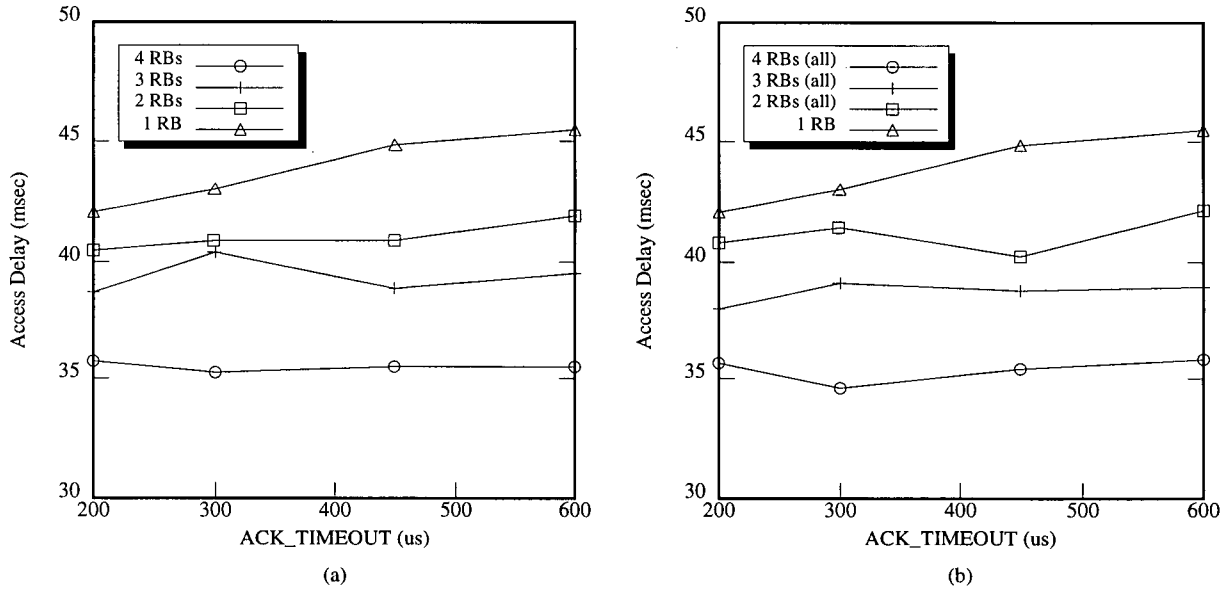

Figure 5.22 Access delay as a function of ACK_Timeout for 15 WTs with capture in log-normal shadowing plus Rayleigh fading channel using Method A (a) and Method B (b).

5.3.4 Effect of Capture Ratio

The capture ratio, c, used in previous sections is 10 dB. In this section, the effect of different values of c is investigated. Figure 5.23(a) and (b) show the saturated throughput and access delay with various values of c for 15 WTs in a log-normal shadowing plus Rayleigh fading channel respectively. As expected, the performance improves with decreasing c because a packet can be more easily to be captured for a smaller value of c. However, the value of c cannot be chosen arbitrary because it depends on the system characteristics such as modulation schemes and coding techniques.

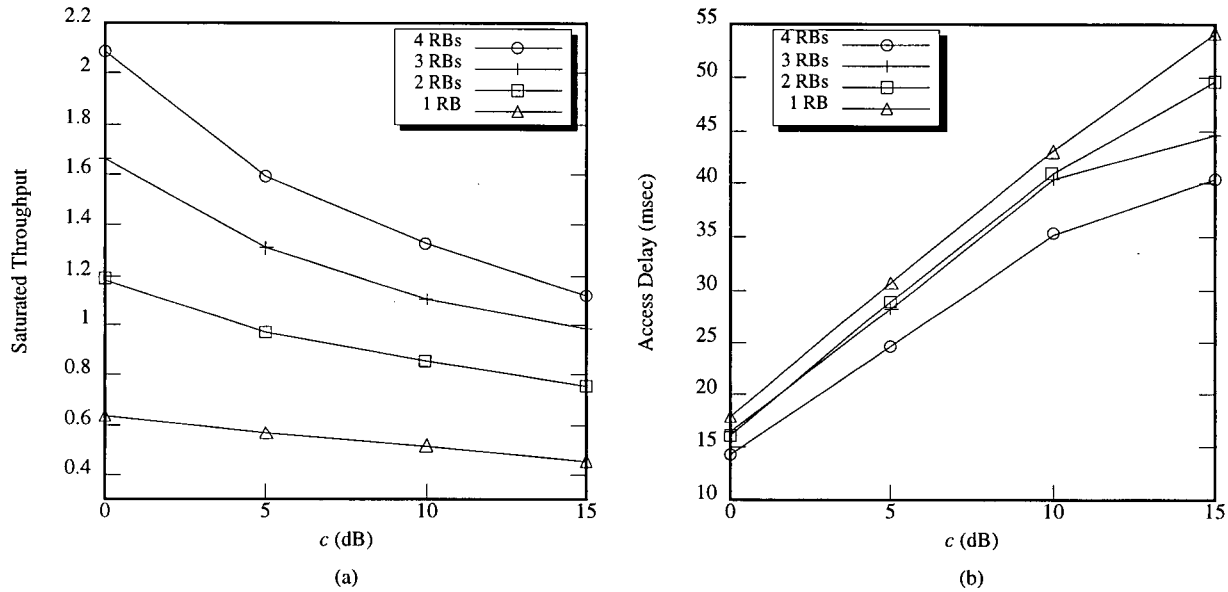

Figure 5.23 (a) Saturated throughput and (b) access delay as a function of c for 15 WTs with capture in log-normal shadowing plus Rayleigh fading channel.

Chapter 6 Conclusions

In this thesis, the performance, in terms of normalized throughput, η, and access delay, τ, of the proposed WLAN with distributed RBs using the IEEE 802.11 MAC protocol is studied extensively by computer simulations. The simulation model is validated against previous results. The channel environments used in the simulation are AWGN, Rayleigh fading, log-normal shadowing and log-normal shadowing plus Rayleigh fading channel. The effect of various parameters, such as number of WTs, number of RBs, n, transmitted power level, T_x, and standard deviation, σ, of the log-normal shadowing are examined. Two methods used for the RBs to return the ACKs are studied. It was found that Method A can provide better performance than Method B in all channel environments and ranges of parameters considered.

The simulation results with no-capture assumption are obtained for all four channel models. In AWGN channel, it is found that η and τ do not change with n. The η is the same for different number of WTs and about 0.9, but τ with more WTs is higher. Thus, using more RBs is not desirable in AWGN channel. With the other three channel models, results show that the performance can always be improved using more RBs. The performance improvement of using multiple RBs to single RB depends on the system parameters, i.e., number of WTs, T_x, σ and n. Use the default values of T_x = 100 mW and σ = 6 dB as an example. In a Rayleigh fading channel, the saturated throughput (access delay), S (τ), with 4 RBs for 15 WTs and 30 WTs can be improved by about 40% (30%) and 100% (40%) respectively. In a log-normal shadowing channel, S with 4 RBs for 15 WTs and 30 WTs can be improved by 28% and 38% respectively. The τ is about the same. In a log-normal shadowing plus Rayleigh fading channel, S with 4 RBs

for 15 WTs and 30 WTs can be improved by 100% and 200% respectively. The τ can be improved by about 50% for both 15 and 30 WTs. Therefore, the results show that the distributed WLAN architecture employing multiple RBs is more effective in a system with a larger number of WTs in terms of performance improvements over a system with a single RB.

In a Rayleigh fading channel, S with any n increases with T_x, but τ is not affected very much by T_x. Because for low T_x each RB can only cover few WTs; therefore, each WT covered by a RB needs only to wait for few other WTs completing their transmissions in order to send its packet. The performance improvement of multiple RBs over single RB at low T_x is much greater, about 10 times from the evaluation range considered in figures, than that at high T_x. In a log-normal shadowing channel, S (τ) decreases (increases) with σ. The performance improvement at high σ is much greater, about 15 times from the evaluation range considered in figures, than that at low σ. In a log-normal shadowing plus Rayleigh fading channel, the performance is more or less independent of T_x and σ. The S with 4 RBs for 30 WTs can be improved by at least 120% over S with a single RB for any values of T_x and σ.

The simulation results with capture are only obtained for a log-normal shadowing plus Rayleigh fading channel. With use of capture, the performance can be improved significantly with increasing n. The performance improvement of multiple RBs over one RBs is greater than that for no capture cases. For T_x = 100 mW and σ = 6 dB, S with 4 RBs and 15 WTs can be improved about 160% over one RB. In general, the performance is not affected significantly by T_x or σ except that the access delay with one RB increases (decreases) with T_x (σ).

The impact of a two-dimensional model, packet size and ACK_Timeout on the performance of distributed RBs are investigated for no capture and capture in a log-normal shadowing plus Rayleigh fading channel. It is found that the configuration of the system (one- or two-dimensional) will affect the performance slightly because the distances between WTs or the distances between WTs and RBs may vary. Thus, it will affect the number of hidden terminals and the occurrence of collisions. The S is independent of packet size, but τ degrades with packet size. Therefore, it is better to use a shorter packet size rather than a longer packet size. However, the packet size depends on the types of message. It is found that the ACK_Timeout does not affect the performance in both no capture and capture cases. As expected, the performance is increased with decreasing the capture ratio because small value of capture ratio allows more packets to be captured easily. However, this value to be chosen depends on the system configuration.

In conclusions, distributed RBs are effective in a channel with fading or shadowing. The performance can always be improved with increasing n over a single RB, especially for a channel severely degraded by fading or shadowing. In a channel with fading or shadowing, a packet might not be received at the RB. Thus, there is a high chance that a packet is discarded at the RB. Multiple RBs can increase the packet reception probability at one of the RBs for fading cases because this is a relatively low probability that a packet is faded at all RBs. For shadowing cases, multiple RBs can be considered as a macrodiversity (multiple-base-station diversity) because if a WT is shadowed from one RB, there is a good chance that the WT might not be shadowed from another RB by adding more RBs. Packets might be faded or shadowed at the WTs so that some WTs may be hidden from each other. While two or more WTs, which are hidden from each other, send the packets at about the same time, those packets are collided and discard at the RB with no-capture. Therefore, for a fixed number of RBs the performance of a system with more WTs is

worse than that with less WTs. Because more WTs increase the number of hidden terminals and thus the number of collisions at RBs is increased as well. With capture, the performance improvement even better than that with no capture. However, it causes the near-far effect problem in which the performance of the WTs close to the RB can be improved greatly.

Among the related topics for further study are the following:

(i) To study the performance by theoretical analysis rather than computer simulation.

(ii) To study the performance with mobile WTs.

(iii) To use RTS/CTS to improve the performance.

(iv) To use different channel for uplink and downlink.

Glossary

τ	Access Delay.
AP	Access Point.
ACK	Acknowledgment.
AWGN	Additive White Gaussian Noise.
T_0	Ambient Room Temperature.
BSA	Basic Service Area.
BSS	Basic Service Set.
BER	Bit-error Rate.
k	Boltzmann's Constant.
c	Capture Ratio.
CS	Carrier Sense.
CSMA/CA	Carrier Sense Multiple Access with Collision Avoidance.
CST	Carrier Sensing Threshold.
CFP	Contention Free Period.
CP	Contention Period.
CW	Contention Window.
DSSS	Direct Sequency Spread Spectrum.
d	Distance between the transmitter and the receiver.
DCF	Distributed Coordination Function.
DIFS	Distributed Coordination Function Interframe Space.
DS	Distribution System.

DSS	Distribution System Services.
T_b	Effective Background Temperature.
T_e	Effective Noise Temperature.
BW	Equivalent Bandwidth of the Receiver.
EIFS	Extended Interframe Space.
ESA	Extended Service Area.
ESS	Extended Service Set.
FCS	Frame Check Sequence.
FHSS	Frequency Hopping Spread Spectrum.
IFS	Interframe Space.
LOS	Line of sight.
LANs	Local Area Networks.
MAC	Medium Access Control.
MPDU	MAC Protocol Data Unit.
MSDU	MAC Service Data Unit.
NAV	Network Allocation Vector.
F	Noise Figure.
ρ	Normalized Offered Load.
η	Normalized Throughput.
n	Number of Radio Bridges.
OBS	Obstructed.
OPNET	OPtimized Network Engineering Tools.

N	Packet Size.
γ	Path Loss Exponent.
PHY	Physical Layer.
PCF	Point Coordination Function.
PIFS	Point Coordination Function Interframe Space.
RBs	Radio Bridges.
RTS/CTS	Ready to Send/Clear to Send.
P_r	Received Power.
G_r	Receiver Antenna Gain.
P_n	Receiver Noise Floor.
RS	Receiver Sensitivity.
d_0	Reference Distance.
S	Saturated Throughput.
SIFS	Short Interframe Space.
SNR	Signal-to-noise Ratio.
σ	Standard Deviation for the log-normal shadowing (dB).
SS	Station Service.
TSF	Timing Synchronization Function.
$P_t(T_x)$	Transmitted Power.
G_t	Transmitter Antenna Gain.
λ	Wavelength.

WIN	Wireless in Building Network.
WLANs	Wireless Local Area Networks.
WTs	Wireless Terminals.
L_σ	Zero-mean Gaussian Distributed Random Variable (dB).

Bibliography

[1] V. C. M. Leung, "Diversity Interconnection of Wireless Terminals to Local Area Networks via Radio Bridges", *Electronics Letters*, vol. 28, no. 5, pp. 489-490, Feb. 1992.

[2] C. T. Lau and C. Leung, "Capture Models for Mobile Packet Radio Networks", *IEEE Transactions on Communications*, vol. 40, no. 5, pp. 917-925, May 1992.

[3] J. C. Arnbak and W. V. Blitterswijk, "Capacity of Slotted ALOHA in Rayleigh-Fading Channels", *IEEE Journal on Selected Areas in Communications*, vol. SAC-5, no. 2, pp. 261-269, Feb. 1987.

[4] V. C. M. Leung and A. W. Y. Au, "A Wireless Local Area Network Employing Distributed Radio Bridges", *ACM/Baltzer Wireless Network Journal*, vol. 2, pp. 97-107, Oct 5, 1995.

[5] V. C. M. Leung, "Internetworking Wireless Terminals to Local Area Networks via Radio Bridges", *Proceedings of the IEEE International Conference on Selected Topics in Wireless Communications*, Vancouver, B.C. pp. 126-129, June 1992.

[6] IEEE, Piscataway, NJ, IEEE 802.11 -- *Wireless LAN Medium Access Control (MAC) and Physical Layer (PHY) Specifications*, Dec. 1994. P802.11/D1.

[7] IEEE, Piscataway, NJ, IEEE P802.11 - *Wireless LAN Medium Access Control (MAC) and Physical Layer (PHY) Specifications*, May. 9, 1997. P802.11D6.1.

[8] S. M. Nor and I. Ismail, "Performance of CSMA-CA MAC Protocol for distributed Radio Local Area Networks", IEEE International Symposium on Personal Indoor and Mobile Radio Communications. vol. 2, pp. 912-914, Toronto, Canada, 1995.

[9] J. Weinmiller, H. Woesner and A. Wolisz, "Analyzing and Improving the IEEE 802.11 MAC Protocol for Wireless LANs", *International Workshop of MASCOTS'96: Modeling Analysis, and Simulation*, pp. 200-206, San Jose, CA, 1996.

[10] J. Weinmiller, H. Woesner, J. P. Ebert and A. Wolisz, "Analyzing the RTS/CTS Mechanism in the DFWMAC Media Access Protocol for Wireless LANs", *Proceedings of IFIP TC6 Workshop Personal Wireless Communications (Wireless Local Access)*, Prague, Czech Republic, pp. 117-130, April 1995.

[11] H. Woesner, J. Weinmiller, J. P. Ebert and A. Wolisz, "Modified Backoff Algorithms for DFWMAC's Distributed Coordination Function", *Proceedings of 2 ITG Fachtagung Mobile Kommunikation '95*, Neu-Ulm, Germany, pp. 363-370. Sept. 1995.

[12] M. A. Visser and M. E. Zarki, "Voice and Data transmission over an 802.11 Wireless network", *IEEE International Symposium on Personal, Indoor and Mobile Radio Communications*, vol. 2, pp. 648-652, Toronto, Canada, 1995.

[13] G. Bianchi, L. Fratta and M. Oliveri, "Performance Evaluation and Enhancement of the CSMA/CA MAC Protocol for 802.11 Wireless LANs", *The Seventh IEEE International Symposium on Personal, Indoor and Mobile Radio Communications*, vol. 2, pp. 392-396, Taipei, Taiwan, Oct 15-18, 1996.

[14] G. Bianchi, "IEEE 802.11--Saturation Throughput Analysis", *IEEE Communications letters*, vol. 2, no. 12, pp. 318-320, Dec 1, 1998.

[15] H. S. Chhaya, "Performance evaluation of the IEEE 802.11 MAC Protocol for Wireless LANs", M. S. thesis, Dep. of Elec. and Comp. Eng, Illinois Institute of Technology, Chicago, Illinois, May 1996.

[16] H. S. Chhaya and S. Gupta, "Performance of Asynchronous Data Transfer methods of IEEE 802.11 MAC Protocol", *IEEE Personal Communications*, vol. 3, no. 5, pp. 8-15, Oct. 1996.

[17] J. H. Kim and J. K. Lee, "Performance Analysis of MAC protocols for Wireless LAN in Rayleigh and Shadow Fading Channels", *IEEE Global Telecommunications Conference,* vol. 1, pp. 404-408, Phoenix, AZ, 1997.

[18] A. Zahedi and K. Pahlavan, "Throughput of a Wireless LAN access point in presence of natural hidden terminals and capture effects", *The 7th IEEE International Symposium on Personal, Indoor and Mobile Radio Communications,* vol. 2, pp. 397-401, Taipei, Taiwan, Oct. 1996.

[19] A. Zahedi and K. Pahlavan, "Natural Hidden Terminal and the Performance of the Wireless LANs", *Annual International Conference on Universal Personal Communications Record.* vol. 2, pp. 929-933, San Diego, CA, 1997.

[20] D. Buchholz, P. Odlyzko, M. Taylor and R. White, "Wireless In-Building Network Architecture and Protocols", *IEEE Network Magazine*, vol. 5, no. 6, pp. 31-38, Nov. 1991.

[21] W. K. W. Cheung, "Performance Study of the IEEE 802.11 Wireless Media Access Control Protocols", M. A. Sc. thesis, Dep. Elec. Eng, Univ. British Columbia, Vancouver, Canada, 1995.

[22] B. P. Crow, I. Widjaja, J. G. Kim and P. Sakai, "Investigation of the IEEE 802.11 Medium Access Control (MAC) Sublayer Functions", *Proceedings of IEEE INFOCOM '97*, vol. 1, pp. 126-133, Kobe, Japan, April 1997.

[23] B. P. Crow, I. Widjaja, J. G. Kim and P. T. Sakai, "IEEE 802.11 Wireless Local Area Networks", *IEEE Communications Magazine*, vol. 35, no. 9, pp. 116-126, Sept. 1997.

[24] L. Tang, "Modeling and Performance Analysis of In-Building Distributed WLAN using CSMA with Spread Spectrum Signaling", M. A. Sc. thesis, Dep. Elec. Eng, Univ. British Columbia, Vancouver, Canada, 1995.

[25] A. W. Y. Au, "Multi-Receiver Performance of Slotted ALOHA Multiple Access with Direct Sequence Spread-Spectrum signalling for Wireless In-Building networks", M. A. Sc. thesis, Dep. Elec. Eng, Univ. British Columbia, Vancouver, Canada, 1993.

[26] C. Roobol, "On the packet delay in Wireless Local Area Networks with Access Port Diversity and Power Control", *Proceedings of 6th International Symposium on Personal, Indoor and Mobile Radio Communications,* vol. 2, pp. 917-920, Toronto, Canada, Sept. 1995.

[27] OPtimized Network Engineering Tools (OPNET) Tutorial Manual, Release 3.0, MIL 3 Inc. Washington, DC. August 1996.

[28] T. S. Rappaport, *Wireless Communications Principles and Practice*. Prentice Hall, Upper Saddle River, NJ, 1996. ISBN 0-7803-1167-1.

[29] T. S. Ho and K. C. Chen, "Performance Analysis of IEEE 802.11 CSMA/CA Medium Access Control Protocol", *IEEE International symposium on Personal, Indoor and Mobile Radio Communications*, vol. 2, pp. 407-411, Taipei, Taiwan, 1996.